

GROUND WATER RESOURCES BETWEEN THE RAKAIA AND ASHBURTON RIVERS

D.M. SCOTT and H.R. THORPE



**PUBLICATION No 6 OF THE
HYDROLOGY CENTRE
CHRISTCHURCH**



Publication no. 6 of the Hydrology Centre, Christchurch (1986)



**GROUND WATER RESOURCES
BETWEEN THE RAKAIA AND
ASHBURTON RIVERS**

D.M. SCOTT and H.R. THORPE

**PUBLICATION NO. 6 OF THE
HYDROLOGY CENTRE
CHRISTCHURCH**

**CHRISTCHURCH
MARCH 1986**

GROUND WATER RESOURCES BETWEEN THE
RAKAIA AND ASHBURTON RIVERS

D.M. SCOTT and H.R. THORPE

Hydrology Centre, Ministry of Works and
Development, Christchurch

Publication No. 6 of the Hydrology Centre
Christchurch, 1986, 105 p, ISSN 0112-1197

The hydrologic components of the ground water system between the Rakaia and Ashburton Rivers are identified. An unsteady, finite difference model is used to predict how that system might react to a large expansion of irrigation supplied by ground water.

National Library of New Zealand
Cataloguing-in-Publication data

SCOTT, D. M., 1946-

Groundwater resources between the Rakaia and Ashburton rivers / by D.M. Scott and H.R. Thorpe. - Christchurch [N.Z.] : Hydrology Centre, Ministry of Works and Development for the National Water and Soil Conservation Authority, 1986 - 1 v. - (Publication ... of the Hydrology Centre, 0112-1197 ; no. 6)

551.490993174

1. Water, Underground--New Zealand--Ashburton County. I. Thorpe, H. R. (Hugh Rankin), 1936-. II. Hydrology Centre (Christchurch, N.Z.). III. National Water and Soil Conservation Authority (N.Z.). IV. Title. V. Series: Publication of the Hydrology Centre Christchurch ; no. 6.

Published for the National Water and Soil Conservation
Authority by the Hydrology Centre, Ministry of Works
and Development, P.O. Box 1479, Christchurch

ABSTRACT

The stimulus for this investigation was the proposal to implement the Lower Rakaia Irrigation Scheme using water from the Rakaia River. It was apparent that with a very significant ground water resource available, it might be practical and economic to develop ground water for irrigation in some areas while constructing a river supplied system for the remainder. An overall understanding of the aquifer system between the Ashburton and Rakaia Rivers and how this might change under the impact of future irrigation development was sought.

Recharge of the aquifers is primarily by drainage from precipitation with significant inputs from the Rakaia River, leaky stock races and irrigation return flows. Most recharge from rainfall occurs in the winter and there is a marked summer fall in piezometric levels in areas away from the rivers. Pumpage for irrigation is increasing very rapidly but there has been no detectable effect on long-term piezometric levels. The present Ashburton-Lyndhurst Irrigation Scheme has a significant effect on ground water quality in some areas and further irrigation will probably raise nitrate-nitrogen concentrations to 15-20 g m⁻³. An alternative water supply for rural households may have to be considered.

An unsteady, finite difference numerical model of the proposed irrigation area was developed, calibrated and used to examine eight options for ground water supplied irrigation. Calibration involved indirect solution of the inverse problem, based on flow net analysis of steady-state heads. Although substantial regional drawdowns were predicted, all options tested could be supplied from the aquifer system. Whichever option is chosen, some existing irrigation wells will be detrimentally affected by lowered piezometric levels.

Regional drawdown caused by extensive ground water pumpage will induce additional leakage from the rivers. This will not be detectable for the Rakaia River, but the effect could be marked on the low summer flow of the Ashburton River, and very severe on the Wakanui Creek.

CONTENTS

| | | |
|-------|--|----|
| | ABSTRACT | |
| 1 | INTRODUCTION | 1 |
| 1.1 | The study area | 1 |
| 2 | SYSTEM CHARACTERISTICS | 4 |
| 2.1 | Hydrogeology | 4 |
| 2.2 | Well specific capacities | 7 |
| 2.3 | Aquifer pumping test results | 7 |
| 2.4 | Surface water - ground water interactions | 11 |
| 2.4.1 | Rakaia River | 11 |
| 2.4.2 | Ashburton River | 14 |
| 2.4.3 | River flow and recharge | 14 |
| 2.5 | Piezometric surfaces | 15 |
| 2.5.1 | Depth to standing water-level | 17 |
| 2.6 | Long-term water-level records | 17 |
| 2.7 | Hydrochemistry | 21 |
| 2.7.1 | Zone 1. Non-irrigated, riparian recharge areas | 22 |
| 2.7.2 | Zone 2. Non-irrigated, non-riparian areas | 23 |
| 2.7.3 | Zone 3. Non-irrigated piedmont area | 23 |
| 2.7.4 | Zone 4. Border-strip irrigated lands | 23 |
| 2.7.5 | Changes of water quality with depth | 24 |
| 2.7.6 | Seasonal changes of water quality | 24 |
| 3 | SYSTEM INPUTS AND OUTPUTS | 26 |
| 3.1 | Deep drainage from precipitation and irrigation | 26 |
| 3.1.1 | Soil moisture model | 26 |
| 3.1.2 | Soil moisture model calibration | 28 |
| 3.1.3 | Soil moisture model results | 29 |
| 3.1.4 | Soil moisture budget for the whole study area | 31 |
| 3.1.5 | Irrigation return water from Ashburton- Lyndhurst Irrigation Scheme | 32 |
| 3.2 | River recharge | 33 |
| 3.2.1 | Ashburton River | 33 |
| 3.2.2 | Rakaia River | 36 |
| 3.2.3 | Rakaia River underflows | 38 |
| 3.2.4 | Recharge of aquifers on the south bank of the Rakaia River | 40 |

| | | |
|-------|---|----|
| 3.2.5 | Recharge of confined aquifer by vertical leakage through the clay-bound gravels underlying the Rakaia River | 42 |
| 3.2.6 | Summary of information on recharge from the Rakaia River | 42 |
| 3.3 | Leakage from stock races and the Rangitata Diversion Race | 43 |
| 3.4 | Water Extraction | 44 |
| 3.4.1 | Municipal and industrial water use | 44 |
| 3.4.2 | Agricultural water use | 44 |
| 3.5 | Spring leakage | 45 |
| 3.6 | Submarine leakage | 46 |
| 3.7 | Elements of the water balance | 46 |
| 4 | GROUND WATER MODELLING | 47 |
| 4.1 | Introduction | 47 |
| 4.2 | Method | 48 |
| 4.2.1 | Ground water flow model | 48 |
| 4.2.2 | Parameter estimation method | 54 |
| 4.2.3 | Summary of modelling approach | 58 |
| 4.3 | Calibration | 58 |
| 4.3.1 | Soil moisture model | 58 |
| 4.3.2 | Lumped parameter ground water model | 60 |
| 4.3.3 | Finite difference model calibration | 64 |
| 4.4 | Finite difference model simulations | 75 |
| 4.4.1 | Options considered | 75 |
| 4.4.2 | Analysis of results | 78 |
| 4.4.3 | Impact of ground water development - spatial description | 80 |
| 4.4.4 | Effects on existing wells | 85 |
| 4.4.5 | Alternative irrigation development options | 88 |
| 4.4.6 | Impact of ground water development - temporal description | 91 |
| 4.4.7 | Leakage zone effects | 94 |
| 5 | SUMMARY AND CONCLUSIONS | 96 |
| 5.1 | Introduction | 96 |
| 5.2 | Summary | 96 |
| 5.2.1 | Hydrogeology | 96 |
| 5.2.2 | Piezometric levels | 96 |
| 5.2.3 | Hydrochemistry | 97 |

| | | |
|----------|---|-----|
| 5.2.4 | Aquifer recharge | 97 |
| 5.2.5 | Aquifer output | 98 |
| 5.2.6 | Model summary | 98 |
| 5.3 | Conclusions | 99 |
| 5.3.1 | Prospects for expansion of ground water use | 99 |
| 5.3.2 | Piezometric level controls | 99 |
| 5.3.3 | Ground water quality changes | 99 |
| 5.3.4 | Potable water supplies | 99 |
| 5.3.5 | Reduction of Ashburton River flows | 99 |
| 5.3.6 | Reduction of Rakaia River flows | 99 |
| 5.3.7 | Water availability | 100 |
| 5.3.8 | Consequences of development | 100 |
| 5.3.9 | Saltwater intrusion | 100 |
| 5.3.10 | Artificial recharge | 100 |
| 5.3.11 | Accuracy of prediction | 100 |
| 6 | ACKNOWLEDGEMENTS | 101 |
| 7 | REFERENCES | 102 |
| APPENDIX | Details of selected existing wells. | 105 |

LIST OF FIGURES

| | | |
|-----|---|----|
| 1.1 | Ashburton-Rakaia ground water study area. | 2 |
| 2.1 | The variation of transmissivity with depth beneath the Canterbury Plains between the Ashburton and Rakaia Rivers. | 5 |
| 2.2 | Specific capacity of wells in the study area. | 8 |
| 2.3 | Water-level records in the Rakaia River, Rakaia River bed and Caunters well. | 12 |
| 2.4 | Water-level records from Rakaia River, adjacent bores at Rakaia Township and barometric pressure at Christchurch. | 13 |
| 2.5 | Water-level records from Rakaia River and bores at Dobsons Ferry Rd. | 13 |
| 2.6 | Water-level records from the Ashburton River and adjacent bores at River Rd and Wilsons Rd. | 15 |
| 2.7 | Piezometric contours for May 1978. | 16 |
| 2.8 | Variation of standing water-level between October 1978 and April 1982 | 18 |
| 2.9 | Depth to standing water-level, April 1982. | 19 |

| | | |
|------|---|----|
| 2.10 | Long-term rainfall at Winchmore Irrigation Research Station and ground water levels at Longs Rd, Lauriston and Charing Cross. | 20 |
| 2.11 | Water sales on the Ashburton-Lyndhurst Irrigation Scheme. | 21 |
| 2.12 | Location of wells used in water quality survey and chemical zones deduced from the results. | 22 |
| 2.13 | Changes in ground water depth in zone 2 wells. | 24 |
| 2.14 | Seasonal changes of nitrate-nitrogen in shallow and deep wells compared with estimates of subsurface drainage. | 25 |
| 3.1 | Relationship between the ratio of actual to potential evapotranspiration and soil moisture level. | 27 |
| 3.2 | Mean monthly rainfall, pan evaporation and drainage at Winchmore Irrigation Research Station. | 31 |
| 3.3 | Loss gauging sites on the Ashburton and Rakaia Rivers. | 35 |
| 4.1 | Conceptual model of soil and ground water systems. | 47 |
| 4.2 | Section of the finite difference grid showing the node reference convention. | 50 |
| 4.3 | Alternative node numbering convention for internal and boundary nodes. | 52 |
| 4.4 | Portion of a streamtube. | 54 |
| 4.5 | Irrigation demand and rainfall drainage for irrigation strategy 1. | 60 |
| 4.6 | Monthly drainage, irrigation return, irrigation pumpage used in the lumped parameter model, together with water-level records at Charing Cross. | 61 |
| 4.7 | Long-term water-level fluctuations simulated using the lumped parameter model. | 63 |
| 4.8 | Finite difference model boundary and grid. | 65 |
| 4.9 | Steady-state piezometric contours, together with streamlines drawn to complete the flow net analysis. | 66 |
| 4.10 | Patterns of coefficients a_i and b_i at model nodes. | 69 |
| 4.11 | Segmentation of finite difference model developed from flow net analysis. | 70 |
| 4.12 | Location of nodes and observed head. | 71 |
| 4.13 | Performance of the automatic optimisation technique in reducing the objective function. | 73 |
| 4.14 | (a) Contours of transmissivity for the calibrated model. | 74 |
| | (b) Steady-state piezometric levels simulated using the transmissivity distribution shown in figure 4.14 (a). | 74 |

| | | |
|------|---|----|
| 4.15 | (a) Observed and simulated piezometric levels at Charing Cross and node 122. | 76 |
| | (b) Observed and simulated piezometric levels at Griggs Rd and node 232. | 76 |
| 4.16 | Simulated piezometric levels for node 122 showing a range of representative levels. | 79 |
| 4.17 | Simulation I results (scheme 3/high water use). | 81 |
| 4.18 | Simulation II results (scheme 4/high water use). | 82 |
| 4.19 | Simulation III results (scheme 6/high water use). | 83 |
| 4.20 | Simulation VII results (scheme 9/high water use). | 84 |
| 4.21 | Schematic illustration of typical well showing local drawdown. | 86 |
| 4.22 | Location of the 56 existing wells used in assessment of impact of ground water development. | 87 |
| 4.23 | Comparison of simulations II and IV showing the effect of a change in scheme shape from scheme 4 to scheme 7. | 88 |
| 4.24 | Comparison of simulations III and V (high/low water use strategies) on scheme 6. | 89 |
| 4.25 | Comparison of simulations VII and VIII (low water use strategy) on scheme 9. | 90 |
| 4.26 | Comparison of simulations III and VI. Effects of artificial recharge on scheme 6. | 90 |
| 4.27 | Long-term simulated piezometric levels at nodes 122, 150 and 232 for simulations 0, I, II, III and VII. | 92 |
| 4.28 | Long-term simulated piezometric levels at: | |
| | (a) Node 122 for simulations 0, VII and VIII. | |
| | (b) Node 150 for simulations III and VI. | 93 |

LIST OF TABLES

| | | |
|-----|--|----|
| 2.1 | Results of aquifer tests where observation wells were available. | 9 |
| 2.2 | Results of step-drawdown aquifer tests. | 10 |
| 2.3 | Ground water level records used in examining interaction of aquifer system and rivers. | 12 |
| 3.1 | Annual and irrigation season drainage derived from daily values of evaporation and precipitation at Winchmore Irrigation Research Station (1950-1981). | 29 |

| | | |
|------|--|----|
| 3.2 | Winchmore annual average climatic values for 1950-1981. | 30 |
| 3.3 | Estimate of average annual ground water recharge by deep drainage of precipitation. | 32 |
| 3.4 | Estimate of average annual (Oct-Sept) ground water recharge by deep drainage from irrigation at Winchmore (1970-1979). | 32 |
| 3.5 | Results of loss gaugings in the Ashburton River. | 34 |
| 3.6 | Losses and gains from reaches of the Rakaia River. | 37 |
| 3.7 | Darcy velocities derived from tracer dilution tests. | 40 |
| 3.8 | Parameters adopted in computation of seepage through the south bank of the Rakaia River. | 41 |
| 3.9 | Irrigation water use between the Rakaia and Ashburton Rivers. | 45 |
| 3.10 | Elements of annual water balance for the Ashburton-Rakaia ground water system. | 46 |
| 4.1 | Alternative irrigation strategies. | 59 |
| 4.2 | Irrigation demands and lumped parameter model water-level ranges at Charing Cross for the postulated irrigation schemes. | 63 |
| 4.3 | Alternative ground water development areas. | 77 |
| 4.4 | Ground water development simulations. | 77 |
| 4.5 | Impact of ground water development on existing wells. | 86 |
| 4.6 | Minimum, maximum and range of simulated levels at selected nodes. | 94 |
| 4.7 | Minimum, mean and maximum simulated leakage zone flows. | 94 |

1 : INTRODUCTION

The investigation was planned to determine the hydrologic components of the ground water system between the Rakaia and Ashburton Rivers and to predict how the system might react to a large expansion of irrigation supplied by ground water.

The original concept of the Lower Rakaia Irrigation Scheme was to irrigate some 64 000 ha, predominantly with surface water from the Rakaia River. Competition for the use of the surface waters of the Rakaia is already occurring and will intensify as more irrigation schemes are proposed.

Ground water is already used in some parts of the scheme area, new wells are being drilled at a rapid rate and there is scope for much more development. To allow for future multiple use of the Rakaia River waters it is desirable to fully develop the ground water resource before taking river water. In management terms, therefore, the objective of the investigation was to evaluate the potential for expanded ground water abstraction and provide a rational basis for management of this resource.

The ultimate development of the ground water resource will also be affected by engineering, agricultural and economic factors but these are beyond the scope of this study.

1.1 The Study Area

The study area shown in figure 1.1 is bounded by Mt Hutt and the foothills of the Southern Alps, the north branch and main Ashburton Rivers, the Pacific Ocean and the Rakaia River. It comprises some 1350 km² of the Canterbury Plains, sloping steadily from an elevation of 500 m at the foot of Mt Hutt down to the sea coast.

Water resources in this area are managed by the South Canterbury Regional Water Board (SCRWB), with the exception of a narrow strip of land along the south bank of the Rakaia River which is administered by the North Canterbury Regional Water Board (NCRWB).

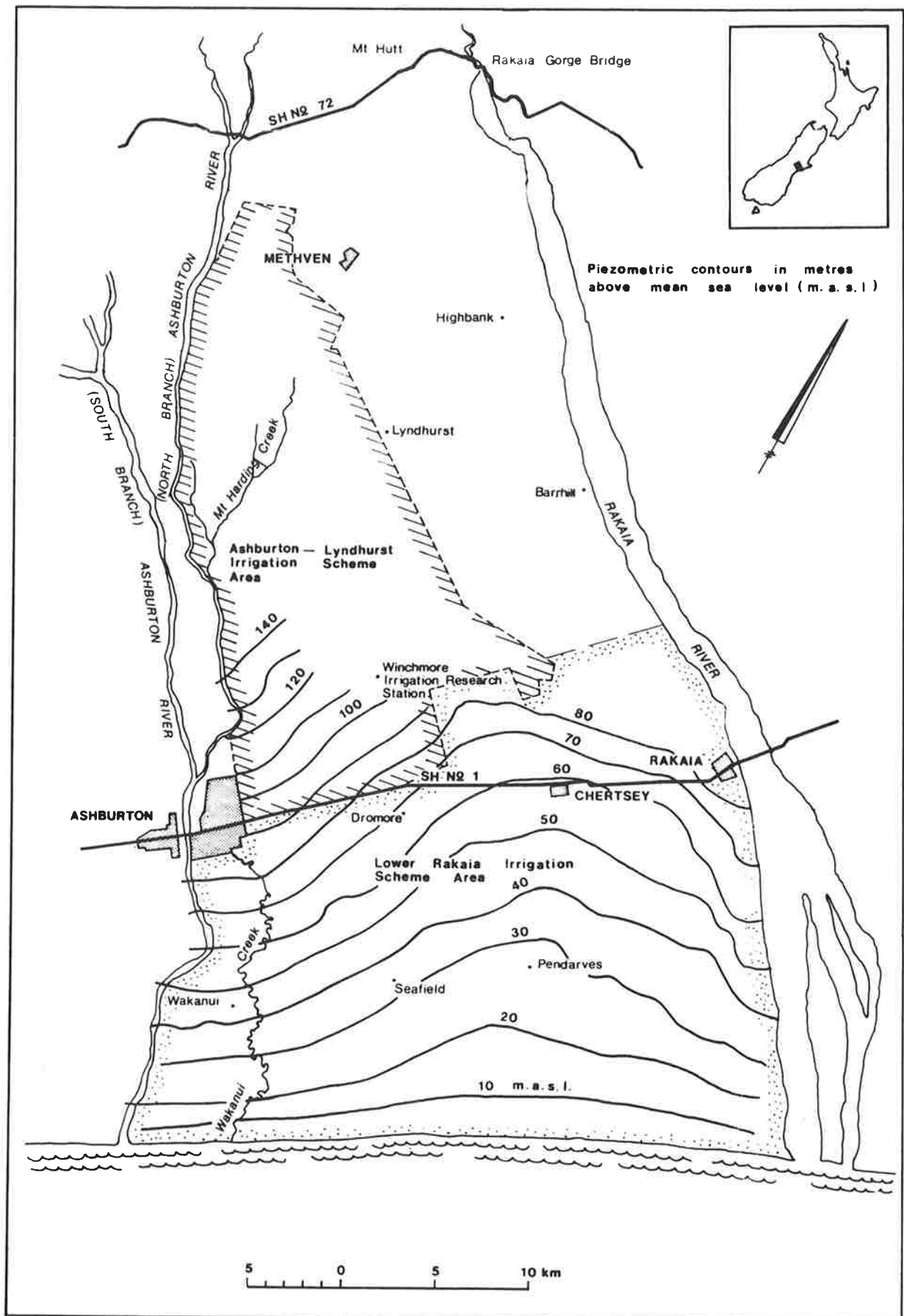


Figure 1.1 Ashburton-Rakaia ground water study area

Current land use in the area is predominantly pastoral with some cereal and crop farming. Included in the study area is the existing 26 000 ha Ashburton-Lyndhurst Irrigation Scheme (ALIS) and the 1050 ha South Rakaia Irrigation Scheme, and there are a rapidly increasing number of well owners who are also irrigating individually. The spread of irrigation has meant an intensification of agricultural activity and a swing to more cropping and horticulture. These changes can be expected to continue as further development proceeds.

Present consumptive water use in the area is dominated by irrigation, as the only sizeable town is Ashburton and the only significant industrial water user is the Fairton freezing works.

The development of ground water resources in this area has been in progress for many years, but accelerated rapidly in the 1970's. By mid 1981 a total of 136 rights to take ground water for irrigation had been granted by the regional water boards. Within the study area the nominal area irrigated from ground water is 9290 ha, with an average (since 1973) of 102 ha per farm (some irrigation was done prior to 1973, but the land areas are not known). There is, as yet, no indication of any long-term trends in the response of the ground water system to this pumpage.

2 : SYSTEM CHARACTERISTICS

2.1 HYDROGEOLOGY

The geology and hydrology of sections of the Canterbury Plains have been described by various workers (Collins, 1950; Oborn, 1955, 1960; Suggate, 1958, 1963, 1973; Mandel, 1974; Wilson, 1973, 1976, 1979).

The area between the Rakaia and Ashburton Rivers is typical of the Canterbury Plains and consists of a series of coalescing, late Cenozoic, gravel fans derived from erosion of the Southern Alps. The fans consist of glacial outwash, inter-glacial and post-glacial alluvium with a discontinuous loess cover on older surfaces (Scott, 1980). Wilson (1973) noted that the Pleistocene gravels extend to considerable depths, 620 m at Chertsey and 540 m at Seafield, as proved by petroleum exploration bores within the study area; however, there are no ground water bores deeper than 150 m and very few deeper than 80 m. Below these gravels are further coarse and fine sediments of the early Pleistocene or Pliocene. Wilson (1973) remarked upon the increase in aquifer yield on the Canterbury Plains with distance from the Alps in both post-glacial and buried glacial outwash. Scott confirmed this observation by analyses of drillers logs from the study area. He also confirmed Wilson's (1979) observation that transmissivity decreases with depth (figure 2.1), noting:

"zones of relatively high transmissivity appear at different depths; the higher transmissivities are found within the upper 40 m of the gravels. These zones are interpreted as associations of broad, thin, ribbonlike aquifers following infilled channels. Wells tapping a specific depth range or zone of thin aquifers are widely scattered across the lower plains and a simple plot of transmissivity against absolute level of the well collar did not reveal any obvious pattern.

The data suggest that the aquifers are subparallel to the present-day land surface and are laterally continuous, at least near the coast. The former is as expected as the gradient of the land surface near the coast has changed little during the late Pleistocene. The lateral continuity of the aquifers also is not unexpected as the Rakaia River has the capacity to spread gravel across the entire lower fan when in flood and probably did so during late Quaternary times. Deep wells are most

common mid-way between the two rivers because the water table is deeper there. Wells tapping shallow high-yielding aquifers are restricted to the coastal region ..." (Scott, 1980 pp. 71-72).

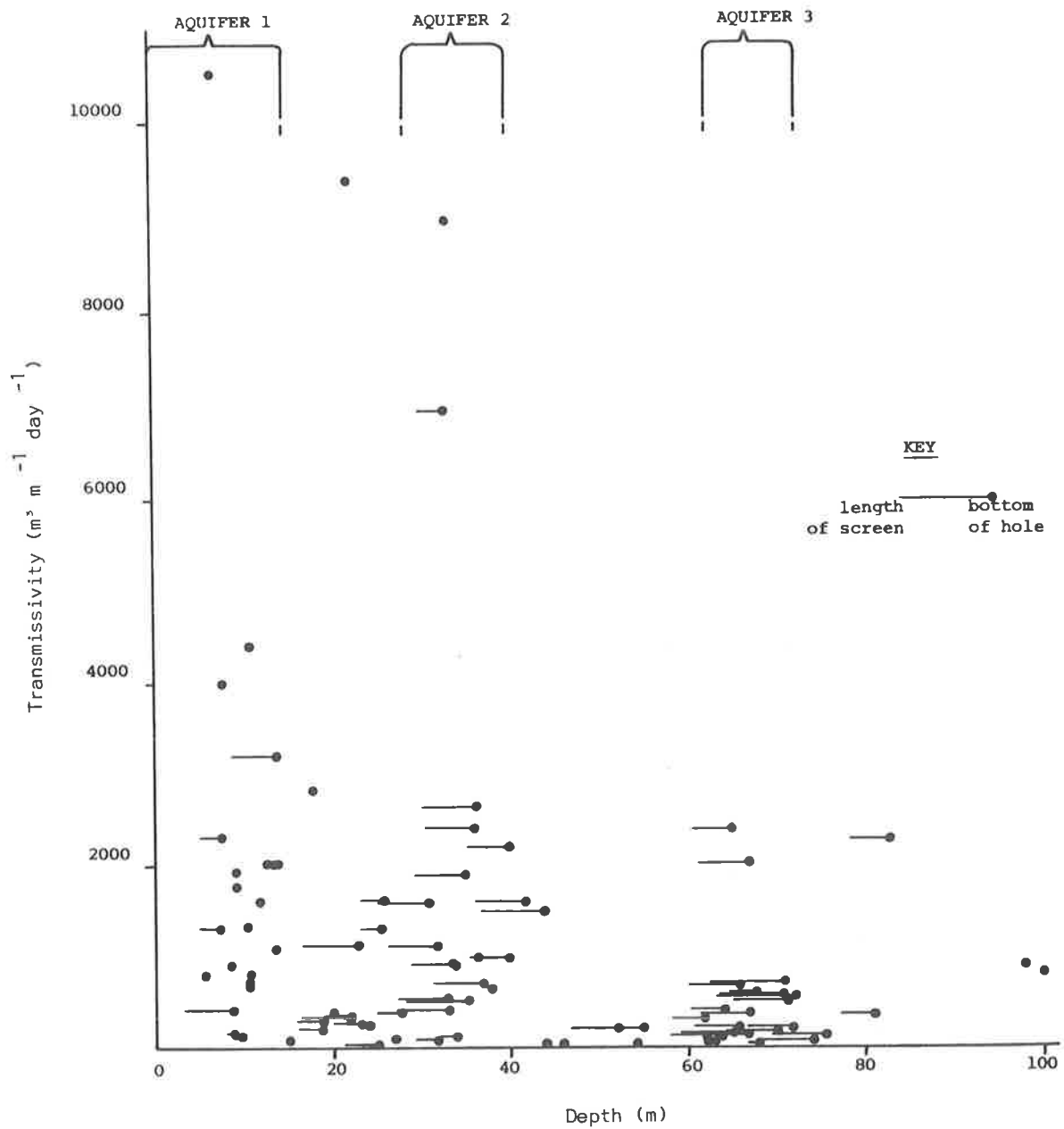


Figure 2.1 The variation of transmissivity with depth beneath the Canterbury Plains between the Ashburton and Rakaia Rivers (after Scott, 1980)

The discontinuous loess cover, which lies on the land surface in mid Canterbury, may also occur as aquitards or aquicludes at depth and could account for the large differences in static water-level which occur in some areas. Differences in water-level between two aquifers at a site can be as much as 20 m, whereas in other areas differences are very small. In all cases where static water-levels were measured in adjacent wells the level decreases with depth.

In discussing his observations Scott noted:

"The processes that led to the deposition of the gravel layers of the Canterbury Plains affect the direction of ground water movement and the hydraulic properties of the gravels. Since about late Wanganui times (Pliocene), rivers draining the Southern Alps have delivered gravel to the region of the Canterbury Plains (Oborn and Suggate, 1959) at greater and lesser rates ...

Ice advances have been accompanied by deposition of outwash fans that have coalesced to form the Canterbury Plains. Each advance has been followed by a retreat phase when the previous outwash deposits were dissected in the upper reaches of the fans (Soons and Gullentops, 1973; Wilson, 1973, 1976). During interglacial periods when sea levels were high and glaciers, if present, were mere vestiges near the Main Divide as today, outwash deposits near river gorges were dissected, reworked and redeposited downstream on the lower fan.

In general, the grain size of the bed material in braided rivers decreases, and the sorting increases, with distance from the sediment source (Bradley et al., 1972). Since the length of the interglacial and postglacial Rakaia River is about twice the length of the glacial Rakaia River, the sorting of interglacial sediments will be higher than that of glacial sediments for any given distance from the present-day coast, assuming that a glacier delivers unsorted material to the river source.

This model suggested that the better sorted and hence more permeable interglacial gravels serve as aquifers near the present coast. During the longer interglacial, alluvial deposits from adjacent river valleys in the Alps might have coalesced (or interdigitated) on the lower portions of the fans, ultimately forming a laterally continuous

veneer near the present coast. As sea level rose, the changing base level would have had the effect of increasing the thickness of the aquifers as the rivers adjusted to the new grade induced by the shifting storm beach." (Scott, 1980 pp. 72-73).

There is no evidence of a declining trend in the water table caused by pumping, nor of long-term increases of water-level caused by existing irrigation development.

2.2 WELL SPECIFIC CAPACITIES

Figure 2.2 maps wells for which hydraulic information is available. The information is expressed as specific capacity ($\text{litres sec}^{-1} \text{metre}^{-1}$) and the pattern revealed confirms the observations of Wilson (1976, 1979) and Scott (1980) that on the Canterbury Plains the permeability of the gravels decreases with distance from the coast and from the rivers.

The boundary between the Burnham (glacial outwash) and Springston (post-glacial) formations is depicted on figure 2.2 (Suggate, 1973). The higher yielding bores are mostly, but not exclusively, associated with the younger Springston gravels. The preponderance of essentially dry or low yielding wells in the upper plains area does not preclude the presence of irrigation water supplies, although the probability of finding good supplies is reduced. The great depth to water table in this area has discouraged systematic drilling to date. In any particular locality the wells tend to be of a similar depth, but even so the variation of specific capacity from well to well is apparent and it is not possible to predict well yields.

2.3 AQUIFER PUMPING TEST RESULTS

Transmissivities were obtained at seventeen sites by a variety of methods. Table 2.1 shows in detail the data gained from six pump tests in which both transmissivity and storage coefficient were obtained in standard tests where observation wells were used. Table 2.2 shows data gained from step-drawdown tests (Eden and Hazel, 1973; Clark, 1977) which do not permit calculation of storage coefficient. Although the number of transmissivity values is limited, the spatial pattern is similar to the specific capacities, i.e., highest values near the Rakaia River, along the coast and in the Wakanui area.

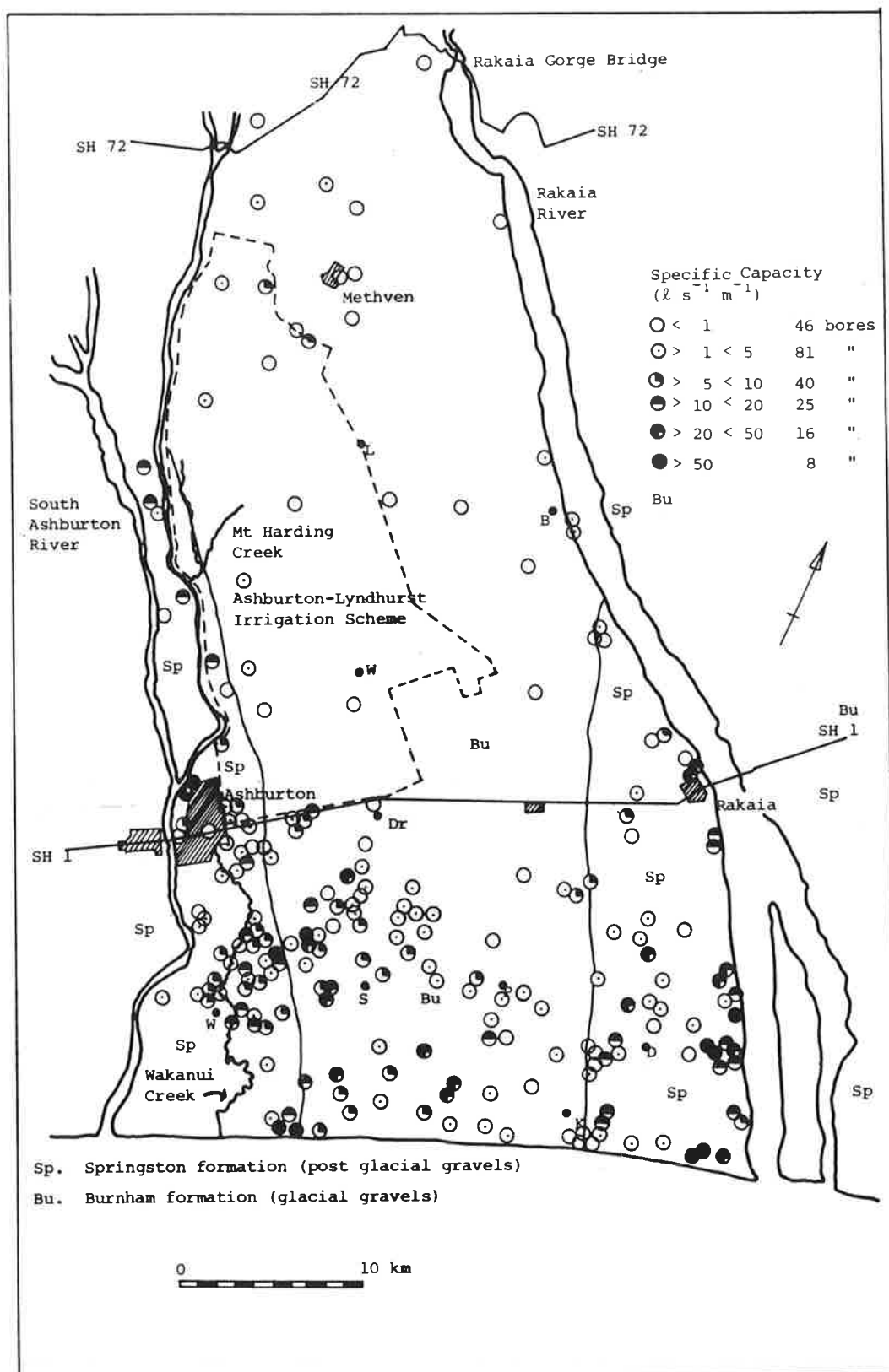


Figure 2.2 Specific capacity of wells in the study area

Table 2.1 Results of aquifer tests where observation wells were available

| Site and Map Ref. | Pumping Well | | | Observation Well | | | T (m ² d ⁻¹) | S | Method of Analysis |
|---|----------------------------|--|----------------|------------------|--------------|----------------------------|--|----------------------|--------------------|
| | Depth (m) | Rate (m ³ d ⁻¹) | Duration (hrs) | Name | Distance (m) | Depth (m) | | | |
| Walnut Ave S92:231128 | 18.0-19.5 and 27.0-28.5 | 2750 | 170.5 | New Railway | 100.0 | 17.0-18.5 and 22.5-24.0 | 1990 | 5x10 ⁻⁵ | Walton |
| Milton Rd S92:234083 | 33.0-39.0 | 2200 | 180.0 | B | 20.0 | 33.0-39.0 | 2240 | 1.1x10 ⁻⁵ | Walton |
| | | | | C | 50.0 | 33.0-39.0 | 2765 | 1.4x10 ⁻⁴ | |
| | | | | D | 100.0 | 33.0-39.0 | 2795 | 1.4x10 ⁻⁴ | |
| | | | | E | 34.9 | 33.0-39.0 | 2930 | 1.2x10 ⁻⁴ | |
| | | | | F | 82.0 | 33.0-39.0 | 3050 | 1.2x10 ⁻⁴ | |
| | | | | G | 151.1 | 33.0-39.0 | 3420 | 2.2x10 ⁻⁴ | |
| Elgin Rd S92:275081 | 17.1-23.2 | 1900 | 174.0 | B | 9.75 | 17.5-23.5 | 1870 | 5.2x10 ⁻⁴ | Walton |
| | | | | C | 24.8 | 17.5-23.5 | 1890 | 6.8x10 ⁻⁵ | |
| | | | | D | 50.0 | 17.5-23.5 | 2050 | 7.6x10 ⁻⁵ | |
| | | | | E | 15.05 | 17.5-23.5 | 1490 | 2.7x10 ⁻⁴ | |
| | | | | F | 39.9 | 17.5-23.5 | 1980 | 4.6x10 ⁻⁵ | |
| | | | | G | 79.9 | 17.5-23.5 | 2190 | 4.5x10 ⁻⁵ | |
| West Bros S92:369031 Tested by SCRWB | 37.2 | 1831 | 3.0 | WW | 39.5 | 30.8-37.2 | 3840 | 3.5x10 ⁻⁶ | Walton |
| | | | | WS | 20.0 | 31.1-37.2 | 3670 | 1.7x10 ⁻⁶ | |
| | | | | WW,WS | - | - | 4340 | - | |
| | | | | WW,WS | - | - | 4160 | - | |
| | | | | WW,WS | - | - | 4450 | - | |
| Kingsbury S93:513093 Tested by SCRWB | 25.9 | 2800 | 72.0 | KW | 45.4 | 26.0 | 995 | 3.1x10 ⁻² | Walton |
| | | | | KE | 18.05 | 26.0 | 1090 | 4.6x10 ⁻² | |
| | | | | KS | 75.8 | 26.0 | 3480 | 2.4x10 ⁻¹ | |
| | | | | KW | 45.4 | 26.0 | 3300 | - | Hantush-I |
| | | | | KE | 18.05 | 26.0 | 3200 | - | |
| | | | | KS | 75.8 | 26.0 | 3580 | 1.5x10 ⁻⁴ | |
| | | | | KE,KW,KS | - | - | 2960 | - | Hantush-II |
| | | | | KE,KW,KS | - | - | 3000 | - | Hantush-III |
| Leadley S92:314084 | 36.6 | 3925 | 18.7 | SCCB | 645.0 | - | 2740 | 6x10 ⁻⁴ | Chow |

Table 2.2 Results of step-drawdown aquifer tests.

| Site and Map Reference | Screen Depth (m) | Transmissivity (m ² day ⁻¹) |
|---|-------------------------|---|
| Walnut Ave, Ashburton S92:231128 | 18.0-19.5 and 27.0-28.5 | 1800 |
| Milton Rd S92:234083 | 33.0-39.0 | 2300 |
| Elgin Rd S92:275081 | 17.1-23.2 | 1500 |
| West St, Ashburton S92:230127 | 17.0-18.5 and 22.5-24.0 | 1825 |
| Rakaia Township A S93:472293 | 10.5-13.5 | 1940 |
| Rakaia Township B S93:472292 | 41.0-44.0 | 1900 |
| Rakaia Golf Course B S93:499257 | 12.0-15.0 | 6800 |
| Rakaia Golf Course C S93:499256 | 35.0-41.0 | 900 |
| Dobsons Ferry Rd A S93:573157 | 5.5-8.5 | 14 000 |
| Dobsons Ferry Rd B S93:574158 | 32.0-35.0 | 733 |
| Winters Rd (Hewitt) S92:427063 | 59.0-74.0 | 7000 |
| Allen's bore : Dorie S93:503182 | 38.7-43.3 | 1190* |
| Doak's bore : Elgin S92:332077 | ? -33.0 | 2660* |
| Butterick's : Elgin S92:290060 | 28.7-35.7 | 1770* |
| Armstrong's bore : Dorie S93:470167 | 46.0-49.0 | 1000 |
| Ward's bore : Newlands S92:323144 | 67.4-72.0 | 930 ⁺ |
| Moore's bore : Wrights Rd S92:347026 | 32.0-35.0 | 1200 ⁺ |
| Leadley's bore : Seafield S92:313086 | 31.4-35.1 | 1000 ⁺ |

+ Data supplied by SCRWB

* Data supplied by T T McMillan and Son, Well Drillers

At Walnut Ave, Milton Rd and Elgin Rd both standard and step-drawdown tests were done to check the reliability of the latter. In all three, the transmissivities derived from the step-drawdown tests were about 20% lower than those from the standard tests. This degree of approximation is acceptable, given the many uncertainties in this kind of analysis.

At Rakaia Township, Rakaia Golf Course, and Dobsons Ferry Rd, step-drawdown tests were done in adjacent wells of different depths, and marked differences of transmissivity were measured (table 2.2). At the township and golf course sites, a 20 m thick aquiclude separated the two pumping levels and the different transmissivities were anticipated. At Dobsons Ferry Rd, although the well log indicated apparent aquitards, there was no significant change in static water-level at any depth during drilling, therefore all levels were hydraulically connected in the vicinity. Nevertheless, the transmissivity over the depth interval 5.5-8.5 m was about $14\ 000\ \text{m}^2\ \text{day}^{-1}$, whereas at the 32-35 m level it was only $730\ \text{m}^2\ \text{day}^{-1}$. There were other water bearing layers at 13.75-17.5 m and 19.0-20.75 m, which would all contribute to the transmissivity of the total formation.

The gravels of the Canterbury Plains form a vertical sequence of layers of varying hydraulic conductivity (see section 2.1). The layers of higher hydraulic conductivity are separated by aquitards of lower conductivity which, nevertheless, may be capable of transmitting large volumes of water horizontally because of their considerable total thickness. The values in tables 2.1 and 2.2 were obtained from tests on one interval of this vertical sequence, and therefore do not represent the ability of the full depth of gravels to transmit water.

Measured storativities (table 2.1) are typical of confined or semi-confined aquifers, with the exception of Kingsbury's which is unconfined.

2.4 SURFACE WATER - GROUND WATER INTERACTIONS

Water-level recorders located in wells close to the Rakaia and Ashburton Rivers have provided some understanding of the response of aquifers to flood events in the rivers. Instrument locations and well details are given in table 2.3. Examination of the water-level records from these wells has confirmed the type of aquifer deduced from the well logs.

2.4.1 Rakaia River

A river level record was obtained at Rakaia Rail Bridge and compared to records from the wells listed in table 2.3. All the unconfined aquifers respond to flood events in the Rakaia River, which indicates that hydraulic connections exist (figures 2.3, 2.4, 2.5). Furthermore, since aquifer head is less than river head, some recharge will occur (see section 3.2.4).

Table 2.3 Ground water level records used in examining interaction of aquifer system and rivers

| Site | Map Ref. | Aquifer type | Depth (m) |
|----------------------|------------|-------------------|-----------|
| Rakaia River Bed | S82:431321 | Unconfined | 6.0 |
| Caunters | S82:432313 | Log not available | |
| Rakaia Town A | S93:472293 | Unconfined | 13.5 |
| Rakaia Town B | S93:472292 | Confined | 44.0 |
| Rakaia Golf Course B | S93:499257 | Unconfined | 15.4 |
| Rakaia Golf Course C | S93:499256 | Confined | 41.3 |
| Dobsons Ferry Rd A | S93:573157 | Unconfined | 8.5 |
| Dobsons Ferry Rd B | S93:574158 | Semi-confined | 35.0 |
| River Rd | S92:255047 | Unconfined | 3.6 |
| Wilsons Rd | S92:265031 | Unconfined | 5.6 |

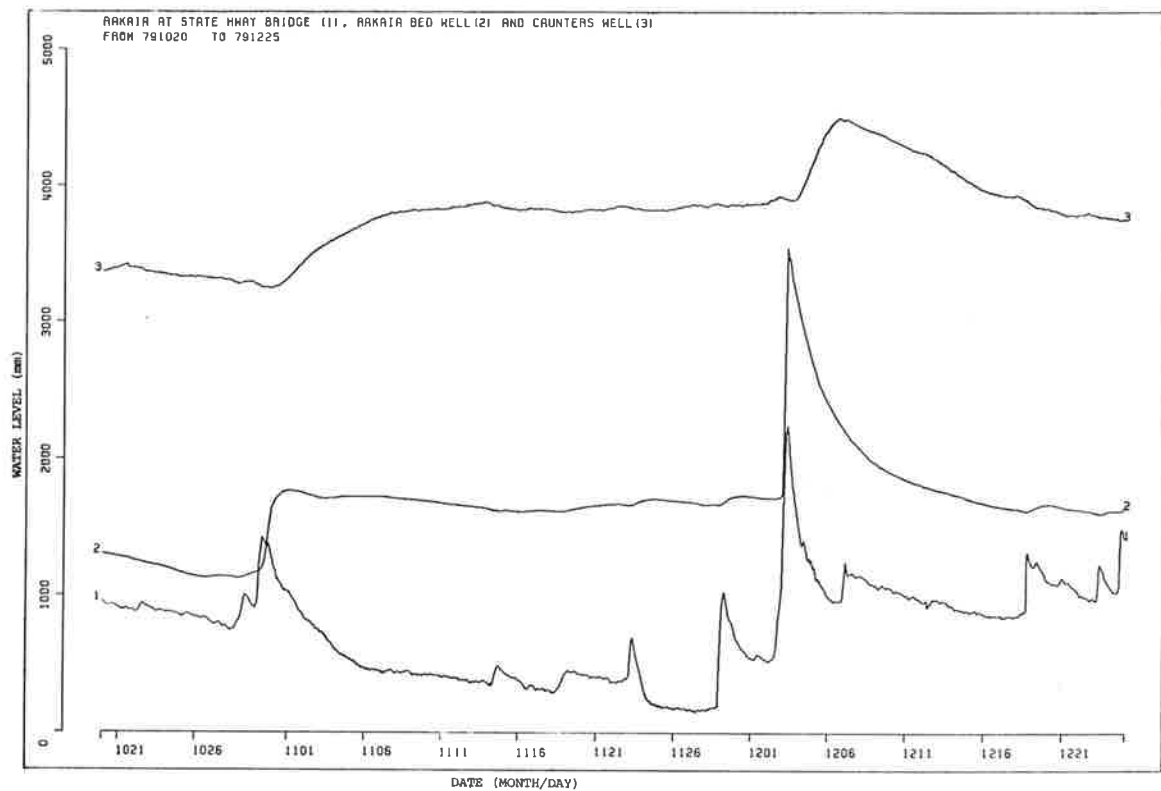


Figure 2.3 Water-level records in the Rakaia River (1), Rakaia River bed (2) and Caunters well (3)

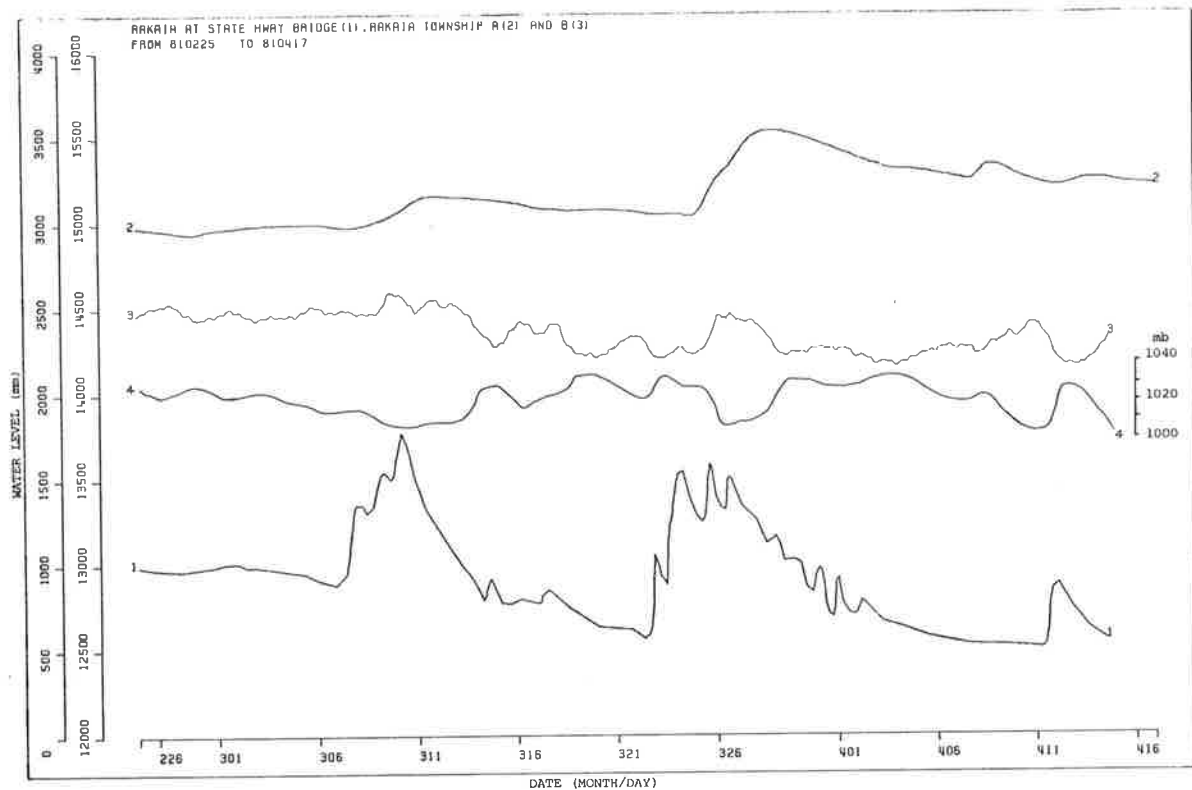


Figure 2.4 Water-level records in the Rakaia (1), adjacent bores at Rakaia Township (2 and 3) and barometric pressure at Christchurch (4)

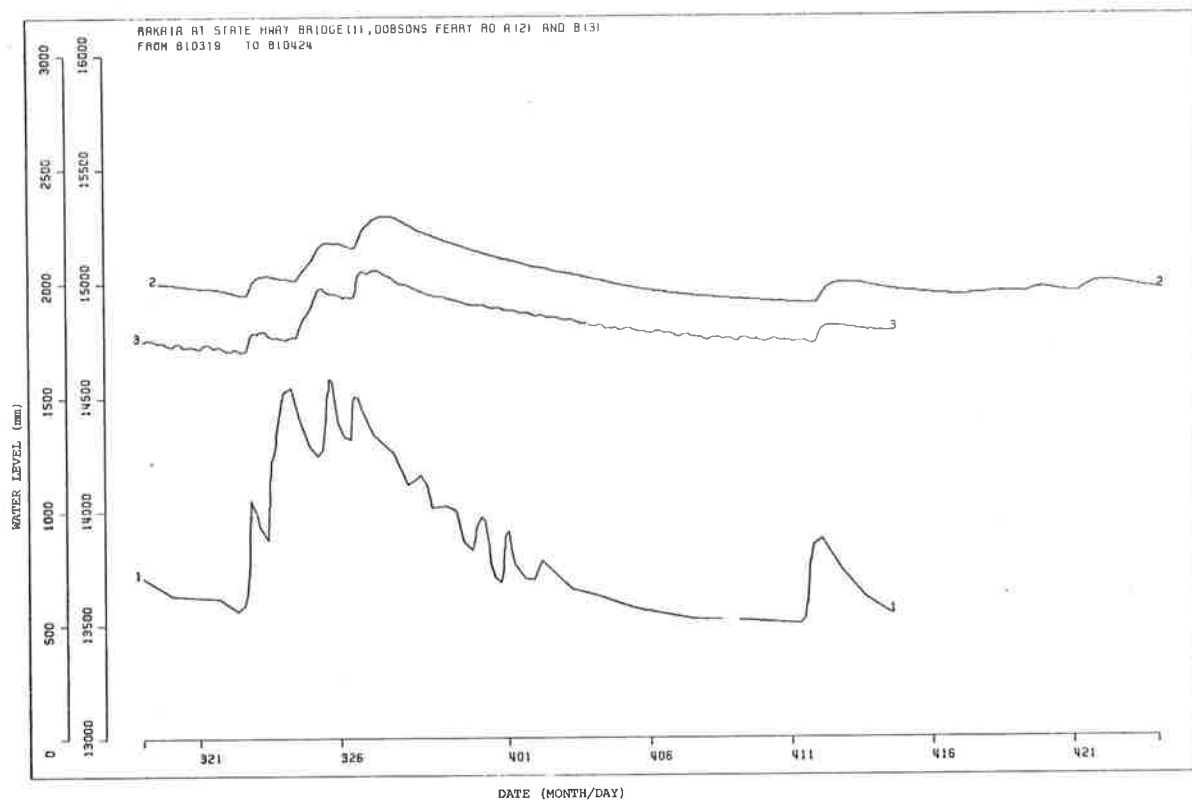


Figure 2.5 Water-level records from Rakaia River (1), and bores at Dobsons Ferry Rd (2 and 3)

The confined aquifers at Rakaia Township and golf course do not respond to river events. The short-term fluctuations in the records are caused by changes of barometric pressure (figure 2.4). This is a phenomenon which is observed only in confined aquifers. This observation, together with the large head differences between confined and unconfined aquifers at the township, golf course and a further well at Northbank Rd (S93:528293), strongly suggest that a continuous aquiclude exists beneath the full river width. Wells drilled into the river bed near the golf course also encountered the top of the aquiclude. The aquiclude must extend from a point somewhat upstream of the township to below the golf course, a distance of at least 6 km. Borelog information suggests that this aquiclude also extends several kilometres laterally from the south bank of the Rakaia, and thus protects the river from the effects of varying piezometric levels in the deeper aquifers.

At Dobsons Ferry Rd the water-level records confirm the absence of a confined aquifer, as had been deduced from the drillers logs. Both shallow and deep bores respond similarly to flood events (figure 2.5).

2.4.2 Ashburton River

Water-level records were obtained on the Ashburton River at State Highway 1 (SH 1) and also from bores in River Rd and Wilsons Rd (figure 2.6). The River Rd bore was within 100 m of the river and responded closely to freshes and floods, whereas the Wilsons Rd bore, about 1500 m from the river, did not. It did, however, show response to a nearby drainage ditch which filled during heavy local rainfall. Both wells were less than 6 m deep (table 2.3).

Shallow piezometers were also installed along Milton Rd and Wakanui School Rd in transects at right angles to the river, 300 and 638 m long, respectively. The piezometric gradients along these lines were very flat, 0.0003 and 0.0002, respectively. Thus, despite the high transmissivity in this unconfined aquifer (table 2.1) the loss of water from the Ashburton River under natural ground water levels would be small.

2.4.3 River Flow and Recharge

The pressure waves generated in the unconfined aquifers by flood waves in the rivers show that the process is one of filling the aquifers. That is, the recession from the peak water-level in the aquifers is much slower than that from the open channel flood wave. As a corollary of this, flood waves of a

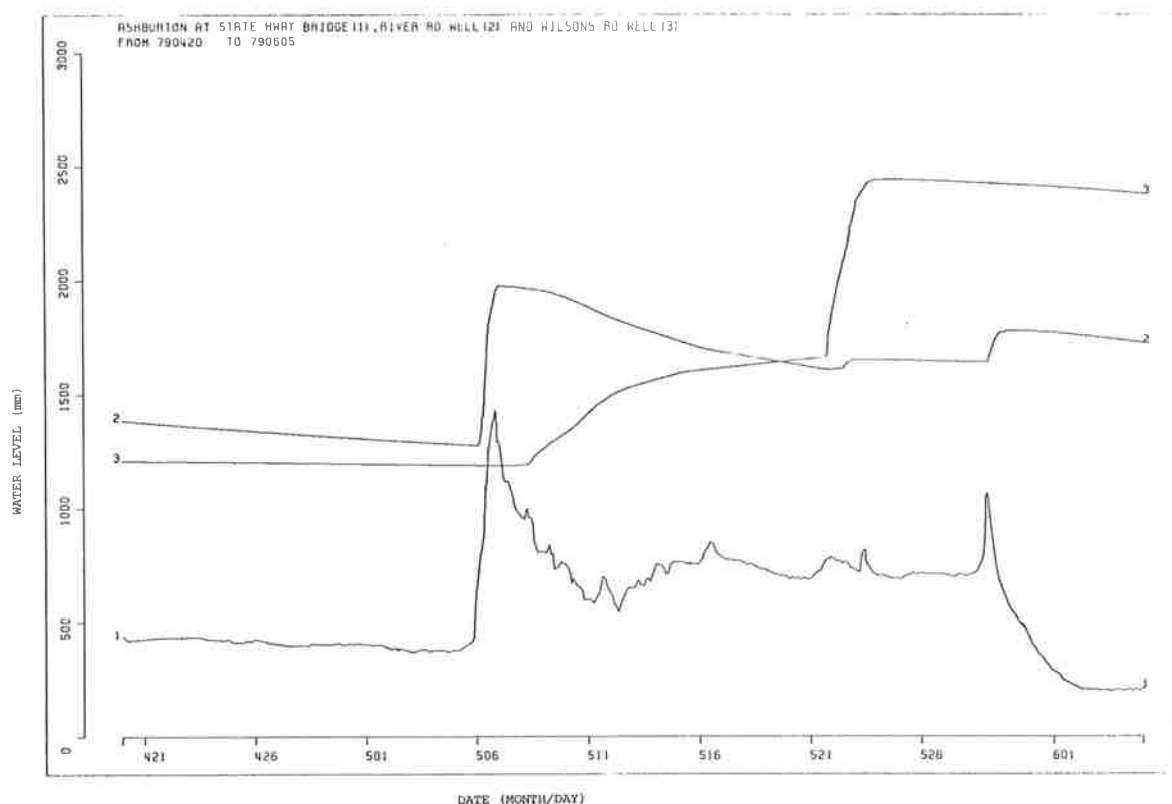


Figure 2.6 Water-level records from the Ashburton River (1) and adjacent bores at River Rd (2) and Wilson Rd (3)

given magnitude generate pressure waves of different amplitude, depending on the antecedent water-level in the aquifer. High antecedent aquifer levels result in small pressure waves and vice versa (figures 2.3, 2.4, 2.5, 2.6). The tentative conclusion to be drawn from this is that the losses from the rivers to the aquifers are not likely to be proportional to river flows, as has been suggested (Stephen, 1972), but will also depend upon conditions within the aquifers.

2.5 PIEZOMETRIC SURFACES

Piezometric surveys were done in conjunction with the SCRWB on three occasions, May and October 1978 and April 1982. The 1978 surveys were outside the irrigation season and should represent reasonably natural conditions. The 1982 survey was right at the end of the season and may be slightly lower than natural levels. North and east of a line joining Rakaia, Winchmore Irrigation Research Station and Methven there are insufficient data to permit contouring.

Figure 2.7 shows the piezometric map from May 1978, which is typical. From this, the general lines of flow of ground water have been inferred. There is an indication of loss from the Rakaia River between SH 1 and Dobsons Ferry Rd.

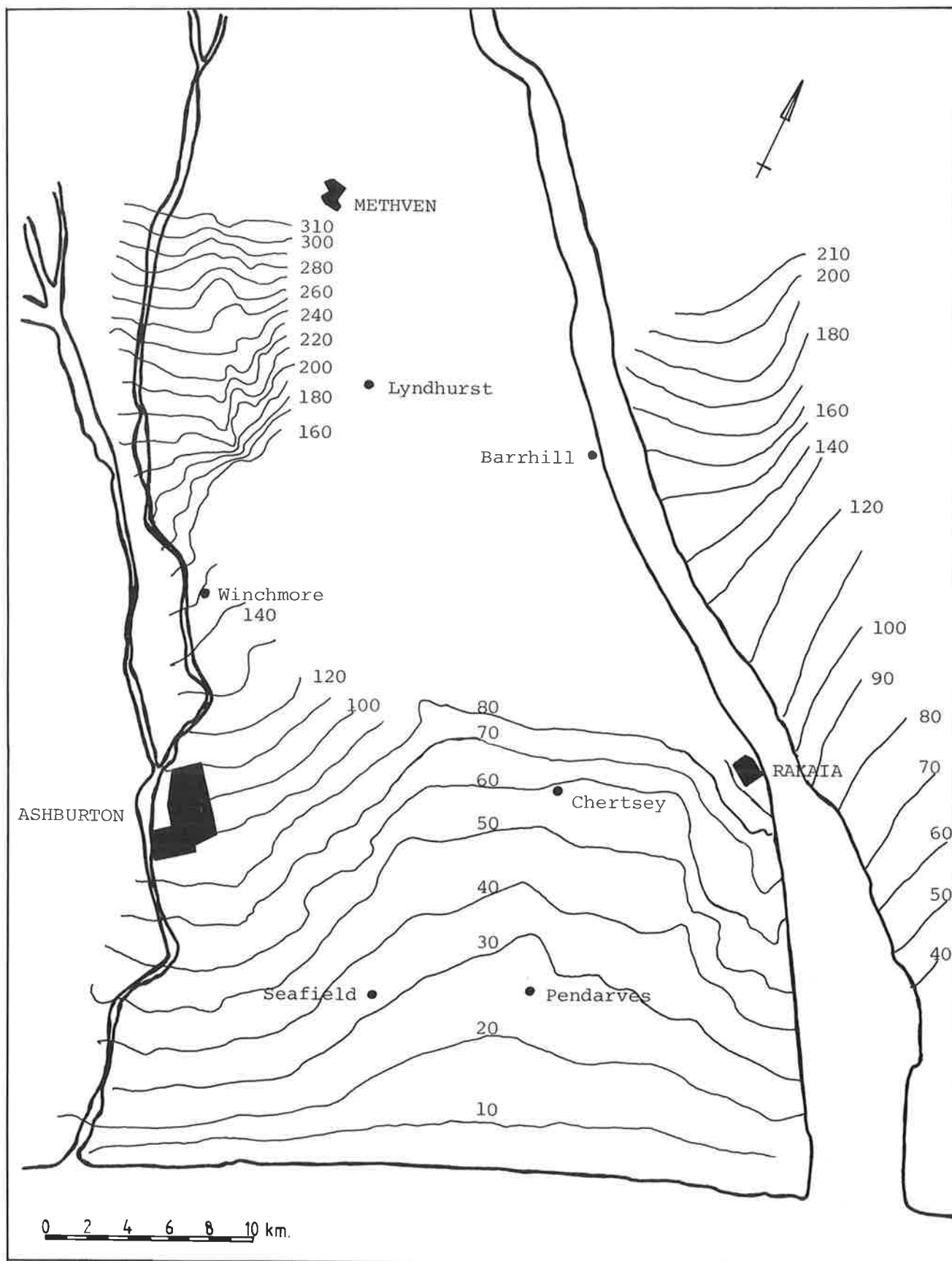


Figure 2.7 Piezometric contours for May 1978 (metres above mean sea level)

There is, however, no clear indication of loss from the Ashburton River, except perhaps the North Ashburton in the reach above and below Winchmore. These observations are supported by flow gaugings of the rivers (see sections 3.2.1 and 3.2.2).

Figure 2.8 shows the differences in piezometric level between the extreme high of October 1978 and the very low levels of April 1982, indicating the range of natural fluctuations.

2.5.1 Depth to Standing Water-Level

Because of the generally flat terrain, contours of depth to standing water-level can be drawn. Figure 2.9 depicts the depths measured in April 1982. These were the greatest depths recorded since the first comprehensive water-level data collection was begun by the SCRWB in 1974.

The apparent anomaly near the mouth of the Wakanui Creek is due to the drop in land surface elevation from the plain proper into the Wakanui Valley.

2.6 LONG-TERM WATER-LEVEL RECORDS

The construction of the Rangitata Diversion Race (RDR) and the border-strip irrigation schemes in the post World War II period aroused concern about possible problems from deep drainage of waste water. In an attempt to monitor these effects a network of observation bores was sunk and these have been monitored on a monthly basis, some since 1944.

Records of depth to ground water for three bores in, or near the ALIS have been compiled and plotted (figure 2.10). Well No. 49 (Longs Rd, Map Ref. S82:080442) is above the ALIS and would not be influenced by irrigation. Well No. 54 (Lauriston, Map Ref. S92:200264) is in the middle, and No. 41 (Charing Cross, Map Ref. S92:350087) is 10 km beyond the downstream end of the scheme where water-levels might be affected by high drainage inputs.

Rainfall data at Winchmore Irrigation Research Station are plotted on figure 2.10 as cumulative departure from the mean in order to display the long-term rainfall pattern.

The Longs Rd, Lauriston and Charing Cross records show the behaviour of wells which terminate at 18.3, 25 and 30.5 m, respectively.

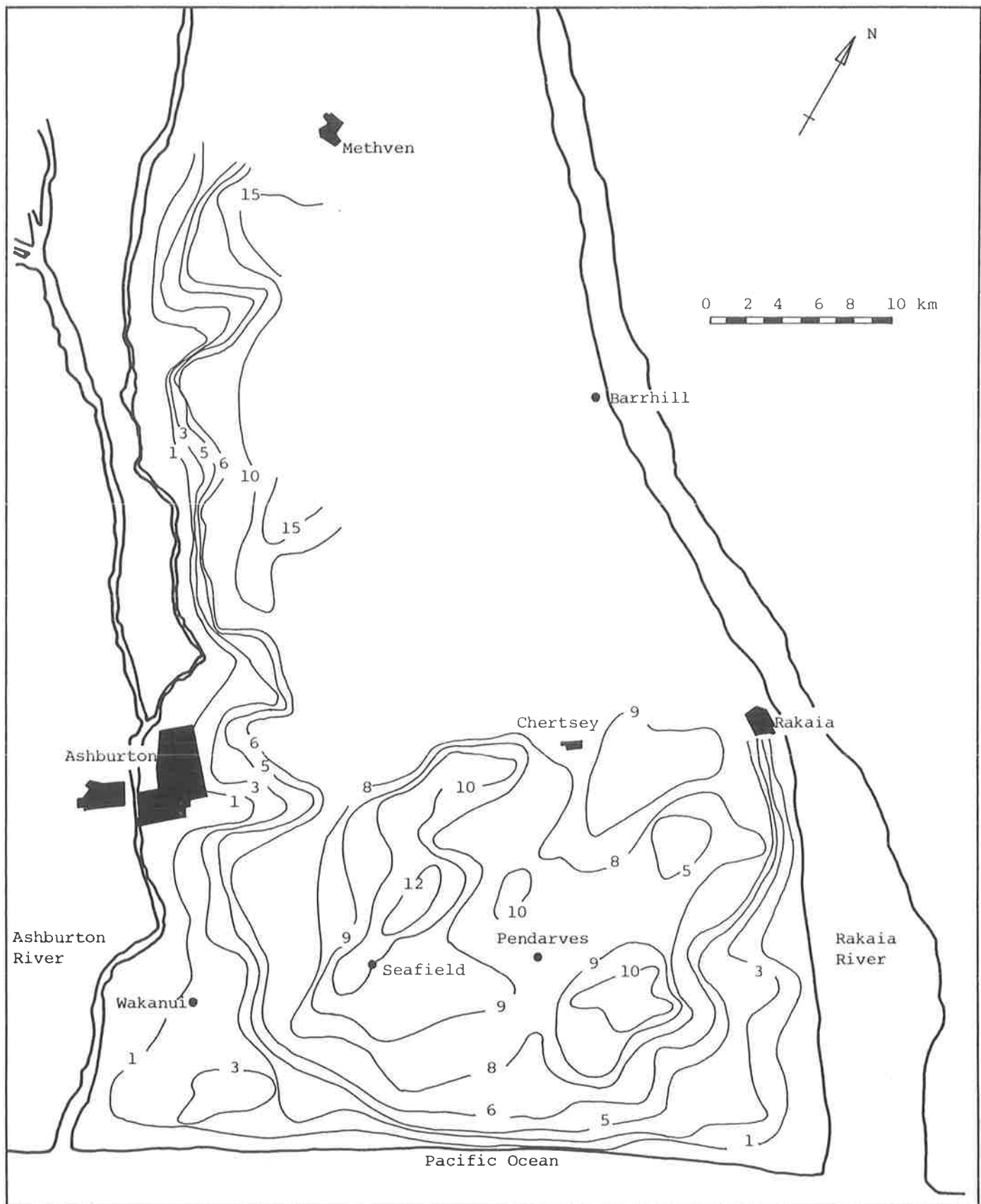


Figure 2.8 Variation of standing water-level (m) between October 1978 and April 1982

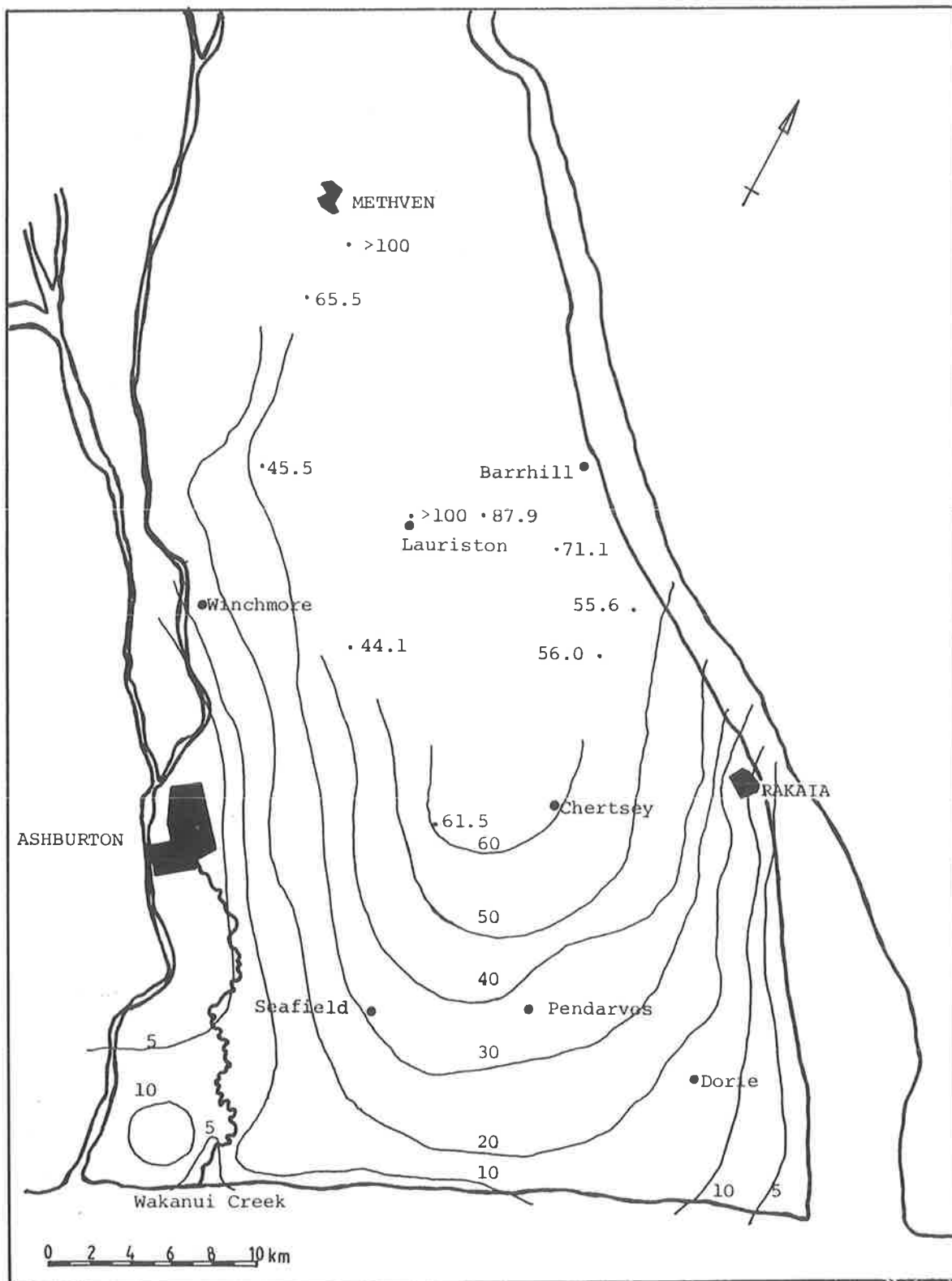


Figure 2.9 Depth to standing water-level, April 1982 (metres below ground)

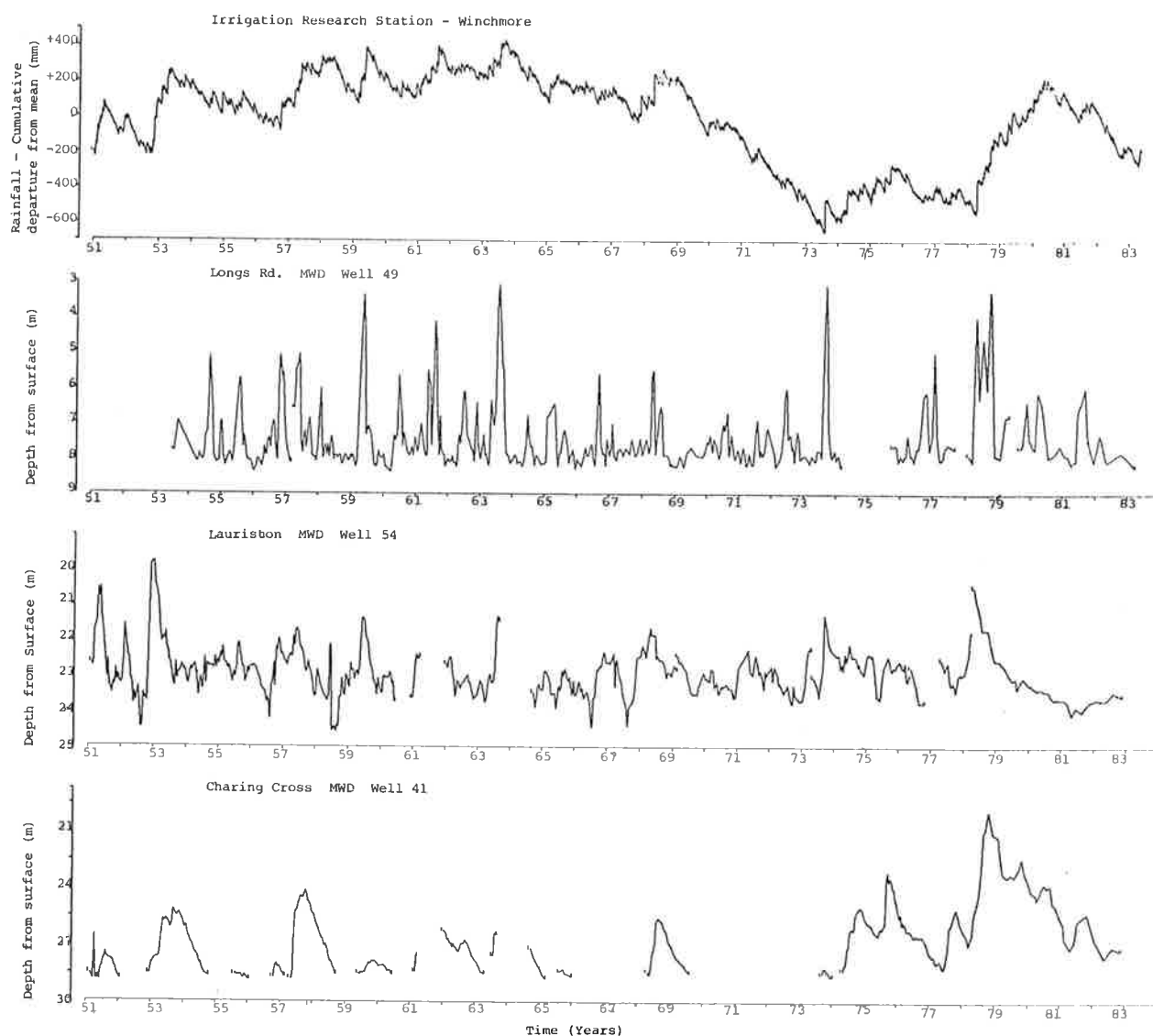


Figure 2.10 Long-term rainfall at Winchmore Irrigation Research Station and ground water levels at Longs Rd, Lauriston and Charing Cross

The Longs Rd well responds sharply to short wet periods, and perhaps even to individual rain events, although the monthly readings do not show this conclusively. The well behaves as though the aquifer at that point has low storativity (i.e., is confined) and in fact the well log suggests that this could be the case. The Lauriston well behaviour is more subdued, probably because low summer levels are precluded by the application of irrigation water. At Charing Cross the well response is to longer term rainfall patterns and the water-level correlates with the rainfall cumulative departure from the mean.

The steep increase in water sales for the ALIS, plotted in figure 2.11, indicates larger irrigation return flows. None of the wells show any long-term response either to increased application of irrigation water or to increased pumping from the aquifers. Rainfall variation dominates ground water levels.

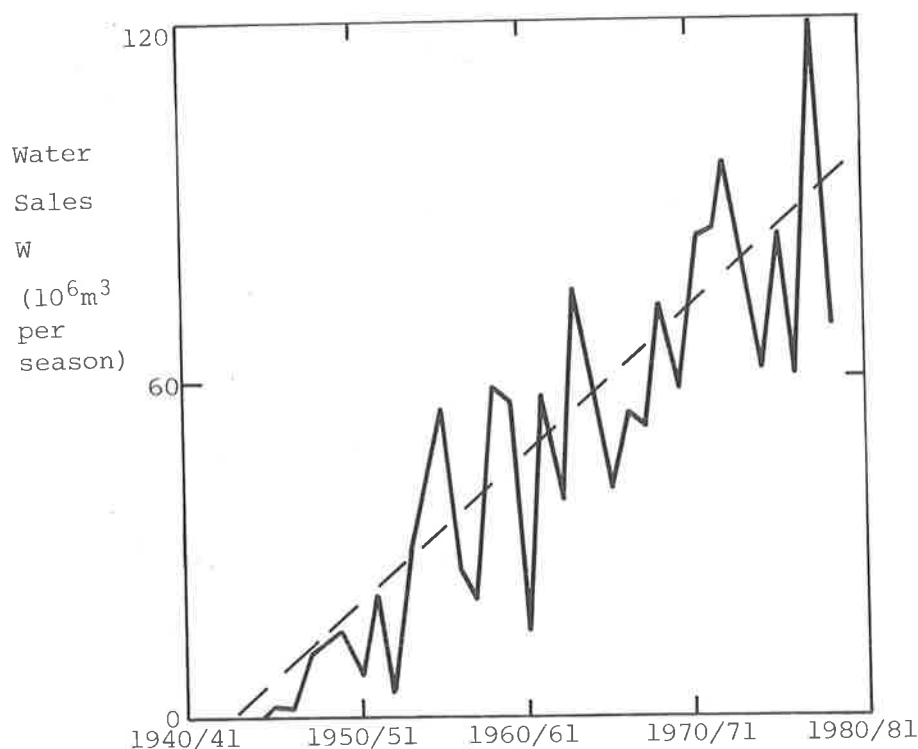


Figure 2.11 Water sales on the ALIS have increased $2.62 \times 10^6 \text{ m}^3 \text{ yr}^{-1}$ since 1944 (after Maidment et al., 1980)

2.7 HYDROCHEMISTRY

Knowledge of the spatial and temporal distribution of chemical constituents in a water-table aquifer is valuable in understanding the sources of recharge, flow paths, relationships between land use and water quality, and for predicting the impact of future changes in land use. The hydrochemistry of the area was studied by Burden (1982) as part of this investigation and is summarised below.

Figure 2.12 shows the location of 26 wells from which monthly water samples were taken and analysed over a one year period. On the basis of these analyses the aquifer has been divided into four chemical zones.

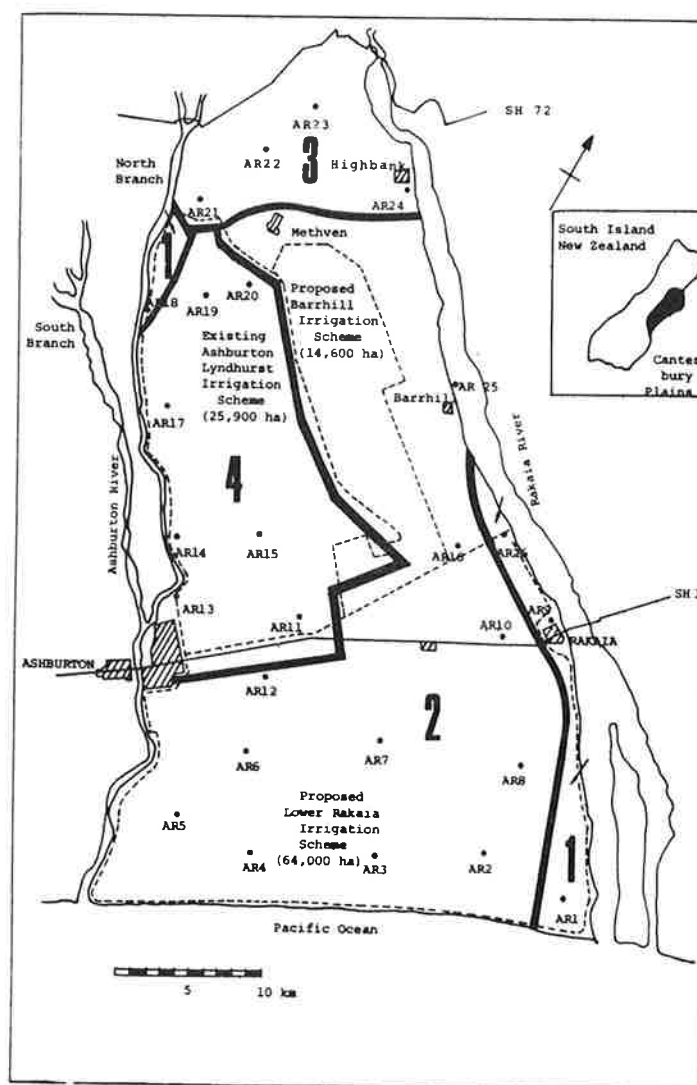


Figure 2.12 Location of wells used in water quality survey and chemical zones deduced from the results (after Burden, 1982)

2.7.1 Zone 1. Non-irrigated, Riparian Recharge Areas

Ground water in zone 1 closely reflects the chemical character of the adjacent rivers. In general, it has low total dissolved solids. Proportionately, however, Ca^{++} and HCO_3^- are high in relation to Na^+ , Cl^- and nitrate-nitrogen ($\text{NO}_3\text{-N}$). Although $\text{NO}_3\text{-N}$ concentrations are low, the effect of nitrate leaching from grazed pasture is already evident. Zone 1 areas coincide with river reaches in which flow gaugings indicated loss to ground water.

2.7.2 Zone 2. Non-irrigated, Non-riparian Areas

The chemistry of shallow ground water in this area indicates that the major source of recharge is drainage from non-irrigated pasture, either directly above or up-flow of the sampling point. Nitrate-nitrogen in ground water derives principally from the oxidation and subsequent leaching of nitrogen species in stock urine, and sulphate derives from superphosphate fertilizer. Both these species increase in zone 2. Quin (1979) estimated that the leaching process under these conditions would produce concentrations of $\text{NO}_3\text{-N}$ between 4 and 10 g m^{-3} . Since concentrations such as these are already found in the shallow ground water, this is indirect evidence that recharge in this zone is almost entirely from drainage of excess rainfall. Na^+ and Cl^- derived from rainfall are high near the coast but decrease rapidly inland, as would be expected.

2.7.3 Zone 3. Non-irrigated Piedmont Area

Zone 3 recharge is by drainage from non-irrigated pasture and runoff from the slopes of Mount Hutt. The chemical character of zone 3 ground water is similar to that of zone 2, except that Na^+ , Mg^{++} , SO_4^{--} and Cl^- are lower, because of the distance from the sea, and so is $\text{NO}_3\text{-N}$. Conversely, the ratio of $\text{NO}_3\text{-N}/\text{Cl}^-$ is higher. Nitrate-nitrogen concentrations are reduced because this is an area of high rainfall and drainage, and even though stocking rates are high, the drainage is dilute. The $\text{NO}_3\text{-N}/\text{Cl}^-$ ratio remains high because of exceptionally low chloride content. Overall ionic concentrations are low.

2.7.4 Zone 4. Border-strip Irrigated Lands

Recharge in this area is from both irrigation return water and drainage from precipitation, in the approximate ratio 60:40 (see sections 3.1 and 3.2) and this combined drainage dominates the quality of the shallow ground water (<30 m below water table). Shallow zone 4 ground water is similar in character to zone 2 water, except that Na^+ and Cl^- are lower and $\text{NO}_3\text{-N}/\text{Cl}^-$ is higher. Na^+ and Cl^- are lower because the irrigation water applied is taken from the Rangitata River, which is low in these ions. The low Cl^- level and the extra $\text{NO}_3\text{-N}$ leached under irrigation (Quin, 1979), lead to a higher $\text{NO}_3\text{-N}/\text{Cl}^-$ ratio. Overall, the total dissolved solids in ground water below the irrigated area is less than that below the dry land, because of the diluting effect of the extra drainage from the irrigation water.

2.7.5 Changes of Water Quality with Depth

In zones 2 and 4 (away from rivers and hills), the recharge is overwhelmingly by drainage from the surface, carrying with it dissolved constituents. Thus, ground water at the water table has a composition very similar to that of the subsurface drainage, whereas at greater depths the water may be either older, or have a larger component of recharge from rivers. The deeper water, therefore, has lower $\text{NO}_3\text{-N}$ and Cl^- but higher HCO_3^- than that near the water table (figure 2.13).

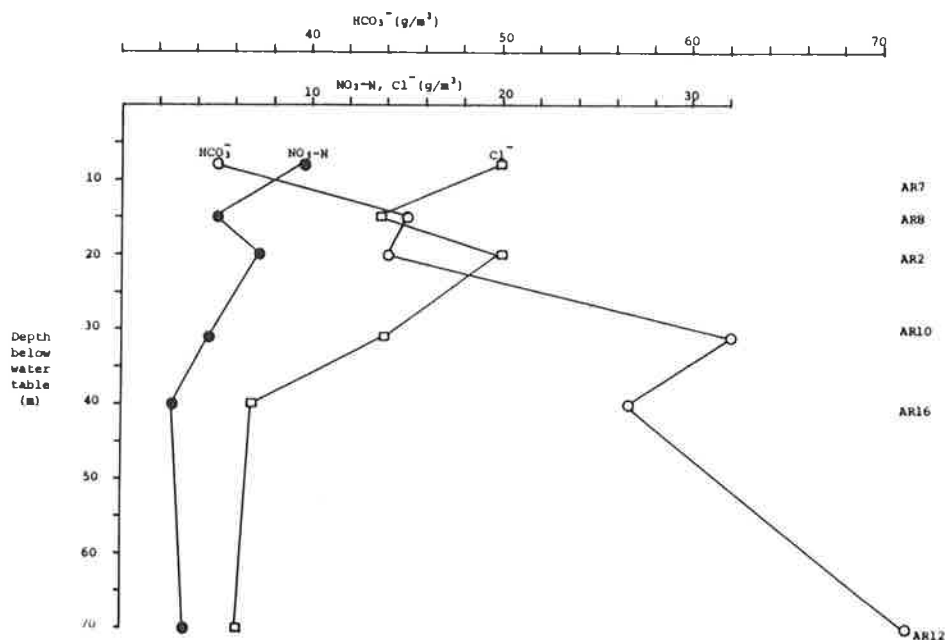


Figure 2.13 Changes in ground water depth in zone 2 wells. Concentrations are means of up-to ten values (after Burden, 1982)

2.7.6 Seasonal Changes of Water Quality

Figure 2.14 shows characteristic seasonal changes of $\text{NO}_3\text{-N}$ in shallow and deep wells for both irrigated and non-irrigated areas, compared with estimates of sub-surface drainage for the same time span. Shallow wells showed a seasonal trend coinciding with the pattern of drainage; deep wells did not. Nitrate-nitrogen levels in wells in irrigated areas tended to peak in summer, whereas those in non-irrigated areas and near influent rivers peaked in winter. Depth from ground level to water table has some effect on seasonal variations since peaks are transmitted rapidly from subsoil to water table in areas where the water table is close to the surface (i.e., near rivers).

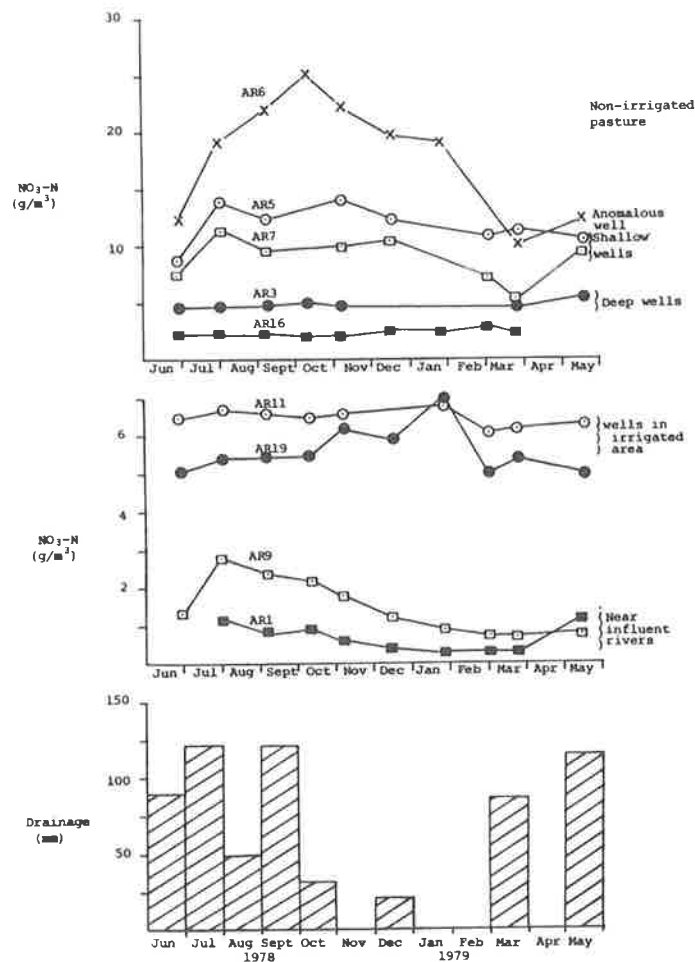


Figure 2.14 Seasonal changes of nitrate-nitrogen in shallow and deep wells compared with estimates of subsurface drainage (after Burden, 1982)

In areas away from the rivers, the greater thickness of unsaturated gravels tends to adsorb and smooth seasonal peaks. Similarly, where wells draw water from deep below the water table, the process of downward dispersion from the water table homogenizes the seasonal chemical loadings of the aquifer.

The seasonal variations of $\text{NO}_3\text{-N}$ were caused by changes in the volume of drainage reaching the water table and not by changes in concentration (Quin and Burden, 1979). The temporal variation of other major ions (i.e., Cl^- , SO_4^{--} , Na^+ , Ca^{++} , K^+ , and Mg^{++}) generally followed that of $\text{NO}_3\text{-N}$. Quin (1979) estimated that irrigation of pasture produces a drainage water with a concentration of $\text{NO}_3\text{-N}$ of $14\text{-}17 \text{ g m}^{-3}$, therefore as irrigation expands, the nitrate concentrations in the ground water near the water table can be expected to rise significantly.

3 : SYSTEM INPUTS AND OUTPUTS

The significant inputs and outputs to the system are:

- (i) Deep drainage from precipitation and irrigation return water.
- (ii) Recharge from rivers.
- (iii) Deep drainage from leaky stock races.
- (iv) Pumpage.
- (v) Spring flows.
- (vi) Submarine leakage.

A complete water balance cannot be attempted because of the unmeasured seepage across the seaward boundary of the study area.

3.1 DEEP DRAINAGE FROM PRECIPITATION AND IRRIGATION

3.1.1 Soil Moisture Model

A soil moisture model was used in a simple water budget to route excess rainfall through the soil profile to produce drainage. The soil was assumed to have a uniform water holding capacity over the model area and surface runoff was ignored. Rainfall and actual evapotranspiration were used to calculate soil moisture levels at daily time steps using the relationship

$$S_i = S_{i-1} + R_i + I_i - E_i - D_i \quad 3.1$$

where S_i is the soil moisture level at the end of day i and R_i , I_i , E_i and D_i are rainfall, irrigation, actual evapotranspiration and drainage below the soil moisture zone for day i , all in units of length. Equation 3.1 was used with the constraints that the calculated soil moisture level could not exceed the specified field moisture capacity nor fall below permanent wilting point. Drainage was calculated from rainfall excess after the previous day's soil moisture level had been adjusted by the rainfall, irrigation and evapotranspiration depths.

Actual evapotranspiration was calculated from potential evapotranspiration using an empirical relationship adapted from the irrigation demand assessment model described by Power, Broadhead and Hutchinson in a Ministry of Works and Development, Christchurch Hydrology Centre unpublished report WS 182. The

relationship takes account of the soil moisture condition,

$$E_i/PE_i = 1 \text{ for } S_{i-1} > W(1 - 0.67/PE_i)$$

and for lower soil moisture levels

3.2

$$E_i/PE_i = (0.2 + S_{i-1}/W)/(1.2 - 0.67/PE_i)$$

where PE_i is the potential evapotranspiration depth for day i and W is the maximum available soil moisture for the particular soil (e.g., 50 mm). Equation 3.2 allows evapotranspiration to continue at the potential rate for high soil moisture levels. Lower soil moisture levels cause a reduction in the actual evapotranspiration rate below the potential rate and this reduction is greatest when the potential evapotranspiration rate is high. This effect is illustrated in figure 3.1 and is intended to allow for the fact that plant transpiration ability can limit high potential evapotranspiration rates.

Potential evapotranspiration was calculated using the procedure given by Smart (1978),

$$PE_i = K_p N_i E_{pan} \quad \text{for } E_{pan} \leq 5 \text{ mm}$$

and

3.3

$$PE_i = K_p N_i 1.904(E_{pan})^{0.6} \quad \text{for } E_{pan} > 5 \text{ mm}$$

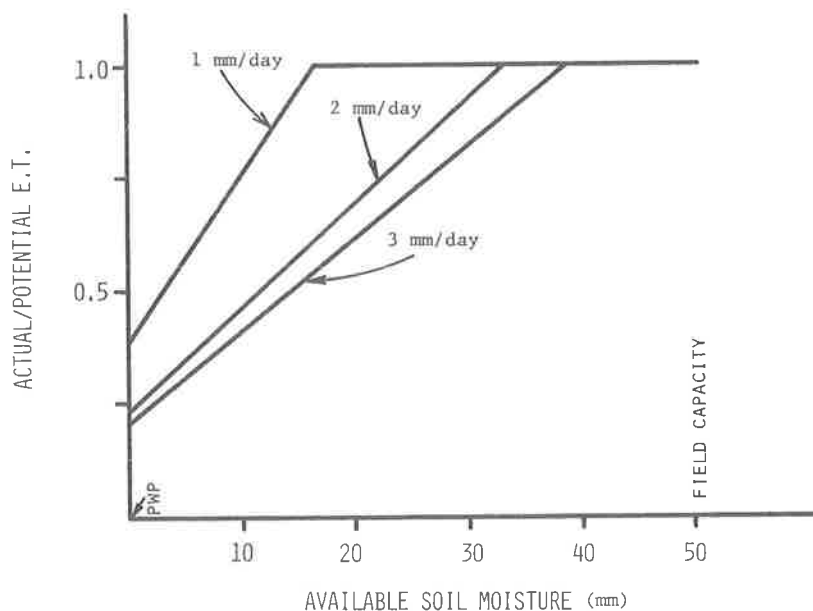


Figure 3.1 Relationship between the ratio of actual to potential evapotranspiration and soil moisture level

where K_p is the pan reduction factor (set at 0.85), E_{pan} is the daily pan evaporation and N_i is a factor based on the length of day i allowing for the seasonal variation in plant growth. N_i is approximated by the relationship

$$N_i = 0.2 [\cos (2\pi N_{day}/365) + 1] + 0.6 \quad 3.4$$

where N_{day} is the day number of day i . The constants in eqn 3.4 have been based on the relationship between potential evapotranspiration and open water evaporation measured by Heine (1976).

The exponential reduction for E_{pan} greater than 5 mm/day makes allowance for the greater influence of advected energy on an evaporation pan than on an irrigated pasture. This is necessary since advected energy is a very significant factor influencing evaporation in Canterbury.

The calculation of actual evapotranspiration and soil moisture levels departs from the method used in the irrigation demand assessment model in two respects. Firstly, the excess water retention factor which allows soil moisture levels to temporarily exceed field capacity has not been incorporated, and secondly, the soil moisture budget does not allow for soil moisture levels below permanent wilting point. Soil moisture budget based estimates tend to underestimate recharge (Rushton and Ward, 1979) and the above modifications compensate by causing a small increase in the calculated drainage.

3.1.2 Soil Moisture Model Calibration

Soil moisture model calibration was done using the daily rainfall and pan evaporation recorded at Winchmore, assuming a soil of 50 mm available soil moisture. The average annual rainfall measured at Winchmore for the period 1950-1980 was 760 mm. Walsh and Scarf (1980) give average rainfalls for 10 rainfall sites in the area below SH 1. The arithmetic mean of these annual values is 738 mm, which is within 3% of the Winchmore value.

Maidment et al. (1980) have classified the soils within the model area into two groups with water holding capacities of 85 and 45 mm. The shallower soil is the predominant one and so a water holding capacity of 50 mm has been adopted as being representative.

Drainage of excess soil moisture from the soil moisture zone eventually reaches the ground water system as recharge. The drainage is delayed in its passage

through the unsaturated material below the soil, but the volume that eventually becomes recharge will be conserved. The time distribution of recharge can be approximated by assuming that the drainage is lagged in time before becoming recharge. This allows a proportion of the excess rainfall to reach the ground water relatively quickly.

Drainage from irrigation return flow was calculated using the weekly records of water sales on the ALIS. Water volumes were converted to application depths using the ALIS area for the corresponding season. These applications were incorporated in the soil moisture model input to calculate the total drainage under irrigation. The difference between this and the drainage without irrigation produced the distribution of irrigation return flows.

3.1.3 Soil Moisture Model Results

The results of the soil moisture model are summarised in table 3.1. The mean annual drainage at Winchmore is 307 mm, but 75% of this occurs during the

Table 3.1 Annual and irrigation season drainage derived from daily values of evaporation and precipitation at Winchmore Irrigation Research Station (1950-1981).

| | Minimum | Mean | Maximum | Standard Dev. | Coeff. of Var. |
|-----------------------------|---------|------|---------|---------------|----------------|
| Annual (Oct-Sept) | | | | | |
| Rainfall (mm) | 491 | 760 | 1122 | 142 | 19% |
| Sunken pan evaporation (mm) | 808 | 1002 | 1302 | 119 | 12% |
| Drainage (mm) | 44 | 307 | 599 | 144 | 47% |
| Irrigation Season (Oct-Mar) | | | | | |
| Rainfall (mm) | 212 | 386 | 771 | 130 | 34% |
| Sunken pan evaporation (mm) | 578 | 762 | 1067 | 115 | 15% |
| Drainage (mm) | 0 | 74 | 406 | 93 | 127% |

winter. Drainage is extremely variable during the period October-March, with four seasons showing zero drainage and seven seasons where drainage was less than 10 mm over six months. For the period 1970-1980, the mean annual drainage from a surface irrigated area at Winchmore was calculated to be 807 mm (i.e., an increase of 500 mm above natural drainage).

Drainage is not very sensitive to changes in the available soil moisture. An increase of 20% (to 60 mm) resulted in a reduction in drainage of 4.6% and a 100% increase (to 100 mm) reduced drainage by 17.2%. Hence, the assumption that the soil water holding capacity is homogeneous over the model area will not introduce large errors in the recharge estimate.

The low available soil moisture level quickly limits actual evapotranspiration as soil moisture levels fall. For the period simulated, the total actual evapotranspiration was 64% of potential evapotranspiration, while potential evapotranspiration was 92% of total rainfall (table 3.2).

Table 3.2 Winchmore annual average climatic values for 1950-1981.

| | |
|------------------------------|---------|
| Precipitation | 760 mm |
| Actual evapotranspiration | 449 mm |
| Potential evapotranspiration | 698 mm |
| Pan evaporation | 1002 mm |

Monthly rainfall, evaporation and drainage are plotted in figure 3.2. Because there is no typically wet month, the drainage is concentrated in the low evapotranspiration winter period. The pan evaporation record shows a distinct long period cyclic component. However, the more random nature of the rainfall dominates the resulting patterns of drainage.

Approximately 60% of the total volume of irrigation water drains to ground water. Because this calculation assumed that the weekly water sales are uniformly spread over the irrigable area, the estimate of irrigation return flow is conservative.

The soil moisture model was also used to estimate potential irrigation demand. The calculated daily demands were used as input for the ground water simulations (section 4.3.1).

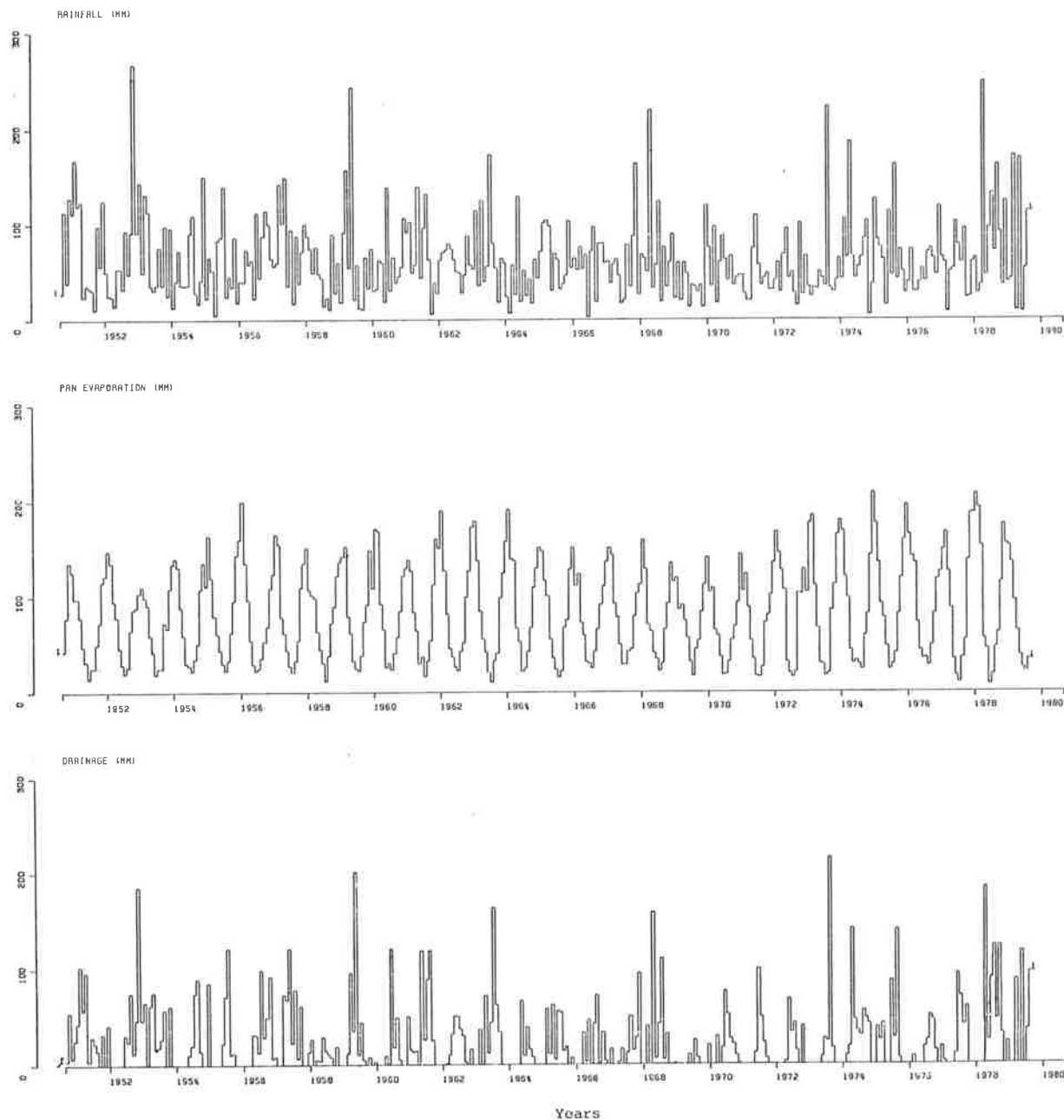


Figure 3.2 Mean monthly rainfall, pan evaporation and drainage at Winchmore Irrigation Research Station

3.1.4 Soil Moisture Budget for the Whole Study Area

Assuming a uniform soil moisture availability (50 mm) and evaporation rate (1002 mm; sunken pan) apply to the entire study area, it is possible to extrapolate from the Winchmore computations and make an estimate of average

annual deep drainage for the study area as a whole (table 3.3). The area was divided into sub-areas of equal rainfall, and drainage computed pro rata for each sub-area. Runoff from streams on Mt Hutt was not included in this estimate, but it is small in relation to direct rainfall on the study area.

Table 3.3 Estimate of average annual ground water recharge by deep drainage of precipitation

| Avg. Ann. Precip. (mm) | Sub-area (km ²) | Avg. Ann. Deep Drainage (mm) | Avg. Ann. Deep Drainage (m ³ x 10 ⁶) |
|------------------------|-----------------------------|------------------------------|---|
| 650 | 22 | 200 | 4.4 |
| 675 | 150 | 225 | 33.8 |
| 725 | 276 | 275 | 75.9 |
| 775 | 403 | 325 | 131.0 |
| 825 | 184 | 375 | 69.0 |
| 875 | 68 | 425 | 28.9 |
| 950 | 94 | 500 | 47.0 |
| 1100 | 120 | 650 | 78.0 |
| 1300 | 38 | 850 | 32.3 |
| TOTAL | 1355 | | 500.3 |

Average annual rainfall over the study area is 820 mm. Average annual deep drainage over the study area is 370 mm which is equivalent to $500 \times 10^6 \text{ m}^3 \text{ yr}^{-1}$. Annual variability of drainage over the whole study area is high, as indicated by table 3.1.

3.1.5 Irrigation Return Water from Ashburton-Lyndhurst Irrigation Scheme

A similar extrapolation was done by applying the Winchmore data (table 3.4) to the ALIS land under surface irrigation. Application rates of irrigation water were extracted from records of weekly water sales from the ALIS for the period 1970-79.

Table 3.4 Estimate of average annual (Oct-Sept) ground water recharge (mm) by deep drainage from irrigation at Winchmore (1970-1979).

| Minimum | Mean | Maximum | Standard Dev. | Coeff. of Var. |
|---------|------|---------|---------------|----------------|
| 320 | 500 | 641 | 125 | 25% |

The area under surface irrigation within the ALIS was about 14 000 ha in 1981 and is increasing at a rate of 260 ha yr^{-1} (Maidment et al., 1980). The volume of deep drainage from surface irrigation of 14 000 ha in a year of typical water demand is $70 \times 10^6 \text{ m}^3$. The variability of this figure from year to year is about the same as for rainfall, as would be expected.

Recharge from irrigation waste water will increase slowly as the irrigation scheme continues to develop. The computation assumes that irrigation water is uniformly applied to the whole area during the season at times taken from the record of weekly water sales. The fact that water is applied at greater depth to only part of the irrigated area, means that actual drainage will be somewhat greater than the computed drainage.

3.2 River Recharge

River loss gaugings have been done in both the Rakaia and Ashburton Rivers. Such gaugings can only be done when river flow is steady. Concurrent gaugings along the river length, with correction made for water abstractions or tributary inflows, allow calculation of the loss or gain of surface flow in each reach. It is not usually possible to directly assess whether the loss is to the left bank, the right bank or merely underflow within the river bed gravels and parallel to the surface flow.

3.2.1 Ashburton River

Three sets of gaugings of the Ashburton River were done. Two under low summer flow conditions, covering both the north and south branches between SH 72 and the coast, and the third under winter conditions, with higher flows but covering only the north branch of the river from Ollivers Rd to the coast (figure 3.3). Results are given in table 3.5.

Both branches of the Ashburton are losing water from the upper reaches (elevation greater than about 250 m). The North Ashburton continues to lose water as far down as Pages Rd (elevation 115 m), but the South Ashburton is gaining water at about the same rate through this reach. As the north branch is slightly higher than the south there could merely be a transfer via ground water from one branch to the other. Between 115 m elevation (Pages Rd) and 90 m (SH 1) the river system gains water consistently, but from SH 1 to the coast there is no consistent trend between sets of gaugings. Overall, there is evidence of a net loss from the aquifers to the river.

Table 3.5 Results of loss gaugings in the Ashburton River.

| Site | Discharge ($\text{m}^3\text{sec}^{-1}$) | | | Loss/Gain ($\text{m}^3\text{sec}^{-1}$) | | |
|------------------------------|---|-----------|-----------|---|------------|-----------|
| | 20.2.78 | 29.1.79 | 31.7.79 | 20.2.78 | 29.1.79 | 31.7.79 |
| Ashburton : North Branch | | | | | | |
| Old SH Bridge | 2.90 | 4.20 | -) |) | | - |
| Methven Aux | 1.40 abs. | 1.20 abs. | -) |) | | - |
| RDR siphon | 1.50 | 2.50 | -) | no change) | 0.50 loss | - |
| Flemings Rd | 0.08 | 1.00 | -) | 1.42 loss) | 1.50 loss | - |
| Swamp Drain | 0.21 inp. | 0.24 inp. | -) |) | | - |
| Thompsons Track | 0.39 | 1.65 | -) | 0.10 gain) | 0.41 gain | - |
| Braemar Rd | 0.18 | 0.60 | -) | 0.21 loss) | 1.05 loss | - |
| Mt Harding Creek | 0.67 inp. | 1.14 inp. | -) |) | | - |
| Ollivers Rd | 0.71 | 1.30 | 5.80 | 0.14 loss) | 0.44 loss | - |
| Greenstreet waste | - | 0.21 inp. | -) | -) | -) | - |
| Digbys Bridge | 0.43 | 0.76 | 4.81 | 0.28 loss) | 0.75 loss | 0.99 loss |
| Rawles Crossing | - | 0.95 | -) | -) | 0.19 gain | - |
| Rawles Crossing waste | 0.19 inp. | 0.30 inp. | 0.26 inp) |) |) | - |
| Pages Rd waste | 0.42 inp. | 0.30 inp. | 0.47 inp) |) |) | - |
| Pages Rd | 0.70 | 1.25 | -) | 0.34 loss) | 0.30 loss | - |
| At confluence | 1.40 | 1.81 | 5.65 | 0.70 gain) | 0.56 gain | 0.11 gain |
| Ashburton : South Branch | | | | | | |
| RDR siphon | 2.4 | 2.05 | -) | -) | - | - |
| Above Taylors Stream | 1.3 | 1.28 | -) | 1.1 loss) | 0.77 loss | - |
| O'Shea's intake | 1.0 abs. | 0.50 abs. | -) |) | | - |
| Below O'Shea's | - | 2.72 | -) | -) | 1.94 gain | - |
| Braemar Rd | 1.6 | 2.71 | -) | 1.3 gain) | 0.01 loss | - |
| Ollivers Rd | 2.4 | 3.85 | -) | 0.8 gain) | 1.14 gain | - |
| Blacks Rd | 3.1 | 4.41 | -) | 0.7 gain) | 0.56 gain | - |
| At confluence | 3.6 | - | 18.2 | 0.5 gain | - | - |
| Ashburton : Below Confluence | | | | | | |
| At confluence | 5.0 | 6.2 | 23.85) | -) | -) | - |
| At SH 1 | 5.9 | 8.36 | -) | 0.9 gain) | 2.2 gain) | - |
| Milton Rd | 5.9 | 7.51 | 28.6 | no change) | 0.85 loss) | 4.75 gain |
| Wakanui School Rd | 6.1 | 7.85 | 28.31) | 0.2 gain) | 0.34 gain) | 0.29 loss |
| Croys Rd | 6.4 | 7.77 | 29.21) | 0.3 gain) | 0.08 loss) | 0.9 gain |
| Net change to river flow | | | | +2.0 | +1.1 | - |

Below SH 1, water-level records in the aquifer close to the river have shown that the two are hydraulically connected. The aquifer test in Milton Rd (table 2.1, figure 3.3) indicated medium to high permeabilities with no suggestion of low permeability zones which might impede river losses. Piezometric gradients in Milton Rd and Wakanui School Rd, close to the river, are flat and this probably prevents significant outflows from the river. Losses from the river in the reach from SH 1 to the coast could become significant if water tables adjacent to the river are lowered by pumping.

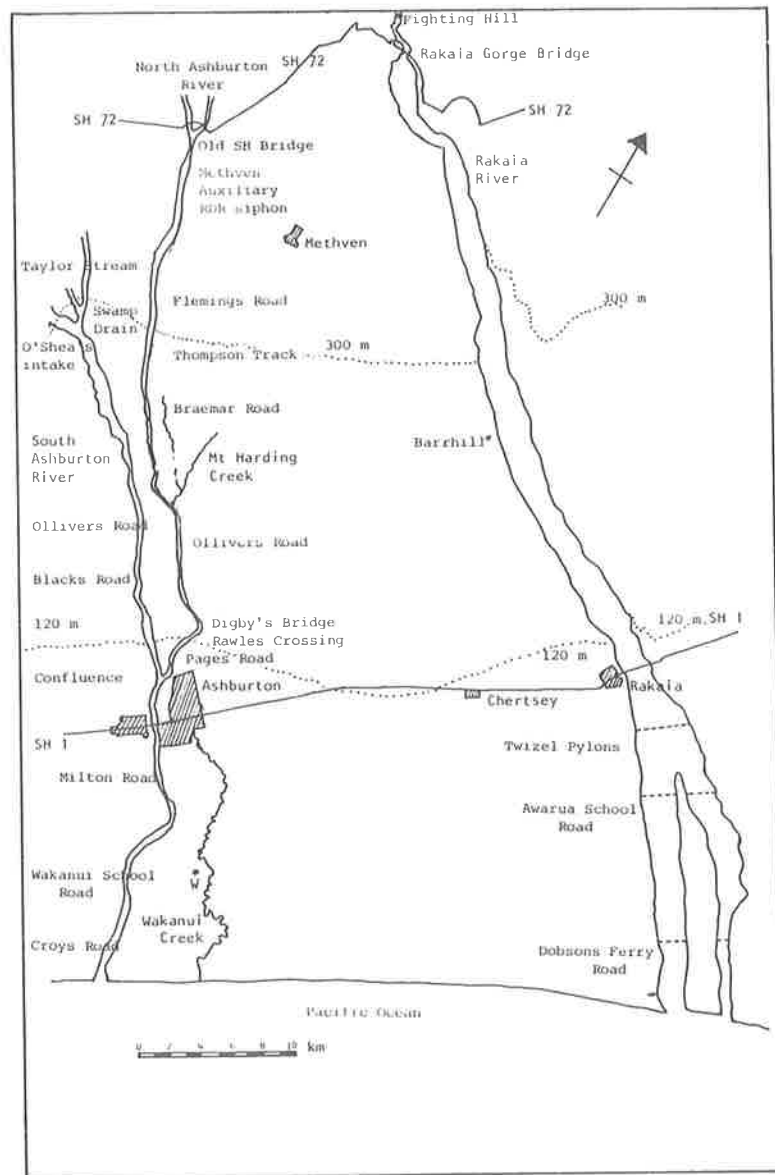


Figure 3.3 Loss gauging sites on the Ashburton and Rakaia Rivers

3.2.2 Rakaia River

Loss gaugings in the Rakaia were extremely difficult to carry out. Firstly, by their nature, calculated flow losses are relatively small differences between measured flows, and hence a very high standard of gauging is required. Secondly, in a river such as the Rakaia, each section contains several braids and multiple gaugings are required, increasing the possibility of error. Thirdly, Coleridge and Highbank power stations discharge varying flows into the river and arrangements had to be made with the Electricity Division of the Ministry of Energy for them to be kept on constant load for at least 24 hours. Fourthly, the vast expanse of gravel river bed acts like an unconfined aquifer with a considerable storage capacity; thus river stage must be in equilibrium with the piezometric level in the river bed gravels. With these cautions in mind eleven series of gaugings were done (figure 3.3).

Table 3.6 summarises the results of these gaugings and includes the results of previous loss gaugings between the Gorge and SH 1 carried out by the North Canterbury Catchment Board (Stephen, 1972). Stephen inferred from his gaugings that losses between Rakaia Gorge and SH 1 were proportional to flow in the river, although data from the present study do not confirm this. Stephen's data indicated losses in several cases substantially higher than measurements made specifically for this study.

Piezometric information from both sides of the river indicated that the river is perched from about Barrhill downstream. Upstream of Barrhill there were no piezometric data points sufficiently close to the river from which conclusions could be drawn. It has been surmised that because the river is deeply incised through this reach it is gaining water from the aquifers (Stephen, 1972), but there is no direct evidence to support this conclusion. Loss gaugings at points between the Gorge and Barrhill (Stephen, 1972; Hicks, MWD, pers. comm.) gave conflicting results. Losses are normally greater below SH 1 than above it. The two sets of gaugings done in summer (table 3.6) differ from the winter gaugings in that the river between SH 1 and Twizel Pylons shows a slight gain. No explanation can be given for this anomaly. It is not caused by high piezometric levels in the aquifers adjacent to the river, since these are lower in summer than in winter.

Accuracy of flow gauging in this type of river is probably about 5%, and individual discharges in table 3.6 should be considered in this light.

Table 3.6 Losses and gains from reaches of the Rakaia River ($\text{m}^3 \text{sec}^{-1}$).

| Date | Discharge at Fighting Hill (Rakaia Gorge) | Net Losses (-) and Gains (+) | | | | Total Loss |
|------------|---|------------------------------|---------------------|-----------------------------------|---------------------------------|------------|
| | | Fighting Hill to SH 1 | SH to Twizel Pylons | Twizel Pylons to Awarua School Rd | Awarua School Rd to Corbetts Rd | |
| 25.8.71 | 77 + 21* | -5 | - | - | - | - |
| 22.9.71 | 159 + 20* | -26 | - | - | - | - |
| 9.11.71 | 183 | -14 | - | - | - | - |
| 7.12.71 | 140 | -19.5 | - | - | - | - |
| 11.1.72 | 130 | -16.5 | - | - | - | - |
| 1.3.72 | 105 + 8* | -7 | - | - | - | - |
| 5/6.7.79 | 123 + 25* | -10.5 | -14 | - | -2 | -26.5 |
| 14/15.2.80 | 185 | -9 | +4 | -5 | -3 | -13 |
| 14/15.7.80 | 135 + 25* | -8 | -14 | -9 | -3 | -34 |
| 17/18.8.81 | 110 + 25* | -8 | -9 | -2 | -1 | -20 |
| 24.3.82 | 111 | -9 | +1 | -7 | -6 | -21 |

* Input from Highbank power station
1971-72 data from Stephen (1972) and 1979-82 data from MWD

Nevertheless, apart from the anomalous summer values noted, the repeat gauging series show general consistency and at times up to 20% of surface water disappears into the gravels.

3.2.3 Rakaia River Underflows

It is not obvious if the surface water lost from the Rakaia River actually enters the aquifers or whether it remains as underflow within the confines of the active river bed.

At Rakaia Gorge, where the channel is restricted between essentially impermeable banks with only a shallow gravel bed (Broadbent, 1978), it can be assumed that underflow is small, and thus underflow at sections further downstream must come from channel losses or, more speculatively, from the aquifer system above Barrhill.

In the reach between Rakaia Township and Twizel Pylons, drilling showed that the river is underlain at a depth of about 15 m by a thick layer of clay-bound gravels. Piezometric levels above and below this layer are markedly different, indicating that two separate aquifers exist and that the aquiclude is extensive and continuous. Thus, the unconfined aquifer above the aquiclude and between the river banks is well defined and is the underflow path. The Darcy velocity was measured with the borehole tracer dilution method (Halevy *et al.*, 1967; Drost *et al.*, 1968; Klotz *et al.*, 1979), which involves injecting a tracer into the screened portion of a bore, mixing thoroughly, and recording the rate of disappearance. From this the underflow was calculated.

For this experiment, eight shallow (6 m) wells were excavated and two deeper (15 m) wells drilled across the river bed. The shallow wells were excavated inside a 1 m diameter steel liner, a 100 mm slotted PVC screen was inserted, the liner withdrawn and the hole backfilled. Observation during excavation showed typical medium coarse greywacke gravels with some sand and clay wash. Only in one well was there any evidence of a low permeability layer. In two wells the flow was observed to be at about 45° to the general downstream direction.

The tracer used was a 1% salt (NaCl) solution and detection was by conductivity meter. Inflatable packers were used to isolate a 240 mm length of screen and prevent density currents or natural vertical flows from disturbing the experiment.

The Darcy flow velocity (V_f) is given by (Klotz et al., 1979):

$$V_f = \frac{\pi r \beta}{2 \alpha \gamma} \frac{\ln C/C_0}{t} \quad 3.5$$

where r = internal radius of screen (m)

t = time since injection (days)

C = concentration at time t

C_0 = concentration at time zero

α , β and γ are correction factors determined by the geometry of the injection equipment and borehole.

α is an analytical factor to allow for the thickness and permeability of the screen, gravel pack and aquifer.

β is an empirical factor to correct for the volume occupied by the injection equipment within the screen.

γ is an empirical factor to allow for the flow disturbance created by packers which isolate the section of bore and aquifer under test.

Correction factors selected from the literature (Halevy et al., 1967; Klotz et al., 1979) were:

$$\alpha = 2.5$$

$$\beta = 0.8$$

$$\gamma = 1.4$$

whence $\beta/\alpha\gamma = 0.23$

Because of the empirical nature of $\beta/\alpha\gamma$, an independent check of the method and equipment was made at Burnham, where other workers had established ground water seepage velocity at a point by well to well tracer tests. Assuming a porosity of 0.3 this check suggested that $\beta/\alpha\gamma$ is about 0.15. Velocities derived with the above correction factors are listed in table 3.7, the mean value being 36 or 23 m day⁻¹, depending on which correction factor is adopted.

The water table in the unconfined aquifer below the river is about 2 m below the surface, thus the saturated depth of permeable gravels above the aquitard is about 13 m. The width of the active and inactive bed at Twizel Pylons is

Table 3.7 Darcy velocities derived from tracer dilution tests.

| Test Well | Well Depth (m) | Water Depth in Well (m) | Darcy Velocity (m day ⁻¹) | |
|------------|----------------|-------------------------|---------------------------------------|----------|
| | | | $\beta/\alpha\gamma = 0.23$ | $= 0.15$ |
| A | 5.0 | 3.7 | 21 | 14 |
| B | 6.1 | 5.1 | 10 | 6.5 |
| C | 4.4 | 2.5 | 60 | 39 |
| D | 3.3 | 2.3 | 3.5 | 2.5 |
| E | 4.4 | 2.5 | 4 | 2.5 |
| F | 6.3 | 3.7 | 14 | 9 |
| South deep | 16.1 | 14.1 | 105 | 68 * |
| Pylon 369 | 5.3 | 3.9 | 1 | 0.6 |
| Pylon 370 | 6.2 | 4.6 | 0.2 | 0.1 |
| North deep | 15.2 | 10.0 | 140 | 91 + |
| Mean | | | 36 | 23 |

* Mean of ten velocities in the vertical

+ Mean of eleven velocities in the vertical

about 3.5 km, thus the Darcian flow cross-section is $3500 \times 13 = 45\,500 \text{ m}^2$. The two underflow values computed are therefore:

$$\begin{aligned}
 45\,500 \times 36 &= 1.638 \times 10^6 \text{ m}^3 \text{ day}^{-1} \quad (19 \text{ m}^3 \text{ sec}^{-1}) \\
 \text{or } 45\,500 \times 23 &= 1.047 \times 10^6 \text{ m}^3 \text{ day}^{-1} \quad (12 \text{ m}^3 \text{ sec}^{-1})
 \end{aligned}$$

The tracer dilution method is not capable of defining velocities with accuracy, and the only conclusion to be drawn is that underflow at the Twizel Pylons section of the Rakaia River is $10\text{--}20 \text{ m}^3 \text{ sec}^{-1}$. The mean annual flow of the Rakaia at the Gorge is $200 \text{ m}^3 \text{ sec}^{-1}$ and thus underflow is a significant loss. Comparison of the underflow estimate with channel losses given in table 3.6 demonstrates that although water leaks out of the surface channels at a high rate, much of it remains as underflow, and the actual recharge of the aquifers on either side of the river may be quite small.

3.2.4 Recharge of Aquifers on the South Bank of the Rakaia River

Hydraulic and stratigraphic information enabled an estimate to be made of seepage through the south bank in the reach between SH 1 and the coast (table 3.8). Well logs show that a thick layer of clay-bound gravels exists

Table 3.8 Parameters adopted in computation of seepage through the south bank of the Rakaia River

| Reach | Length (km) | θ (degrees) | Gradient | Transmissivity ($\text{m}^2 \text{ day}^{-1}$) | Q_r Discharge ($\text{m}^3 \text{ sec}^{-1}$) |
|---------------------------------|-------------|--------------------|----------|--|---|
| Township -Twizel Pylons | 5.2 | 50 | .01 | 4 000 | 1.8 |
| Twizel Pylons -Dobsons Ferry Rd | 11.2 | 30 | .005 | 10 000 | 3.2 |
| Dobsons Ferry Rd-coast | 4.5 | 0 | .005 | - | 0 |
| Total | | | | | 5.0 |

at a depth of 15 m from Rakaia Township seawards at least as far as the Twizel Pylons. Above this layer is about 13 m of saturated gravels.

Hydraulic gradients and flow directions were estimated from piezometric maps. From aquifer tests at Rakaia Township, Twizel Pylons and Dobsons Ferry Rd (table 2.2), mean transmissivities in the reaches were calculated.

The discharge through the river bank Q_r in each reach is then calculated as:

$$Q_r = T i l \sin \theta \quad 3.6$$

where T = transmissivity ($\text{m}^2 \text{ day}^{-1}$)

i = hydraulic gradient

l = reach length of river (m)

θ = angle between river and ground water flow directions

For the reach between SH 1 and the coast, the calculation of the actual recharge to the aquifer is $5.0 \text{ m}^3 \text{ sec}^{-1}$ (table 3.8), but considering the gross simplifying assumptions used this should more realistically be taken to be from 3 to $8 \text{ m}^3 \text{ sec}^{-1}$. Once in the aquifers, the flow path of this recharge remains sub-parallel to the river as determined by the water chemistry (see figure

2.14). A similar estimate cannot be made for the reach above SH 1 because of inadequate information, but the piezometric contours (figure 2.7) show that there will be some additional recharge.

3.2.5 Recharge of Confined Aquifer by Vertical Leakage Through the Clay-bound Gravels Underlying the Rakaia River

The major proportion of the loss from the surface channels of the Rakaia River occurs between SH 1 and Awarua School Rd (section 3.2.2). Much of this reach is underlain by a thick layer of clay-bound gravels across which an hydraulic head exists, implying some downward seepage. The existence of a head difference ranging from 13 to 25 m across this clay-bound layer is a strong indication that it is horizontally extensive. An estimate of the rate of seepage through this bed can therefore be made using Darcy's Law.

The assumptions are:

- (i) The clay-bound gravel layer is continuous and uniform beneath the Rakaia River in the reach from SH 1 to Awarua School Rd, an area of 35 km² or 3.5×10^7 m².
- (ii) The average thickness of the layer from borelogs is 20 m.
- (iii) The head difference across the layer averages 15 m.
- (iv) The permeability of the layer is 10^{-8} m sec⁻¹, appropriate for a glacial till (Cedergren, 1977).

The rate of seepage is given by:

$$\begin{aligned} Q &= k i A \\ &= 10^{-8} \times 15/20 \times 3.5 \times 10^7 \\ &= 0.26 \text{ m}^3 \text{ sec}^{-1} \end{aligned}$$

This flow may enter the aquifer system on either side of the river. Because of the assumptions made in this calculation, the result is approximate. However, vertical seepage through the aquitard into the confined aquifer will be low.

3.2.6 Summary of Information on Recharge from the Rakaia River

- (i) The measured losses from the surface channels between the Gorge and Corbetts Rd, measured on five occasions, range from 13 to 34 m³ sec⁻¹.

These losses are not related to in-channel flows. Greatest losses occur between SH 1 and Awarua School Rd.

- (ii) Underflows at a cross-section near the Twizel Pylons are approximately 10 to $20 \text{ m}^3 \text{ sec}^{-1}$.
- (iii) Flow across the south bank of the Rakaia between SH 1 and the sea is 3 to $8 \text{ m}^3 \text{ sec}^{-1}$.
- (iv) Vertical seepage through the clay-bound gravels underlying the river between SH 1 and Awarua School Rd is less than $0.5 \text{ m}^3 \text{ sec}^{-1}$.

These four observations are self-consistent and suggest that the contribution of the Rakaia to the aquifers between the two rivers is less than $8 \text{ m}^3 \text{ sec}^{-1}$.

3.3 LEAKAGE FROM STOCK RACES AND THE RANGITATA DIVERSION RACE

Within the study area, a system of stock races administered and maintained by the Ashburton County Council provides each farm with a water supply. The total rate of water abstraction for stock authorised by water rights administered by the SCRWB and NCRBW is $4.14 \text{ m}^3 \text{ sec}^{-1}$. During the summer, abstraction rates are at the limit authorised, but in winter they may be slightly reduced. Waste discharge into the sea on a year round basis is estimated as $0.15 \text{ m}^3 \text{ sec}^{-1}$, and stock utilisation is not more than $0.2 \text{ m}^3 \text{ sec}^{-1}$ (R J Paterson, Ashburton County Council, pers. comm.). The remainder of the water is lost either by evaporation or seepage into the gravels. Assuming the stock races are on average 60 cm wide and spaced about 1000 m apart across the width of the plains, the area of open water exposed in the races is of the order of $2 \times 10^6 \text{ m}^2$. With average annual sunken pan evaporation at Winchmore of 1.0 m, the evaporative loss from the races is about $2.0 \times 10^6 \text{ m}^3 \text{ yr}^{-1}$ or about $0.06 \text{ m}^3 \text{ sec}^{-1}$, to which should be added a similar quantity of transpired water from vegetation alongside the races. Thus, evapotranspiration losses from the stock races are very small.

Recharge of the aquifers from the stock races can therefore be estimated to be about

$$(4.14 - 0.2 - 0.15 - 0.12) = 3.67 \text{ m}^3 \text{ sec}^{-1}$$

in the summer, and somewhat less in winter. Flow gaugings in the RDR indicate that seepage losses are about $0.026 \text{ m}^3 \text{ sec}^{-1} \text{ km}^{-1}$ of length, and thus for a length of 17 km total seepage losses within the study area from this source are

small, about $0.45 \text{ m}^3 \text{ sec}^{-1}$ (M Duncan, MWD, pers. comm.). The recharge to the aquifers from these two sources is, therefore, approximately $4.15 \text{ m}^3 \text{ sec}^{-1}$.

3.4 WATER EXTRACTION

Water is extracted from the aquifers for domestic, municipal, industrial and agricultural purposes. Domestic consumption is not controlled by water right and the usage is not known accurately. The SCRWB estimates that within the study area rural domestic water use of ground water is about $0.037 \text{ m}^3 \text{ sec}^{-1}$, which is negligible compared to other uses (Walsh and Scarf, 1980).

3.4.1 Municipal and Industrial Water Use

The SCRWB has granted 29 rights to take ground water for municipal and industrial purposes, as of June 1981. The two major users are the Canterbury Frozen Meat Company, which is authorised to take an average daily flow of $0.03 \text{ m}^3 \text{ sec}^{-1}$, and Ashburton Borough with a right to take $0.1 \text{ m}^3 \text{ sec}^{-1}$. Total authorised extraction by municipal and industrial users is $0.187 \text{ m}^3 \text{ sec}^{-1}$, 87% of which is taken by the six largest users (SCRWB data). Approximately 80% of the authorised ground water extraction, including the Ashburton Borough wells, is seasonal and thus the figure, when averaged throughout the year, is small.

3.4.2 Agricultural Water Use

Agricultural use of ground water predominates and is increasing rapidly. Maidment et al. (1980) reported that to September 1979 the SCRWB had issued 101 water rights to irrigators operating between the Rakaia and Ashburton Rivers, of which more than 90% were for ground water. Since that time a further 27 rights have been issued (to June 1981) and are being utilised. In addition, the NCRWB has issued eight rights for agricultural water use in the thin strip of land which falls within its jurisdiction along the south bank of the Rakaia River. Irrigation water use is summarised in table 3.9, and totals $3.217 \text{ m}^3 \text{ sec}^{-1}$.

The actual usage during the irrigation season may be much less than the quantities granted under the rights, depending upon the seasonal rainfall. During the 1980/81 season, which was unusually dry (irrigation season rainfall 65% of long-term normal), the average rates of extraction and power usage for 16 spray irrigators were measured. This information was combined with irrigation power consumption for the entire study area and an average seasonal

Table 3.9 Irrigation water use between the Rakaia and Ashburton Rivers (SCRWB and NCRWB data).

| Year | No. of Rights Issued | Nominal Area (ha) | Nominal Average Daily Flow ($\text{m}^3 \text{sec}^{-1}$) |
|----------------|----------------------|-------------------|---|
| 1969 | 23 | n.d. | 0.250 |
| 1970 | 13 | n.d. | 0.185 |
| 1971 | 4 | n.d. | 0.107 |
| 1972 | 6 | n.d. | 0.105 |
| 1973 | 9 | 969 | 0.362 |
| 1974 | 17 | 1307 | 0.428 |
| 1975 | 15 | 1068 | 0.373 |
| 1976 | 7 | 517 | 0.173 |
| 1977 | 5 | 1176 | 0.197 |
| 1978 | 17 | 2357 | 0.489 |
| 1979 | 10 | 1133 | 0.342 |
| 1980 | 6 | 394 | 0.114 |
| 1981 (to June) | 4 | 370 | 0.092 |
| Total | 136 | 9291 | 3.217 |

water usage was estimated. This was only 39% of the withdrawal rate permitted by water rights at that time. During the 1979/80 season, which was unusually wet (125% of long-term seasonal rainfall), the average seasonal use was only 12.5% of the permitted rate at that time (Price, MWD, pers. comm.).

Thus to summarise, maximum extraction for consumptive municipal, industrial and agricultural use is $3.404 \text{ m}^3 \text{sec}^{-1}$, and is nearly all seasonal.

3.5 SPRING LEAKAGE

Within the study area, springs or seepages occur in the area feeding the Mt Harding and Wakanui Creeks. Flow information for Mt Harding Creek is limited, and it is difficult to estimate the natural discharge, since during the summer this is boosted by waste waters from the ALIS. The natural discharge is estimated to be about $0.33 \text{ m}^3 \text{sec}^{-1}$ (SCRWB data) and when supplemented by irrigation waste water it has been gauged at $1.14 \text{ m}^3 \text{sec}^{-1}$.

The Wakanui Creek is not affected by irrigation waste waters, but does occasionally carry stormwater flows from Ashburton Borough. There is no continuous flow information. During a period of extremely high water-levels in 1978,

the creek was gauged at $3.5 \text{ m}^3 \text{ sec}^{-1}$ near the mouth. The mean flow is estimated to be $1.5 \text{ m}^3 \text{ sec}^{-1}$ near the mouth.

3.6 SUBMARINE LEAKAGE

No direct evidence of submarine leakage has been obtained, but the discrepancy between inputs and outputs to the aquifer system indicates that major losses from the aquifer system must occur in this way.

3.7 ELEMENTS OF THE WATER BALANCE

The water balance equation states that the difference between inputs and outputs is equal to the change in storage. There is no evidence of long-term change of storage in the Ashburton-Rakaia aquifers and therefore mean input should balance mean output. The components are given in table 3.10. The major component for the input is drainage from precipitation, which is highly variable from year to year (see table 3.1) and season to season. The tabulated outputs on an average annual basis are about 12% of the input. The difference between input and output is the seepage across the coastline.

Table 3.10 Elements of annual water balance for the Ashburton-Rakaia ground water system.

| Inputs ($\text{m}^3 \times 10^6 \text{ yr}^{-1}$) | | Outputs ($\text{m}^3 \times 10^6 \text{ yr}^{-1}$) | |
|--|-----|---|-----|
| Precipitation drainage | 500 | Municipal and industrial | 6 |
| Ashburton-Lyndhurst drainage | 70 | Agricultural | 43* |
| Ashburton River | 0 | Mt Harding Creek | 10 |
| Rakaia River | 160 | Wakanui Creek | 47 |
| Stock race leakage | 123 | | |
| RDR leakage | 13 | | |
| Total | 866 | | 106 |

* Actual irrigation use for the 1981/82 season

4 : GROUND WATER MODELLING

4.1 INTRODUCTION

Computer models were used to simulate, for a range of irrigation development options, the long-term ground water response to extensive pumping. The ground water system is dynamic and its inputs and outputs vary with time - indeed irrigation is likely to be high during periods of below average recharge. A study of the ground water response to development must, therefore, provide a measure of the probability of extreme conditions. This has been achieved by simulating the ground water response for a 30 year period, using historic climate data and postulated irrigation schemes.

Two components of the hydrologic cycle (figure 4.1) were treated separately, using a soil moisture model (see section 3.1.1) and ground water flow models. The soil moisture component was simulated using a lumped parameter water budget model to route both rainfall and irrigation water through a soil moisture zone. The calculated mean drainage rate from the soil moisture model was used to estimate the steady ground water recharge rate. This model also estimated

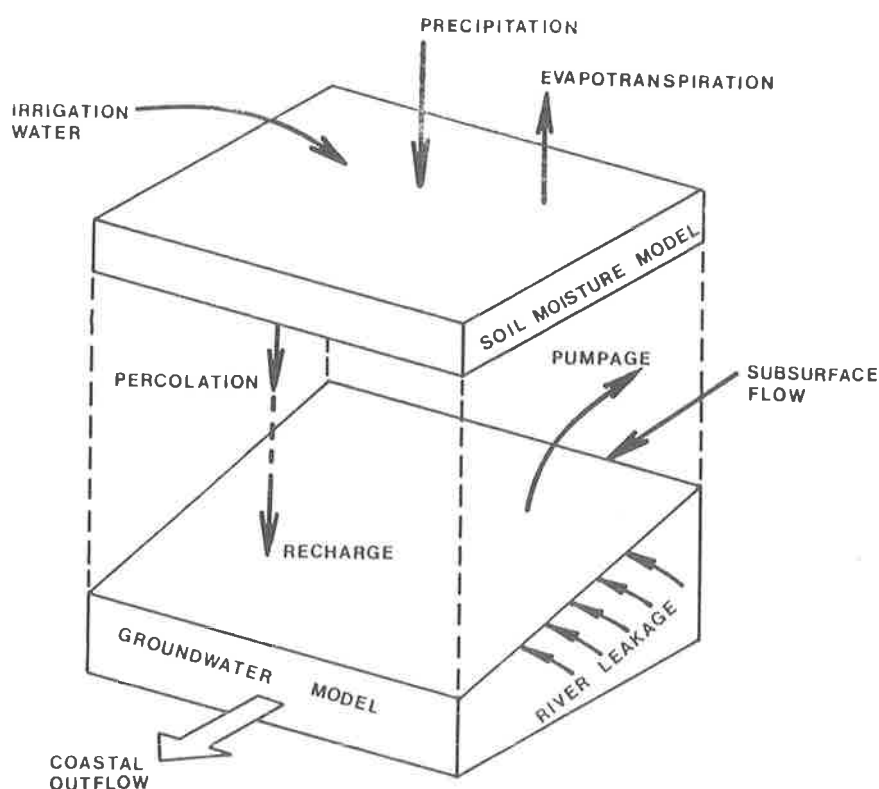


Figure 4.1 Conceptual model of soil and ground water systems

the time-dependent potential irrigation demand required to replenish soil moisture deficits for various irrigation strategies. These demands were used as ground water pumpage rates for the unsteady ground water flow model.

Ground water flow was simulated, using firstly a simple, lumped parameter model, and subsequently a more complex, two-dimensional model. The lumped parameter model was used to assess the adequacy of water balance estimates as input to an unsteady ground water model and, particularly, to determine how the calculated rainfall excess should be lagged before being treated as ground water recharge. The initial simulations using the lumped parameter model demonstrated the particular significance of the unsteady response of the system. The two-dimensional models used finite difference methods. A new approach to the calibration of ground water flow models was developed using a steady-state version of the model. An unsteady version was used to simulate the response to different irrigation development options. The results of the irrigation development simulations have been summarised so that the alternatives considered can be compared. In addition, the effects of the postulated development options on existing irrigation wells are examined.

4.2 METHOD

4.2.1 Ground Water Flow Model

(a) Ground water flow equations

The transient flow of ground water through an aquifer can be described by the equation (Bear, 1972)

$$\nabla(KB \nabla h) = S \frac{\partial h}{\partial t} + W \quad 4.1$$

where K is permeability, B is saturated aquifer thickness, S is aquifer storativity, h is piezometric head, t is time and W is a source/sink term. Equation 4.1 is derived from the equation of continuity and Darcy's Law, using the Dupuit approximation of constant piezometric head in the vertical direction.

For a lumped parameter, or single cell model, the gradient terms are zero and so eqn 4.1 simplifies to:

$$S \frac{\partial h}{\partial t} + W = 0 \quad 4.2$$

where h is calculated for a representative point in the aquifer. For an isotropic confined aquifer, eqn 4.1 can be rewritten as:

$$\frac{\partial}{\partial x} \left(T \frac{\partial h}{\partial x} \right) + \frac{\partial}{\partial y} \left(T \frac{\partial h}{\partial y} \right) = S \frac{\partial h}{\partial t} + W \quad 4.3$$

where the product KB has been replaced by the transmissivity, T .

Equation 4.3 can be applied to flow in an unconfined aquifer if the change in piezometric head is small compared to the saturated thickness of the aquifer. A properly posed problem requires that the region has boundaries of specified head or specified gradient.

(b) Discrete form of ground water equations

Numerical solutions of eqns 4.2 and 4.3 can be found by approximating them in discrete form. The lumped parameter model described by eqn 4.1 can be written in discrete form as

$$S (h_t - h_{t-\Delta t}) / \Delta t + Q_t / A = 0 \quad 4.4$$

where h_t is the piezometric head at time t , Q_t is the net outflow from the aquifer during the period Δt , and A is the effective area of the single cell which represents the aquifer.

For the two dimensional flow problem, superimposing a square grid over the flow region allows eqn 4.3 to be expressed in discrete form using the implicit Crank-Nicholson approximation as:

$$\begin{aligned} & T_{i-1/2,j} \frac{(h_{i-1,j,t} - h_{i,j,t}) + (h_{i-1,j,t-1} - h_{i,j,t-1})}{2} \\ & + T_{i+1/2,j} \frac{(h_{i+1,j,t} - h_{i,j,t}) + (h_{i+1,j,t-1} - h_{i,j,t-1})}{2} \\ & + T_{i,j-1/2} \frac{(h_{i,j-1,t} - h_{i,j,t}) + (h_{i,j-1,t-1} - h_{i,j,t-1})}{2} \\ & + T_{i,j+1/2} \frac{(h_{i,j+1,t} - h_{i,j,t}) + (h_{i,j+1,t-1} - h_{i,j,t-1})}{2} \\ & = S_{i,j} \frac{(\Delta x)^2}{\Delta t} (h_{i,j,t} - h_{i,j,t-1}) + \frac{W_{i,j,t} + W_{i,j,t-1}}{2} (\Delta x^2) \end{aligned} \quad 4.5$$

where $h_{i,j,t}$ is the piezometric head at time t at node i,j of the square grid with sides of length Δx , $T_{i-1/2,j}$ is the transmissivity between nodes i,j and $i-1,j$, and $S_{i,j}$ is the storativity at node i,j . $W_{i,j,t}$ is the source/sink term for node i,j during time t (figure 4.2).

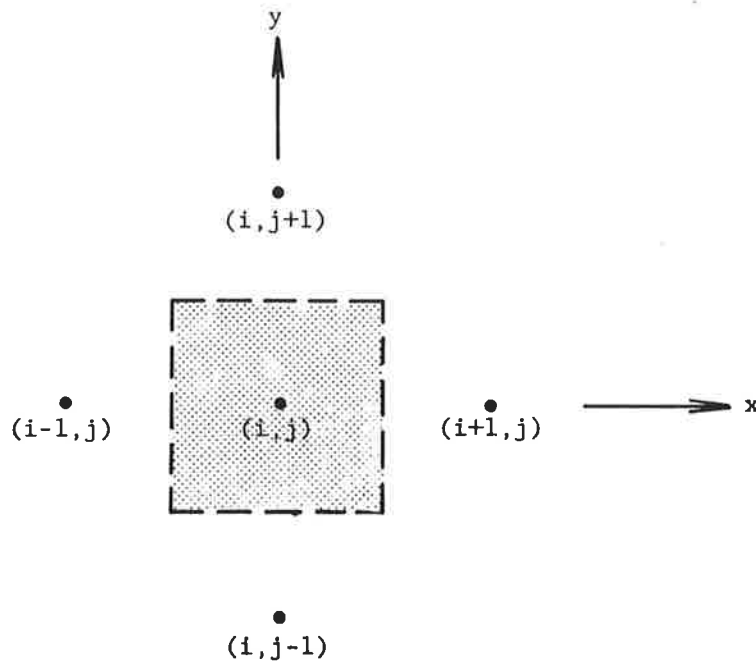


Figure 4.2 Section of the finite difference grid showing the node reference convention

For steady flow $h_{i,j,t} = h_{i,j,t-1}$ eqn 4.5 can be rewritten, omitting the time subscript, as:

$$\begin{aligned}
 & T_{i-1/2,j} (h_{i-1,j} - h_{i,j}) + T_{i+1/2,j} (h_{i+1,j} - h_{i,j}) \\
 & + T_{i,j-1/2} (h_{i,j-1} - h_{i,j}) + T_{i,j+1/2} (h_{i,j+1} - h_{i,j}) \\
 & = W_{i,j} (\Delta x)^2
 \end{aligned} \tag{4.6}$$

The mid-node transmissivities in eqns 4.5 and 4.6 can be approximated by the arithmetic mean of the adjacent node values:

$$T_{i-1/2,j} = (T_{i-1,j} + T_{i,j})/2 \tag{4.7}$$

(c) Numerical methods

The finite difference expressions presented in the previous section must be reorganised in a form suitable for the application of numerical solution methods. For the lumped parameter model, eqn 4.5 can be rewritten to give the predicted piezometric head in an explicit form:

$$h_t = h_{t-\Delta t} - \Delta t Q_t / AS \quad 4.8$$

The net outflow term (Q_t) in eqn 4.8 is the algebraic sum of recharge from excess rainfall and irrigation, and abstractions resulting from pumping and leakage. The leakage describes the net effect of leakage to and from rivers, springs and the sea. Since it is a head dependent term, leakage can be expressed as:

$$L_t = a(h_{t-\Delta t} - b) \quad 4.9$$

where L_t is the leakage rate at time t , and a and b are constant coefficients. The leakage is expressed in terms of $h_{t-\Delta t}$ in order to maintain the fully explicit nature of eqn 4.8.

Substituting the components of the outflow term in eqn 4.8 gives:

$$h_t = h_{t-1} + \Delta t (V_t + A_i I_t - O_t - (ah_{t-1} - b)) / AS \quad 4.10$$

where A_i is the sub-area receiving the I_t irrigation excess, O_t is the pumping rate for time t , and V_t is the aquifer recharge derived from drainage of excess rainfall.

Application of eqn 4.10 to the prediction of piezometric heads requires appropriate values of the coefficients a , b and S . In calibrating this model to match observed water-levels an automatic optimisation procedure was used to minimise the sum of squares of differences between observed and predicted values. The optimisation procedure, VA05A (Hopper, 1973), was also used in the calibration of the finite difference model and is described in section 4.2.2. The procedure treats variables as unrestrained. To constrain the aquifer storativity term it was written as:

$$S = 1/(1+U^2) \quad 4.11$$

so that $0 \leq S \leq 1$ and U becomes a substitute variable in the optimisation.

For two-dimensional flow the finite difference approximations were solved using the procedures described by Hunt (1976). By using the alternative node numbering technique shown in figure 4.3, Hunt writes an expression equivalent to eqn 4.5 as:

$$B(t) + B(t-\Delta t) = 2\Delta x^2 S_0 (h_0(t) - h_0(t-\Delta t))/T_0 \Delta t \quad 4.12$$

where

$$B(t) = a_1 h_1(t) + a_2 h_2(t) + a_3 h_3(t) + a_4 h_4(t) - a_0 h_0(t) - Q_0(t)/T_0 + P_0 \text{hspg}(t)/T_0$$

and

$$a_1 = (T_1 + T_0)/2T_0$$

$$a_2 = (T_2 + T_0)/2T_0$$

$$a_3 = (T_3 + T_0)/2T_0$$

$$a_4 = (T_4 + T_0)/2T_0$$

$$a_0 = a_1 + a_2 + a_3 + a_4 + P_0/T_0$$

In eqn 4.12 the source/sink term has been expressed in terms of the pumpage and leakage flows:

$$W_{i,j,t} \equiv Q_0(t)/A + P_0(h_0 - \text{hspg}_0)/A \quad 4.13$$

where $Q_0(t)$ is the well abstraction rate at node 0 for time t , P_0 is the leakage coefficient at node 0, hspg_0 is the piezometric head of any spring to which leakage occurs and A is the area represented by the finite difference node (Δx^2). Hence the finite difference model treats pumpage and leakage as though they were uniformly distributed over an entire node area.

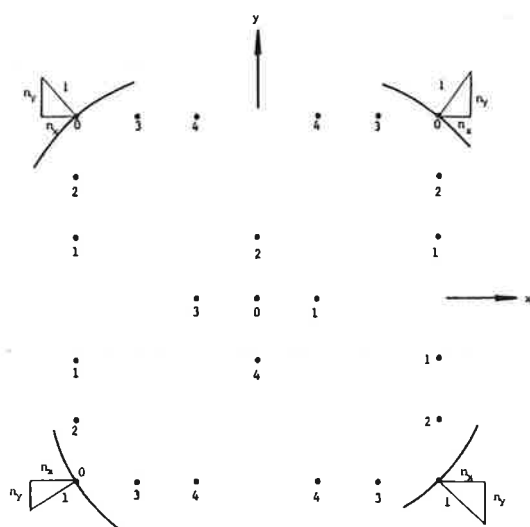


Figure 4.3 Alternative node numbering convention for internal and boundary nodes (after Hunt, 1976)

Hunt (1976) uses the Gauss-Seidel iterative technique (Smith, 1965) to solve the set of simultaneous equations obtained by writing eqn 4.12 for each internal node of the model in the form:

$$h_o = h_o + \frac{B(t) + B(t-\Delta t) - 2\Delta x^2 S_o [h_o(t) - h_o(t-\Delta t)] / T_o \Delta t}{a_o + 2\Delta x^2 S_o / T_o \Delta t} \quad 4.14$$

For the steady flow case, Hunt's node numbering convention can be used to write eqn 4.6 as:

$$\begin{aligned} a_1(h_1 - h_o) + a_2(h_2 - h_o) + a_3(h_3 - h_o) + a_4(h_4 - h_o) \\ = P_o(h_o - h_{spg_o}) / T_o + Q_o / T_o \end{aligned} \quad 4.15$$

where once again the source/sink term has been replaced by the leakage and pumpage terms. Hunt uses the successive over-relaxation method (Smith, 1965) to solve the set of simultaneous equations derived from eqn 4.15 by writing

$$h_o = h_o + \omega(a_1 h_1 + a_2 h_2 + a_3 h_3 + a_4 h_4 - a_o h_o - Q_o / T_o + P_o h_{spg_o} / T_o) / a_o \quad 4.16$$

where ω is the relaxation factor. Smith (1965) gives a procedure for calculating an optimum relaxation factor, ω_{opt} . However, since ω_{opt} is dependent on the coefficient matrix of the simultaneous equations, it changes if the transmissivity distribution is altered. Because the procedure for calculating ω_{opt} requires information from a prior Gauss-Seidel solution ($\omega = 1$), the technique was discarded for the model calibration runs, and instead a value of $\omega = 1.74$ was adopted on the basis of satisfactory results in trial calculations.

The constant head boundary condition is satisfied by maintaining the initial value of head at constant head boundary nodes. Hunt (1976) uses a second-order finite difference approximation to satisfy the specified gradient on the boundary. Using the appropriate node numbering (figure 4.3) gives:

$$N_x(h_4 + 3h_o - 4h_3) / 2\Delta x + N_y(h_1 + 3h_o - 4h_2) / 2\Delta y = G_o \quad 4.17$$

where N_x and N_y are the absolute magnitudes of the outward pointing, unit normal at node O, and G_o is the gradient at node O.

4.2.2 Parameter Estimation Method

Before the two-dimensional finite difference model can be used the transmissivity and storativity parameters must be specified for each node. This effectively involves solving the inverse form of eqn 4.3 so that S and T are calculated from known values of h and W . A solution to the inverse problem can be achieved in two stages by first calculating the transmissivity distribution for steady conditions and then using the partially calibrated model to determine the storativity. This approach has been used here. The steady inverse problem solution is based on a flow net analysis of steady piezometric levels and the unsteady problem reduced to identification of a single parameter by assuming that the aquifer has homogeneous storativity.

(a) Flow net relationships

Hunt and Wilson (1974) use a flow net analysis of steady piezometric contours to calculate the distribution of transmissivity while neglecting rainfall infiltration. The method can be extended to allow for steady vertical recharge as was done by Day (1976) for the case of outflow from springs.

For the section of flow net in figure 4.4

$$Q_o = Q_i + \int_{s=0}^i W n_s ds \quad 4.18$$

where Q_i is the streamtube discharge at section i , W is the vertical recharge rate and n_s is the width of the streamtube at position s . The difference

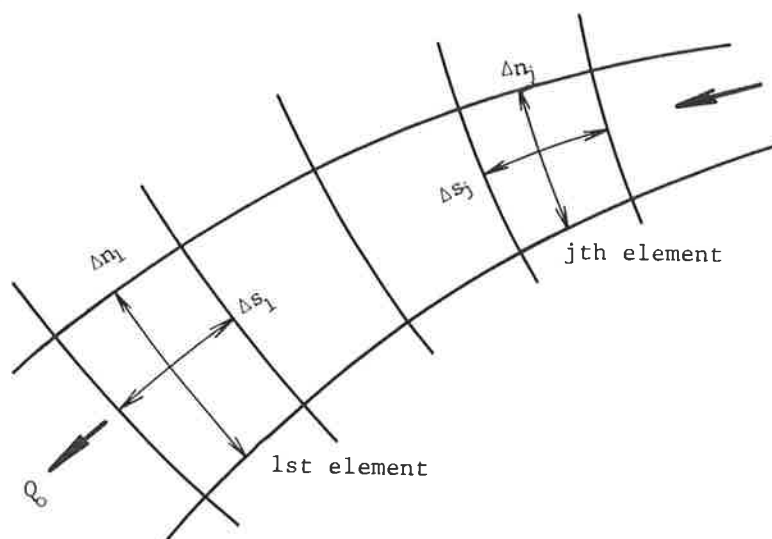


Figure 4.4 Portion of a streamtube

between the flows at section i and the end of the streamtube is given by the integral term which accounts for the vertical flow input between the two sections. Darcy's Law can be used to express flow in terms of transmissivity, head gradient and streamtube width, so that eqn 4.18 becomes:

$$T_o \left(\frac{\partial h}{\partial s} \right)_o n_o = T_i \left(\frac{\partial h}{\partial s} \right)_i n_i + \int_{s=0}^i W n_s ds \quad 4.19$$

Equation 4.19 can be approximated in discrete form, assuming a constant interval between piezometric contours of Δh and homogeneous vertical recharge, as

$$T_i = a_i T_o - b_i W / \Delta h \quad 4.20$$

where $a_i = (n_o / \Delta s_o) / (n_i / \Delta s_i)$

and $b_i = (\Delta s_i / n_i) \sum_{j=1}^i (n_j \Delta s_j)$

For convenience, eqn 4.20 is written in terms of T_o , the reference transmissivity on the downstream boundary of the flow net.

The flow net geometry can be used to derive the values of a_i and b_i for all streamtube elements. When used in conjunction with the finite difference grid, this approach effectively reduces the number of unknowns from the total number of flow net elements to one element on each streamtube.

The geometry of the flow net defines the relative transmissivities along each streamtube but does not give any information about the variation of transmissivity across the streamlines (Hunt and Wilson, 1974). Even when W is specified along a streamtube, a unique solution is not obtained unless W is the only source of flow in the streamtube. However, it is possible to introduce an additional constraint by assuming that the transmissivity can be represented as a continuous two-dimensional function and that therefore the finite difference grid can be used to approximate the transmissivity distribution defined by the flow net geometry.

This approximation has been done by superimposing the finite difference grid on the distributions of the a_i and b_i coefficients and interpolating to obtain

appropriate coefficient values at every node of the grid. The nodes at which the reference transmissivities should be specified can be identified by examination of the flow net. The inverse problem solution involves an iterative procedure that will adjust the initial estimate of these reference transmissivities to achieve a close fit between the predicted and observed piezometric heads.

A non-linear optimisation method is used to determine the reference transmissivities (and hence a transmissivity distribution). An initial estimate of the nv variables in the problem, $\bar{v} = (v_1 \ v_2 \ . \ . \ . \ v_{nv})$ is used to define the nv initial reference transmissivities, \bar{T}_{ref} , according to:

$$\begin{aligned} T_{ref}(1) &= (v_1 + v_2)/2 \\ T_{ref}(i) &= (v_{i-1} + v_i + v_{i+1})/3 \quad \text{for } 2 \leq i \leq nv-1 \\ T_{ref}(nv) &= (v_{nv-1} + v_{nv})/2 \end{aligned} \quad 4.21$$

The smoothing process described by eqn 4.21 is performed to suppress extreme fluctuations in the reference transmissivities. The node transmissivities are calculated from \bar{T}_{ref} with eqn 4.20 and a further smoothing of the transmissivity distribution carried out by putting for each node in turn:

$$T_O = (T_1 + T_2 + T_3 + T_4 + 4T_O)/8 \quad 4.22$$

where the subscripts are based on the node numbering convention defined in section 4.2.1. The smoothed transmissivity distribution is used with the steady finite difference model to obtain the calculated piezometric head, h .

An objective function is defined in terms of the differences between calculated and observed heads at selected nodes, and can be written as:

$$F(\bar{v}) = \sum_{i=1}^{n_h} (h_i - \hat{h}_i)^2 \quad 4.23$$

where \hat{h}_i is the observed steady state piezometric head at node i and n_h is the number of selected nodes with specified head. The automatic optimisation procedure is used to determine a new estimate of v and the process is continued until the objective function is reduced to some predetermined value. The optimisation procedure is VAO5A, from the Harwell subroutine library, which uses a combination of features from Newton-Raphson, steepest descent and Marquardt methods (Hopper, 1973).

The computer program developed to perform the above calculations is documented in a Ministry of Works and Development, Christchurch Hydrology Centre unpublished report, WS 696. The program is written in Fortran IV and has been run using TSO with an IBM 3033 computer. Hunt's (1976) steady-state model and the Harwell subroutine are incorporated in the program.

(b) Unsteady calibration

The second stage of the finite difference model calibration process involves using the transmissivities identified by the above procedure in an unsteady ground water model. The aquifer was assumed to have homogeneous storativity and a trial-and-error approach was taken by adopting a storativity value and examining the ability of the model to match observed piezometric level fluctuations.

The criterion adopted for testing the unsteady model performance is the measure proposed by Nash and Sutcliffe (1970):

$$R^2 = (F_o^2 - F^2)/F_o^2 \quad 4.24$$

where R^2 is the "model efficiency"

$$F_o^2 = \text{initial variance} = \sum_{1}^n (h' - \bar{h}')^2$$

$$F^2 = \text{index of disagreement} = \sum_{1}^n (h - h')^2$$

h' and h are the observed and computed piezometric heads at corresponding times, and \bar{h}' is the mean of the observed values.

To be free of transient effects, unsteady calibration simulations need to be run for some time before the calibration period. A series of simulations were performed using the same starting time and rainfall recharge input to find the value of aquifer storativity that gave maximum model efficiency.

The computer program developed to perform the unsteady model calculations is documented in a Ministry of Works and Development, Christchurch Hydrology Centre unpublished report, WS 697. The program is written in Fortran IV for the IBM 3033 and uses Hunt's (1976) unsteady program as a subroutine.

4.2.3 Summary of Modelling Approach

The methods described in the previous sections were used in the following sequence:

Calibration

- (i) Estimate steady and unsteady drainage from soil using the soil moisture model.
- (ii) Use lumped parameter model to establish the relationship between drainage from the soil moisture zone and aquifer recharge.
- (iii) Estimate \bar{h} representing steady-state conditions from piezometric survey data.
- (iv) Run the steady model with the optimisation procedure to solve the inverse problem for \bar{T} .
- (v) Run the unsteady model with optimum \bar{T} and V_t from the soil moisture model to determine storativity.

Simulation

- (vi) Use the soil moisture model to calculate potential irrigation demand.
- (vii) Run the unsteady model to simulate ground water response to alternative irrigation development options.

4.3 CALIBRATION

4.3.1 Soil Moisture Model

The results of the soil moisture recharge calculations are summarised in section 3.1. Of particular relevance to the ground water model are the calculated long-term average rainfall drainage, which is used as the steady recharge in the finite difference model steady calibration; and the time-dependent drainage and potential irrigation demand, which are used in the unsteady simulations of alternative ground water development options. The calculations of the potential irrigation demand are described in more detail here.

Potential irrigation demand was assessed by calculating the depth of irrigation application required to satisfy deficits in soil moisture on a daily basis, using the soil moisture model with 50 mm available soil moisture. The calculated daily demands were grouped into 10-day blocks to provide simulated water use data for the ground water simulations. A range of water use strategies was considered. Each was described in terms of the soil moisture levels at which irrigation was started and to which the soil was restored

after irrigation. These alternatives and the resulting mean annual demands are described in table 4.1.

Table 4.1 Alternative irrigation strategies.

| Strategy No. | 1 | 2 | 3 | 4 | 5 |
|---|---------|-----|-----|-----|-----|
| Soil moisture restored to: (mm) | 50 | 40 | 35 | 35 | 40 |
| Irrigation applied at soil moisture: (mm) | 25 | 20 | 20 | 15 | 15 |
| Field capacity (mm) | 50----- | | | | |
| Application strategy | 40----- | | | | |
| | 30----- | | | | |
| | 20----- | | | | |
| | 10----- | | | | |
| | 0----- | | | | |
| Permanent wilting point (mm) | 0----- | | | | |
| Mean annual demand (mm) | 326 | 232 | 205 | 167 | 182 |

Two of the tested strategies were used in the ground water simulations. Strategy 1, referred to later as the 'high water use', resulted in applications of 25 to 30 mm with approximately 11 applications in a typical season, and represents a relatively unconstrained approach to water use. Strategy 5, the 'low water use', required applications of 25 to 28 mm with about 7 applications per season, and represents a more constrained water use pattern. The 'low water use' strategy required only 56% of the water needed for the 'high water use' strategy. The time distribution of irrigation demand is shown for strategy 1 in figure 4.5, together with the associated rainfall drainage. Rainfall and pan evaporation for the same period are shown in figure 3.2.

For the unsteady finite difference model the calculated 10-day demand figures for strategies 1 and 5 were applied to the alternative irrigation scheme areas without further adjustment. Thus, irrigation supply system inefficiencies were assumed to be balanced by partial development of the total scheme area.

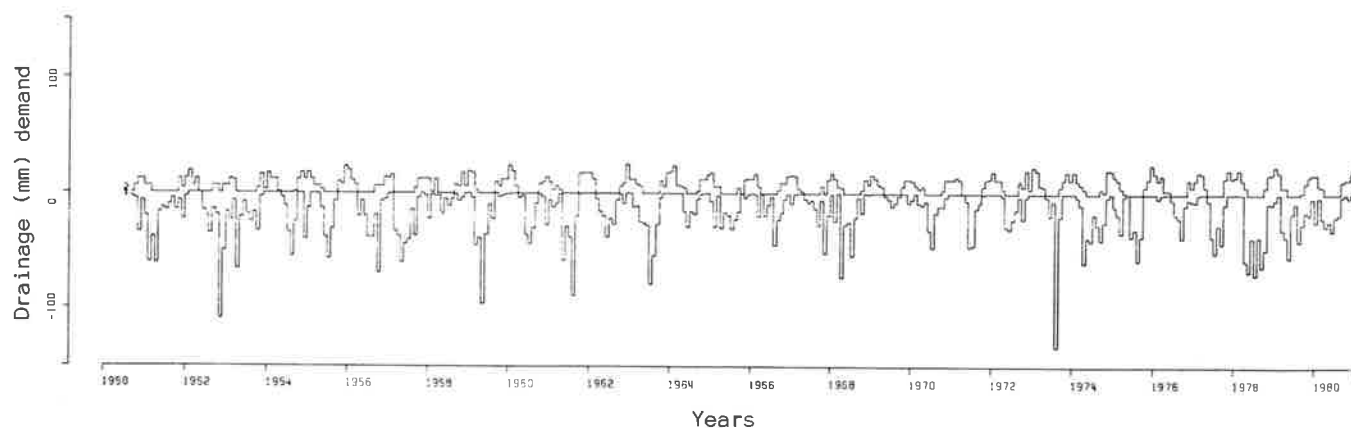


Figure 4.5 Irrigation demand (2) and rainfall drainage (1) for irrigation strategy 1 (high water use)

4.3.2 Lumped Parameter Ground Water Model

(a) Water balance components

The lumped parameter model treats the ground water system as a single cell and requires specification of the rainfall drainage, drainage from irrigation and withdrawals by pumping. The net leakage from and to the rivers and sea is dealt with implicitly and can be determined after the model has been calibrated.

The period from 1970 to 1980 was chosen for application of the lumped parameter model. During that period, pumping of ground water for irrigation began and increased steadily. Ground water abstraction was estimated by assuming that it followed the same temporal pattern as water use on the ALIS and that the installed irrigation systems were used to design capacity during the relatively dry 1977/78 irrigation season. Total pumpage for the 1977/78, 1978/79 and 1979/80 periods was calculated from electrical power consumption, using the relationship between power consumption and pumpage measured in a survey of pumped irrigation in the area (Price, MWD, pers. comm., 1983). From 1973 to 1978 the connected electrical load increased at an average annual rate of 50% (Maidment *et al.*, 1980), therefore the pattern of water use for the total period can be estimated (figure 4.6).

(b) Calibration and validation

The lumped parameter model was used to simulate the ground water level observed at the Charing Cross well. That site was chosen because an unbroken record

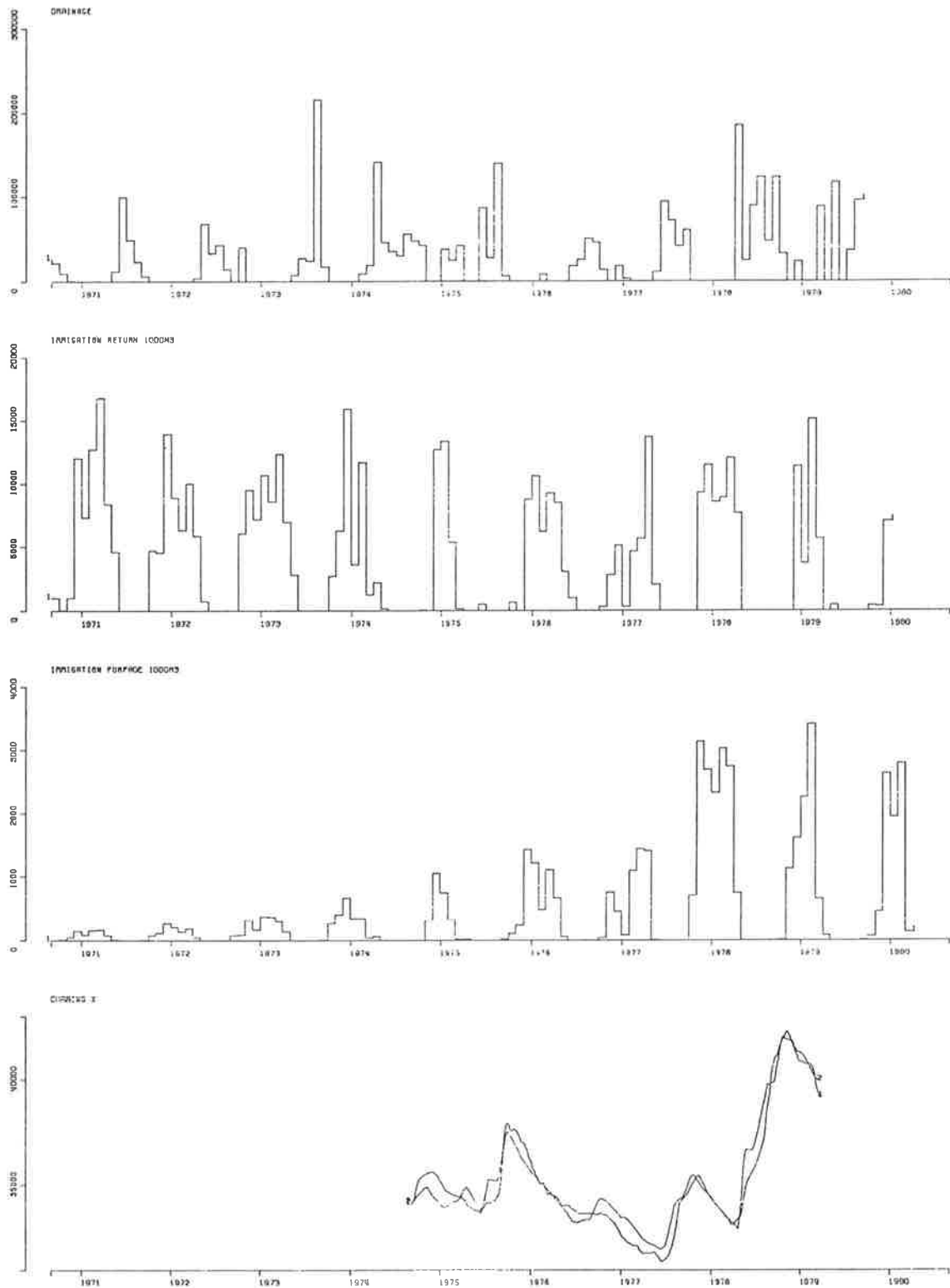


Figure 4.6 Monthly drainage, irrigation return, irrigation pumpage used in the lumped parameter model, together with the observed (1) and simulated (2) water-level records at Charing Cross

of regular water-level observations was available for several years during the 1970-1980 period (figure 4.6) and the site is within the area likely to be irrigated by further ground water development. Observed water-levels and calculated components of the water balance were discretised at 10-day time intervals. The water-level record was divided into two periods: the second, from December 1976 to March 1979, contained the greater range of levels and was used for model calibration, while the first, from September 1974 to December 1976, was used for model validation.

Model calibration was performed by adopting a scheme for the lagging of rainfall drainage and then using the VA05A automatic optimisation procedure to determine the unknowns in eqn 4.11. Initial optimisation runs showed that a significant improvement in model performance was achieved by lagging drainage of excess rainfall to produce:

$$V_t = A \left(\sum_{i=0}^n D_{t-i} \right) / n \quad 4.25$$

with $n = 3$, where V_t is the recharge from drainage occurring in time interval t , A is the effective cell area and D_t is the total drainage occurring in time interval t . Equation 4.25 lags the rainfall drainage over three 10-day periods. Other alternative treatments of rainfall drainage considered were $n = 0$ (no lagging), 1 and 4.

The best fit of the observed water-levels was achieved with the parameter values $a = 7.32 \times 10^5$, $b = 19.7$ and $S = 0.044$ (eqn 4.10). For the calibration period these values gave an RMS error of 0.58 m and a model efficiency $R^2 = 97.3\%$. For the validation period, the RMS error was 0.59 m and model efficiency $R^2 = 75.8\%$. The observed and simulated water-levels are plotted in figure 4.6. The mean observed head for the simulation period (35.2 m) with the above parameter values in eqn 4.9 indicate a mean net leakage out of the system of $13.1 \text{ m}^3 \text{ s}^{-1}$, which should be equivalent to the long-term average recharge, excluding leakage to or from rivers.

(c) Simulation of ground water response to development

The calibrated lumped parameter model was used to simulate ground water levels at Charing Cross for the period 1950 to 1979. Rainfall drainage was lagged according to eqn 4.25 and irrigation water use assessed for the high water use strategy. Because it is a minor component of the system inputs, the irrigation return flow was ignored.

Four ground water development options were considered: no irrigation, and the irrigation of 22 750, 32 130 and 44 800 ha, respectively. For the lumped parameter model, the 10-day ground water abstraction totals were calculated assuming that the irrigation supply system was 70% efficient. The resulting simulated ground water levels are plotted in figure 4.7.

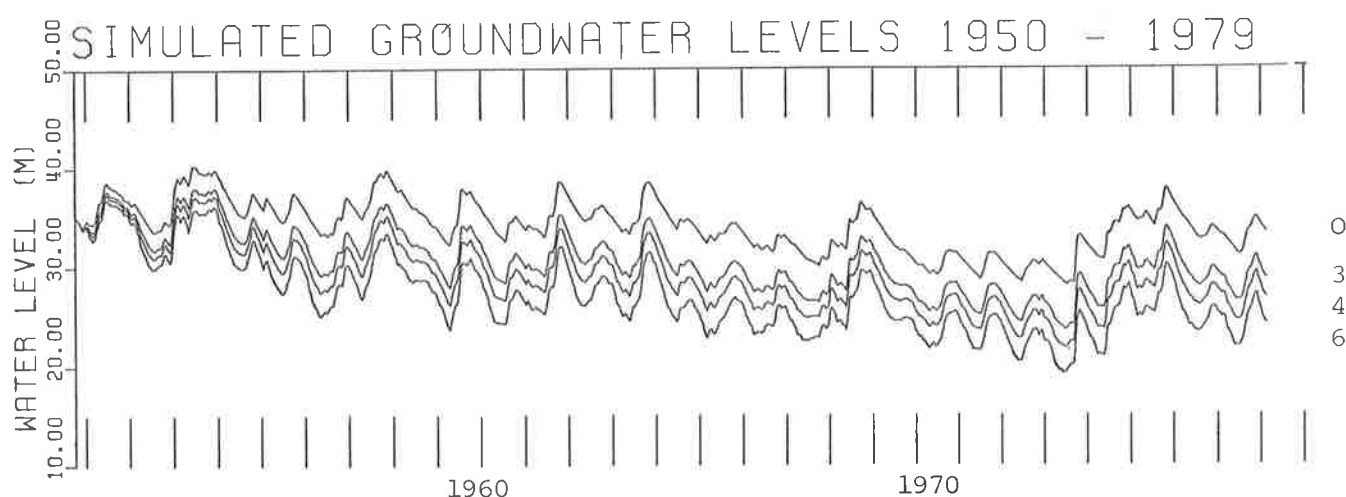


Figure 4.7 Long-term water level fluctuations simulated using the lumped parameter model for no irrigation development and three development alternatives (table 4.2 : schemes 3, 4 and 6)

For each of the three development options the initial model response shows a transient period of several years before a new equilibrium level is reached. A summary of the results is given in table 4.2.

Table 4.2 Irrigation demands and lumped parameter model water-level ranges at Charing Cross for the postulated irrigation schemes (high water use strategy).

| Scheme No. | Area (ha) | Q(10d) (m^3s^{-1}) | Q(annual) (m^3s^{-1}) | Q(peak) (m^3s^{-1}) | Range of Water Levels (m) | | |
|------------|-----------|--------------------------------------|---|---------------------------------------|---------------------------|-------|------------|
| | | | | | h min | h max | Δh |
| 0 | - | - | - | - | 28.12 | 40.23 | - |
| 3 | 22 750 | 10.7 | 3.36 | 21.1 | 23.67 | 38.02 | 4.45 |
| 4 | 32 130 | 15.1 | 4.74 | 29.8 | 21.80 | 37.37 | 6.32 |
| 6 | 44 800 | 21.1 | 6.61 | 41.6 | 19.25 | 36.90 | 8.87 |

Δh is the difference between the minimum water-level for the no irrigation option and the minimum for each of the irrigation development options.

4.3.3 Finite Difference Model Calibration

(a) Model description

The area represented by the finite difference model is shown in figure 4.8 and encompasses the alternative ground water supply areas for the Lower Rakaia Irrigation Scheme (Maidment *et al.*, 1980). The inland boundary was chosen to exclude the area where the absence of observation wells prevented accurate definition of the piezometric surface.

The finite difference grid is square with a node spacing of 1828.71 m (2000 yd); the area represented by each internal node is 334.4 ha. Following Hunt's (1976) convention, the nodes are numbered sequentially along a boundary of specified head (Ashburton River mouth to Rakaia River mouth), along boundaries of specified gradient (Rakaia River boundary, inland boundary and Ashburton River boundary) and then along the series of columns within the model, giving 57 boundary nodes and 244 nodes in all.

The piezometric surveys show that ground water levels tend towards sea level near the coast (figure 4.9). Accordingly, the ocean boundary was specified as a zero head boundary. Flow across the boundary was calculated using a second-order approximation for the gradient at each boundary node.

The inland boundary was specified as a boundary of constant piezometric gradient. The size and direction of the gradient specified for each boundary node were measured from the April 1982 piezometric contour map. Gradient fluctuations along the boundary were smoothed to the specified gradients shown by the vectors plotted in figure 4.8. The average gradient is approximately 1 in 200.

In an early version of the finite difference model, trials were performed with the river boundaries specified as constant head boundaries. This provided a constraint to predicted ground water levels near the rivers, but allowed unrestrained and unrealistic inflow from the rivers when increased ground water abstraction was simulated. For the initial version of the present model, constant boundary gradients were specified for the river nodes. This proved unsatisfactory as it implies that the contribution from the rivers is totally independent of the ground water levels.

Subsequent field work demonstrated that on the Rakaia River side of the model the river water levels and the ground water levels were distinct (figure 4.9).

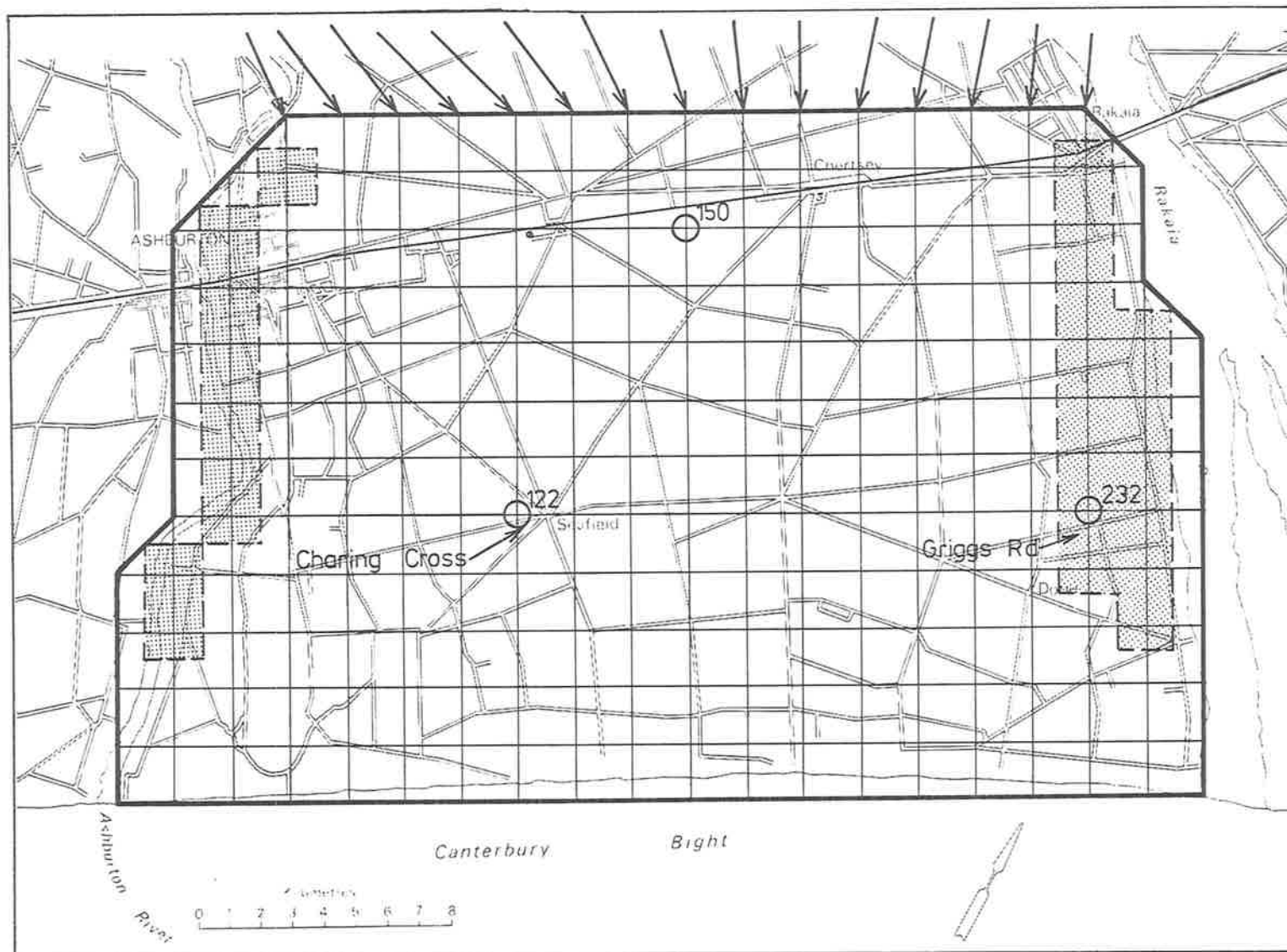


Figure 4.8 Finite difference model boundary and grid. The specified gradients on the inland boundary are indicated by the arrows. The shaded areas are treated as potentially leaky from the rivers. Nodes 122, 150 and 232 have been chosen to provide representative output from the model

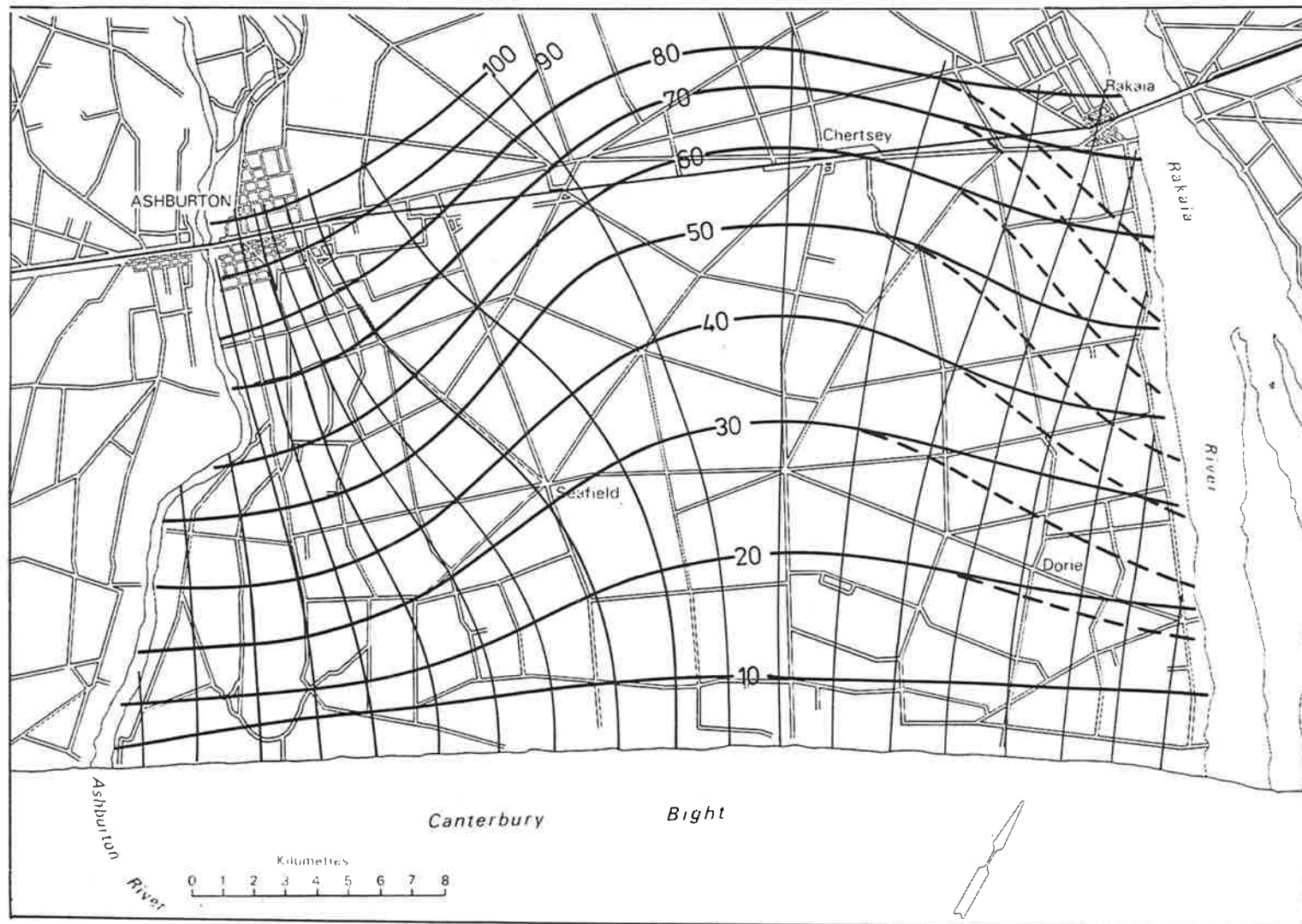


Figure 4.9 Steady-state piezometric contours (m) estimated from May and October 1978 surveys, together with streamlines drawn to complete the flow net analysis. The dashed lines adjacent to the Rakaia River show the contours drawn if unconfined aquifer levels are used

That boundary has now been described as a constant gradient boundary with an adjacent leaky zone. The nodes at which leakage is able to occur are shaded in figure 4.8. A broad zone adjacent to the Rakaia River has been described as a leaky area. The nature and extent of this zone were inferred from borelog and water-level information.

The leakage coefficient used in eqn 4.12 is given by the expression:

$$P = k' A / m' \quad 4.26$$

where k' is the aquitard permeability, m' is the aquitard thickness and A is the area over which leakage occurs. Assuming that the total area of each node is leaky, then for an aquitard thickness of 5 m and permeability of $3 \times 10^{-7} \text{ m s}^{-1}$ the leakage coefficient is $0.02 \text{ m}^2 \text{ s}^{-1}$. The reference head values in this zone were estimated from water-levels observed in shallow wells in piezometric surveys.

On the Ashburton River side of the model, constant gradients were specified and leakage nodes chosen to follow the course of the river. The two nodes adjacent to the coastal boundary were not treated as leakage nodes because the river falls outside the node areas and the low flow gaugings showed no significant river flow changes in that section. The leakage coefficients for the Ashburton River were initially estimated by assuming that the river is partially penetrating the aquifer. From Rushton and Redshaw (1979) a leakage coefficient appropriate for this case can be written for each node as:

$$P = \pi \ell k / \log_e (0.5 \text{ m} / r_r) \quad 4.27$$

where ℓ is the length of river reach, k is aquifer permeability, m is aquifer thickness and r_r is the effective river half width. Assuming that the length of river reach is equal to the node spacing and that the ratio $0.5 \text{ m} / r_r$ is approximately 10, then for a permeability of 1 m day^{-1} the leakage coefficient is $0.03 \text{ m}^2 \text{ s}^{-1}$. This value was used for all the leakage nodes along the Ashburton River. The reference head values along the Ashburton River were estimated from the NZMS1 topographic map.

(b) Flow net analysis

To apply the parameter estimation technique described in section 4.2.2, a flow net analysis was used to establish the spatial distribution of the coefficients a_i and b_i in eqn 4.20. The analysis was performed using a smoothed

piezometric surface derived from the average of the May and October 1978 piezometric surveys to obtain an estimate of a steady-state condition.

The flow net was prepared with a piezometric contour spacing of 10 m. Streamlines were sketched at close intervals, using a trial-and-error approach to ensure that they were orthogonal to the contours. Intermediate streamlines were then removed to produce a set of streamtubes of approximately equal width to match the finite difference model node spacing at the coastal boundary (figure 4.9). The lengths and widths of the streamtube elements were measured from the completed flow net and the a_i and b_i coefficients calculated for each streamtube element, using the relationships given in eqn 4.20.

The next step in applying the parameter estimation technique involved the specification of equivalent coefficient values at each node of the finite difference model, as outlined in section 4.2.2. The resulting distribution of the node coefficients is shown in figure 4.10.

On the river boundaries of the model, coefficients were obtained by extrapolation or were assigned nominal values. The a_i coefficient distribution is a function of the relative proportions of elements along a streamtube, whereas the b_i coefficient distribution reflects the progressive increase of the rainfall drainage recharge area away from the coastal boundary.

The above procedure required a segmentation of the finite difference grid, since each node had to be related to a reference node on the coastal boundary of the model. This was done by using the flow net to determine what model nodes were 'upstream' of each boundary node. The flow net analysis results in the definition, for each node in the finite difference model, of the coefficients a_i and b_i and the appropriate coastal boundary node number. The segmentation of the grid, in which each node is labelled with the same letter as its boundary reference node, is illustrated in figure 4.11.

(c) Parameter estimation

The solution of the steady inverse problem requires quantification of steady-state flow rates and definition of criteria for comparing solutions derived from different transmissivity distributions. The long-term average rainfall drainage of 309 mm/year was used as the steady-state recharge rate. This is equivalent to a uniform flow of $0.0327 \text{ m}^3 \text{ s}^{-1}$ per finite difference node. For this recharge rate the recharge term, W , in eqn 4.20 has the value $9.79 \times 10^{-9} \text{ m s}^{-1}$.

DISTRIBUTION OF COEFFICIENT A
(SCALE FACTOR 10-)

| | | | | | | | | | | | | | | | | | | | |
|----|----|----|----|----|----|----|----|----|----|----|----|----|----|----|----|----|----|----|----|
| | | | 9 | 4 | 1 | 1 | 1 | 1 | 1 | 1 | 2 | 2 | 2 | 2 | 2 | 4 | 5 | 6 | |
| | | 10 | 16 | 6 | 1 | 1 | 1 | 1 | 2 | 4 | 3 | 4 | 4 | 4 | 4 | 6 | 6 | 8 | 10 |
| 20 | 30 | 25 | 8 | 2 | 1 | 1 | 1 | 2 | 2 | 4 | 4 | 5 | 6 | 6 | 8 | 9 | 13 | 15 | |
| 20 | 30 | 29 | 10 | 4 | 2 | 2 | 2 | 3 | 4 | 6 | 7 | 8 | 8 | 8 | 8 | 12 | 15 | 16 | |
| 20 | 28 | 36 | 17 | 7 | 5 | 3 | 4 | 4 | 5 | 7 | 9 | 9 | 9 | 9 | 11 | 14 | 15 | 14 | 16 |
| 20 | 30 | 36 | 24 | 10 | 6 | 6 | 5 | 6 | 7 | 10 | 9 | 9 | 10 | 12 | 14 | 15 | 14 | 16 | |
| 20 | 37 | 37 | 23 | 15 | 9 | 8 | 8 | 7 | 7 | 13 | 13 | 12 | 13 | 12 | 13 | 14 | 14 | 15 | |
| | 30 | 26 | 28 | 22 | 16 | 11 | 10 | 11 | 12 | 12 | 16 | 15 | 15 | 17 | 17 | 17 | 15 | 14 | 15 |
| 30 | 38 | 33 | 28 | 27 | 14 | 13 | 13 | 14 | 14 | 13 | 16 | 16 | 17 | 17 | 18 | 20 | 17 | 23 | 30 |
| 20 | 22 | 29 | 23 | 21 | 14 | 15 | 15 | 14 | 15 | 16 | 17 | 18 | 18 | 18 | 18 | 17 | 16 | 21 | 20 |
| 20 | 21 | 28 | 16 | 18 | 14 | 12 | 12 | 14 | 15 | 16 | 16 | 16 | 18 | 18 | 17 | 15 | 15 | 13 | 12 |
| 10 | 13 | 12 | 10 | 10 | 9 | 10 | 10 | 10 | 10 | 10 | 10 | 10 | 10 | 11 | 10 | 11 | 11 | 11 | 10 |
| 10 | 10 | 10 | 10 | 10 | 10 | 10 | 10 | 10 | 10 | 10 | 10 | 10 | 10 | 10 | 10 | 10 | 10 | 10 | 10 |

DISTRIBUTION OF COEFFICIENT B
(SCALE FACTOR 1000000-)

| | | | | | | | | | | | | | | | | | | | |
|----|----|----|----|----|----|----|----|----|----|----|----|----|----|----|----|----|----|----|----|
| | | | 45 | 30 | 19 | 17 | 13 | 12 | 12 | 15 | 16 | 18 | 14 | 12 | 22 | 25 | 35 | | |
| | | 50 | 50 | 30 | 16 | 13 | 13 | 14 | 16 | 17 | 17 | 20 | 21 | 22 | 25 | 30 | 43 | 48 | |
| | 10 | 40 | 50 | 32 | 15 | 13 | 14 | 14 | 18 | 18 | 18 | 23 | 25 | 25 | 26 | 35 | 45 | 50 | |
| | 10 | 40 | 55 | 30 | 22 | 15 | 15 | 14 | 18 | 19 | 19 | 26 | 28 | 27 | 30 | 38 | 41 | 49 | |
| | 10 | 30 | 55 | 43 | 23 | 19 | 15 | 19 | 20 | 19 | 19 | 24 | 26 | 27 | 30 | 35 | 40 | 45 | 50 |
| | 10 | 30 | 45 | 45 | 27 | 19 | 18 | 19 | 19 | 19 | 20 | 22 | 24 | 24 | 26 | 32 | 35 | 50 | 59 |
| | 10 | 30 | 36 | 35 | 27 | 19 | 18 | 18 | 18 | 18 | 18 | 19 | 22 | 22 | 24 | 24 | 23 | 25 | 30 |
| | 10 | 14 | 20 | 23 | 23 | 17 | 16 | 16 | 17 | 20 | 18 | 19 | 21 | 21 | 20 | 22 | 20 | 21 | 20 |
| 10 | 15 | 14 | 16 | 18 | 14 | 12 | 13 | 13 | 15 | 20 | 15 | 15 | 18 | 19 | 21 | 20 | 18 | 17 | 16 |
| 10 | 12 | 10 | 9 | 11 | 9 | 8 | 11 | 9 | 8 | 7 | 8 | 8 | 7 | 7 | 8 | 9 | 13 | 13 | 12 |
| | 4 | 5 | 5 | 4 | 6 | 6 | 5 | 4 | 5 | 6 | 7 | 7 | 7 | 7 | 7 | 6 | 6 | 6 | 6 |
| | 2 | 2 | 1 | 1 | 1 | 1 | 1 | 1 | 0 | 0 | 0 | 0 | 0 | 0 | 0 | 0 | 1 | 1 | 2 |
| | 0 | 0 | 0 | 0 | 0 | 0 | 0 | 0 | 0 | 0 | 0 | 0 | 0 | 0 | 0 | 0 | 0 | 0 | 0 |

Figure 4.10 Patterns of coefficients a_i and b_i at model nodes

The objective function used by the automatic optimisation procedure provides the basis for comparing alternative solutions and is primarily defined by the differences between simulated and observed piezometric heads. A requirement of the optimisation procedure is that the number of unknowns must not exceed the number of items in the objective function. Hence, to treat 20 reference transmissivities across the coastal boundary as unknowns requires a minimum of 20 nodes with the observed heads specified. An obvious requirement for the selection of these nodes is that there should be at least one in each of the flow net segments of the finite difference model (figure 4.11). In addition, the nodes of observed heads should preferably be in positions where the steady-state piezometric head is well defined or where gradients are high; they should not be on or adjacent to a specified head boundary where they would provide relatively little information.

The positions of the 28 observed heads specified to represent the steady-state piezometric surface are shown in figure 4.12. The observed head was determined from the mean of the piezometric surfaces defined in the May 1978 and April 1982 piezometric surveys. The smoothed contours were used in interpolating levels at the selected nodes. In the region adjacent to the Rakaia River boundary, the observed differences between piezometric levels of the shallow aquifer and

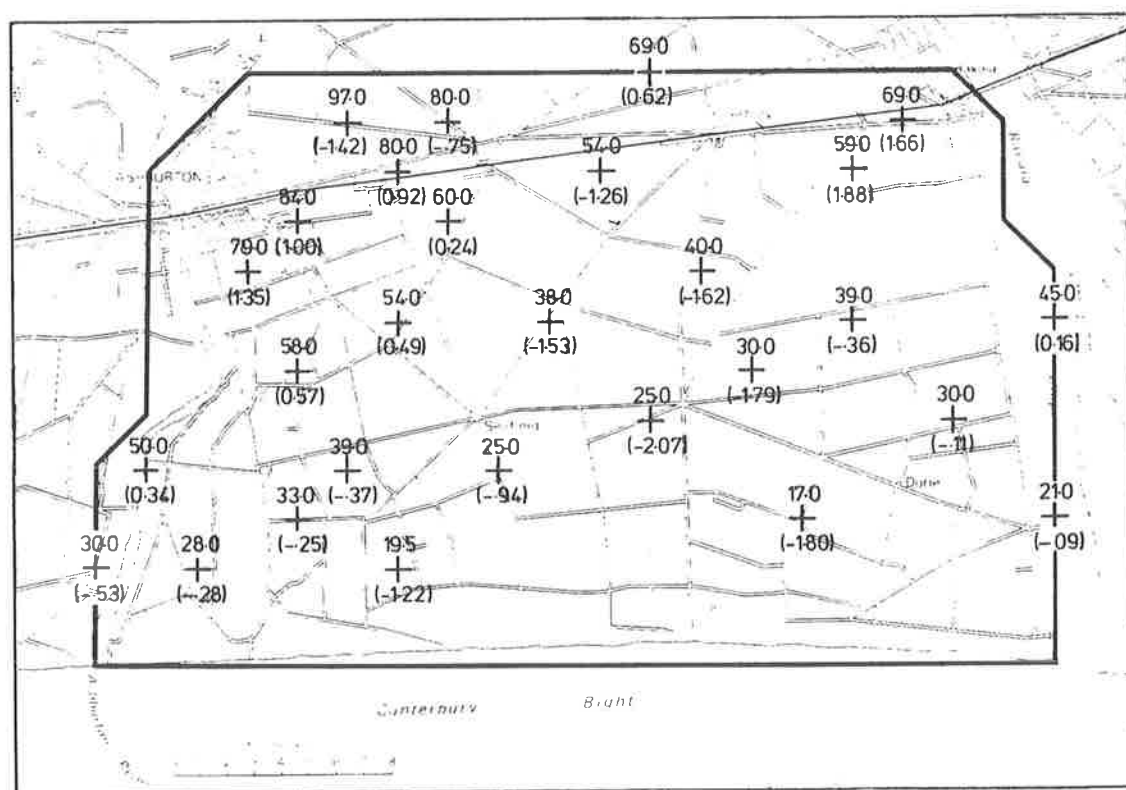


Figure 4.12 Location of nodes and observed head in metres. The value in brackets is the error in the final calibrated model

the deeper aquifer beneath the relatively impermeable material under the river were used to extrapolate the piezometric surface to the model boundary (figure 4.9).

Initial experience with model calibration, using an objective function dependent only upon heads (eqn 4.23), showed that solutions with acceptable errors in head could have quite unacceptable boundary flows and extreme transmissivities. To overcome this problem, a boundary flow term and a maximum transmissivity value were incorporated in the objective function, so that eqn 4.23 was rewritten as:

$$F(\bar{v}) = \sum_{i=1}^{n_h} (h_i - \hat{h}_i)^2 + (Q_b - \hat{Q}_b)^2 + C(T_{\max} - \hat{T}_{\max})^2 \quad 4.28$$

where Q_b is the simulated flow across the inland boundary of the model, \hat{Q}_b is the 'expected' value for flow across the boundary, T_{\max} is the maximum transmissivity for the alternative being evaluated and \hat{T}_{\max} is the 'expected' maximum transmissivity. The coefficient C is the weighting factor which can be used to change the penalty for departures from the expected value.

From an examination of the water balance calculations described in section 3, the following flow criteria were selected for model calibration and comparison of solutions: the flow across the inland boundary of the model should be between 8 and 12 m³ s⁻¹, the total flow from the Rakaia River boundary and adjacent leakage zone should be between 2 and 5 m³ s⁻¹ and the total flow from the Ashburton River should be between -0.5 and +0.5 m³ s⁻¹. The values of the simulated flows from the rivers were used to establish appropriate leakage coefficients.

Because of the tendency of the inverse solution to identify solutions with unrealistically high transmissivities, an 'expected' maximum of 0.7 m² s⁻¹ was set with a weighting factor of 100. This combination of factors was selected after a series of trials showed that a lower maximum value resulted in significantly poorer solutions in terms of piezometric head. A minimum transmissivity of 0.001 m² s⁻¹ was used to prevent excessive transmissivity gradients affecting the numerical stability of the solution procedure.

The performance of the optimisation procedure in reducing the objective function is illustrated in figure 4.13, where the initial reference transmissivities were set to a uniform value of 0.1 m² s⁻¹. Despite the ability of the procedure

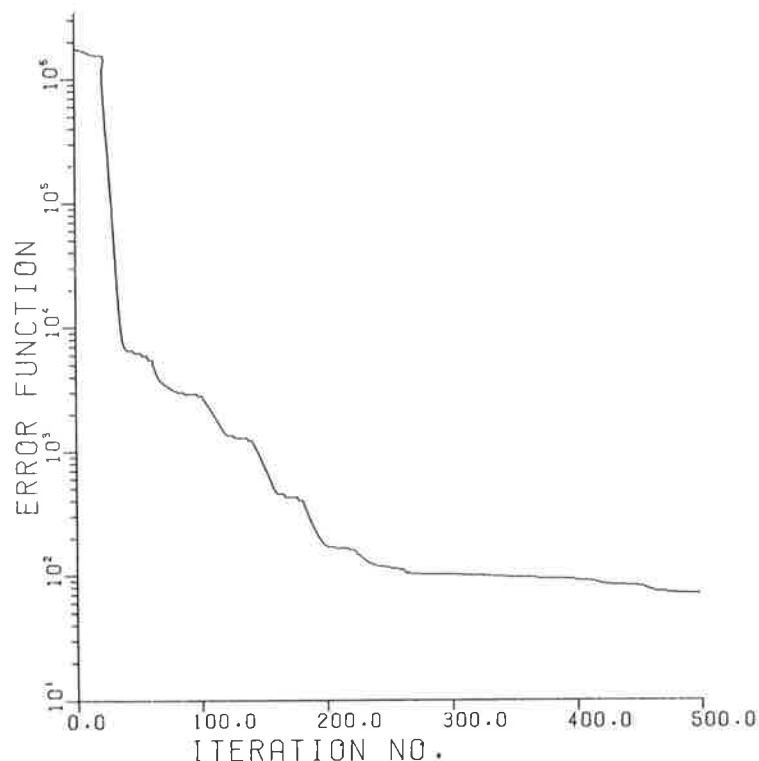


Figure 4.13 Performance of the automatic optimisation technique in reducing the objective function

to achieve such improvements, the calibration procedure was very time consuming as it involved a set of many optimisation runs, and the re-specification of parameters and the objective function before the result indicated in figure 4.13 could be achieved.

The final solution achieved an RMS error in observed head of 1.10 m and a maximum error of 2.07 m. The differences between observed and simulated head are shown in brackets in figure 4.12. Transmissivity contours for this solution are plotted in figure 4.14 (a), with the simulated steady-state heads and the inland boundary flows implied by the solution in figure 4.14 (b). The zone of high transmissivity values was a feature common to all solutions with tolerable reproduction of observed heads. These transmissivities are higher than those measured in pump tests at individual wells. However, the model estimates the total transmissivity of the saturated thickness of the aquifer, whereas values measured at individual wells will relate only to the vertical interval of the aquifer connected to the well. In the complex, vertically heterogeneous aquifer gravels it is possible for these two values to vary markedly, and this was observed in field tests (see table 2.3, Dobsons Ferry Rd, wells A cf. B).

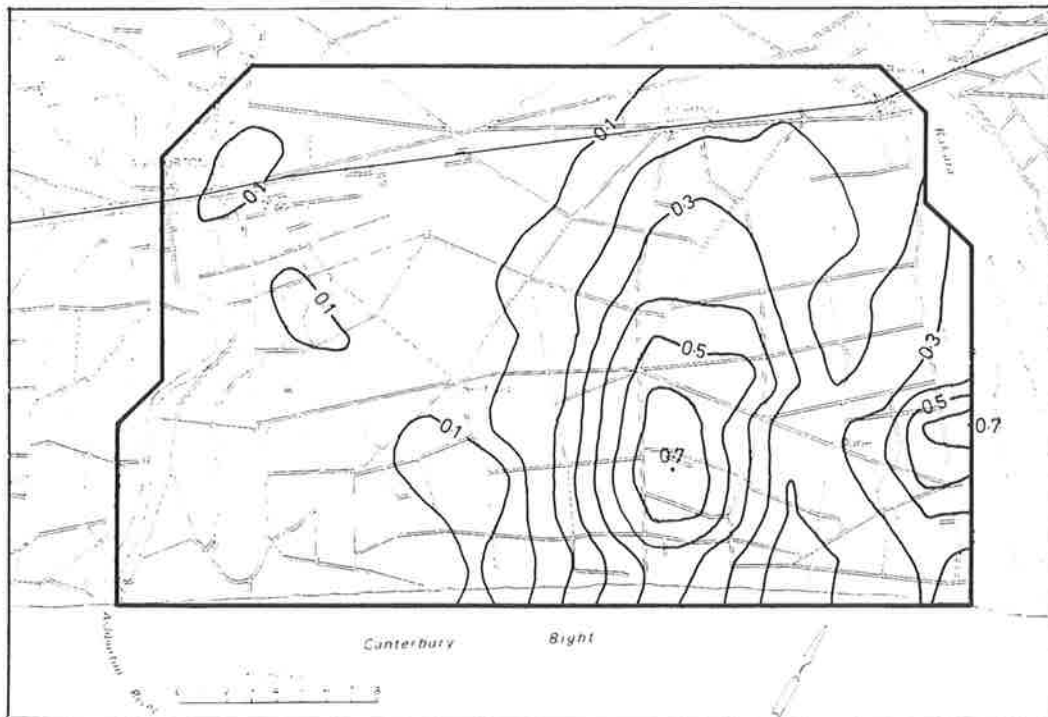


Figure 4.14(a) Contours of transmissivity ($\text{m}^2 \text{s}^{-1}$) for the calibrated model

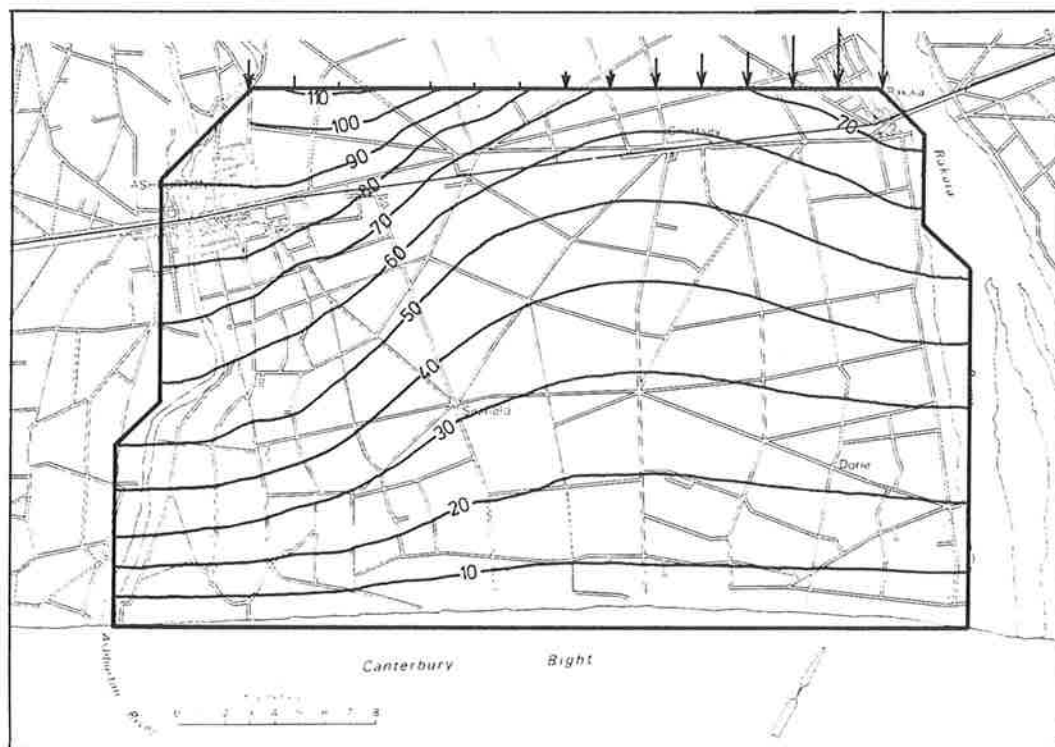


Figure 4.14(b) Steady-state piezometric levels simulated using the transmissivity distribution shown in figure 4.14(a). The arrows on the inland boundary show the relative distribution of flow across that boundary

The distribution of transmissivity across the inland boundary of the model indicates that over 80% of the boundary flow occurs across the Rakaia River half of the inland boundary. This is consistent with the shape of the piezometric surface on the inland side of the model. Extrapolating the streamlines beyond the model area indicates that considerably more than 50% of the inland rainfall recharge will flow to the Rakaia River side of the model region.

(d) Unsteady calibration

The transmissivity distribution calculated using the steady inverse problem solution was used in the unsteady model to determine an optimum homogeneous storativity term. Unsteady simulations were performed for a period of 30 years, using the steady-state head solution as the initial head distribution. The simulation was done with a 10-day time step, and rainfall drainage was lagged using the procedure developed for the lumped parameter model. The unsteady model performance was evaluated by calculating the model efficiency (eqn 4.24), using the piezometric heads calculated at node 122 and those observed at the adjacent Charing Cross well for the period from March 1974 to August 1978. A series of unsteady simulations, using successive readjustments of storativity, resulted in a maximum model efficiency of 78% with a storativity of 0.055, which is close to the value of 0.044 obtained with the lumped parameter model using the same period of observation.

The simulated and observed piezometric heads for the calibrated model are plotted in figure 4.15 for node 122 and the Charing Cross well, and for the corresponding period for node 232 and the adjacent Griggs Rd well.

4.4 FINITE DIFFERENCE MODEL SIMULATIONS

4.4.1 Options Considered

The effects of a range of irrigation development options were examined by performing a series of simulations for several different ground water development areas with alternative water use strategies. Five different scheme areas were considered and are described in table 4.3. These included three of the options considered in conjunction with the development of the Lower Rakaia Irrigation Scheme (Maidment et al., 1980) and a further two alternatives.

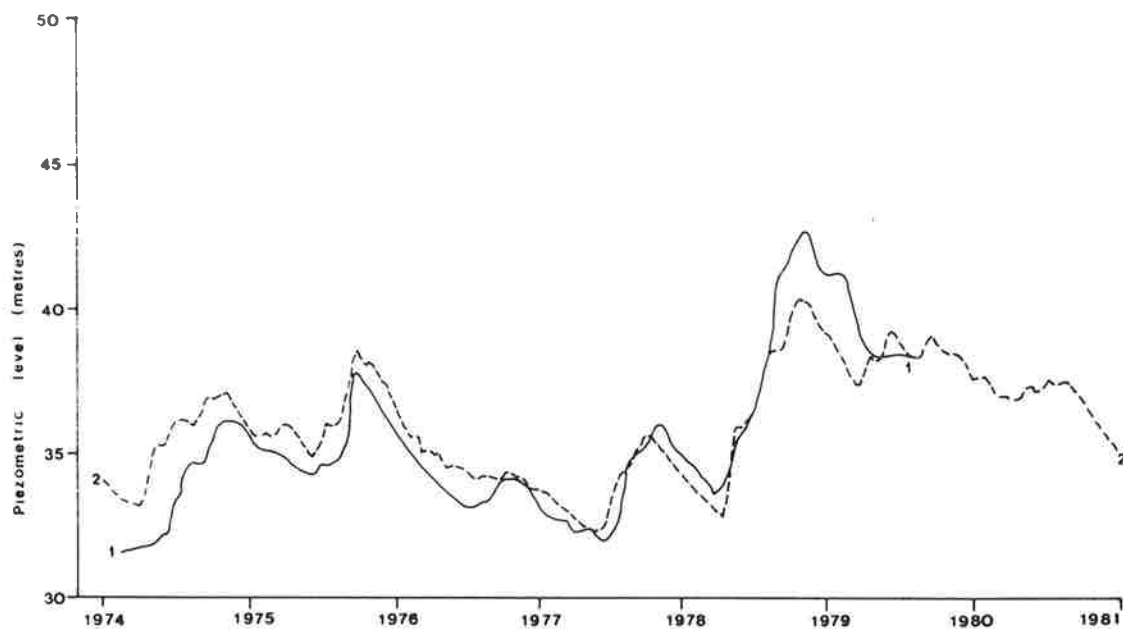


Figure 4.15(a) Observed (1) and simulated (2) piezometric levels at Charing Cross and node 122

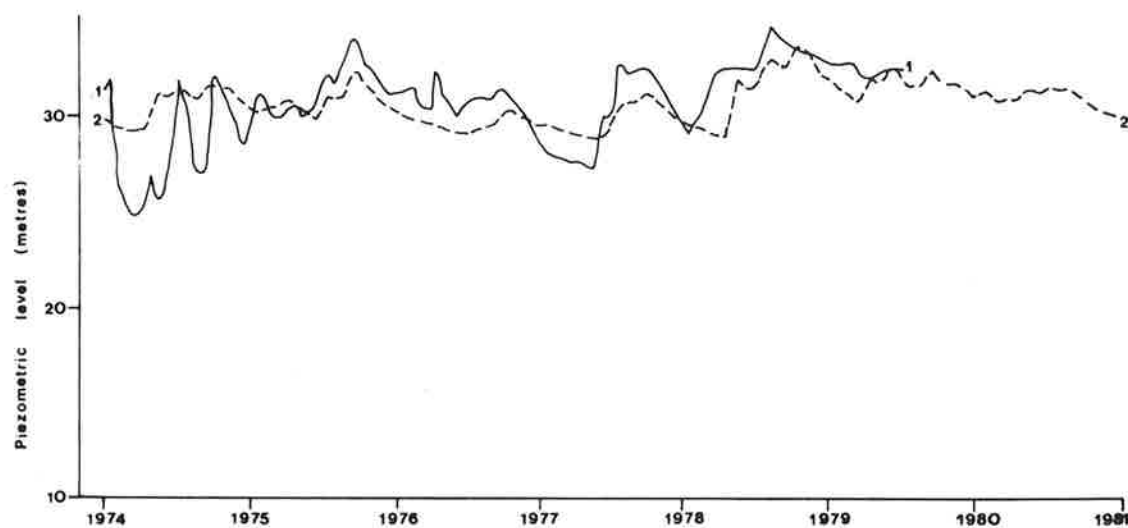


Figure 4.15(b) Observed (1) and simulated (2) piezometric levels at Griggs Rd and node 232

Table 4.3 Alternative ground water development areas.

| Scheme No. | Area (ha) | Comment |
|------------|-----------|---|
| 3 | 22 740 | approximately equivalent to scheme LR3 (described in Maidment <u>et al.</u> , 1980) |
| 4 | 32 070 | approximately equivalent to scheme LR4 |
| 6 | 44 780 | approximately equivalent to scheme LR6 |
| 7 | 32 070 | same total area as scheme 4 with modified boundary |
| 9 | 54 443 | almost complete ground water development |

Alternative ground water development options were represented in the finite difference model by superimposing the finite difference grid over a plan of each scheme and recording those nodes within the ground water development area. For nodes adjacent to scheme boundaries an estimate was made of the proportion of the node area within the boundary.

Eight simulations were performed, each for a 30 year period, using combinations of development areas and water use strategies, as listed in table 4.4. In addition, the results of a simulation for no ground water development have been included to provide a baseline for comparison.

Table 4.4 Ground water development simulations.

| Simulation No. | Scheme No. | Water Use |
|----------------|------------|-----------|
| 0 | no scheme | - |
| I | 3 | high |
| II | 4 | high |
| III | 6 | high |
| IV | 7 | high |
| V | 6 | low |
| VI | 6 | recharge |
| VII | 9 | high |
| VIII | 9 | low |

The water use strategies considered were the high water use (average annual irrigation demand 326 mm) and low water use (average annual irrigation demand 182 mm) options described in section 4.3.1. In addition, one simulation was performed using the high water use strategy in conjunction with artificial recharge for a six month period each year at a rate of $2.0 \text{ m}^3 \text{ s}^{-1}$ distributed over four nodes alongside the inland boundary. This option is referred to here as the 'recharge' option.

4.4.2 Analysis of Results

Simulation experiments performed using an earlier version of the unsteady model illustrated the difficulty of summarising the results in a concise and comprehensible way. A 30-year simulation of 244 nodes with 10-day time steps produces more than 250 000 individual simulated piezometric levels. A range of techniques was tried to summarise the results, using a representative level for each node.

The alternative levels are illustrated for node 122 and simulation II in figure 4.16. The 1 in 5-year minimum was estimated by plotting the annual minima on Gumbel probability paper. Analysis of the auto-correlation of the annual minima showed that persistence in the simulated record was slight enough to allow the use of frequency analysis. However, the annual minimum is maintained for a very short time relative to the period of irrigation water demand and gives a rather severe indication of the impact of ground water development. The 1 in 5-year 90% exceeded level was interpolated from the plot of the Gumbel distribution of the heads exceeded 90% of the time, as an annual series. Though this statistic does include a useful indication of frequency and duration, considerable computational effort is required to calculate it for every node and simulation.

A simpler procedure was used to calculate the 90% value. The simulated levels at each node were sorted in ascending order and the value exceeded 90% of the time taken directly from that series. Analysis of these results showed that, except for simulation VI (recharge), the minimum and 90% exceeded levels can be related by the approximate relationship:

$$(h_{o_i} - h_{min_i}) \approx A(h_{o_i} - h_{90_i}) \quad i = 1, 2, \dots, nt \quad 4.29$$

where h_{o_i} is the initial equilibrium level for node i , h_{min_i} is the minimum level for node i , h_{90_i} is the value exceeded 90% of the time at node i , A

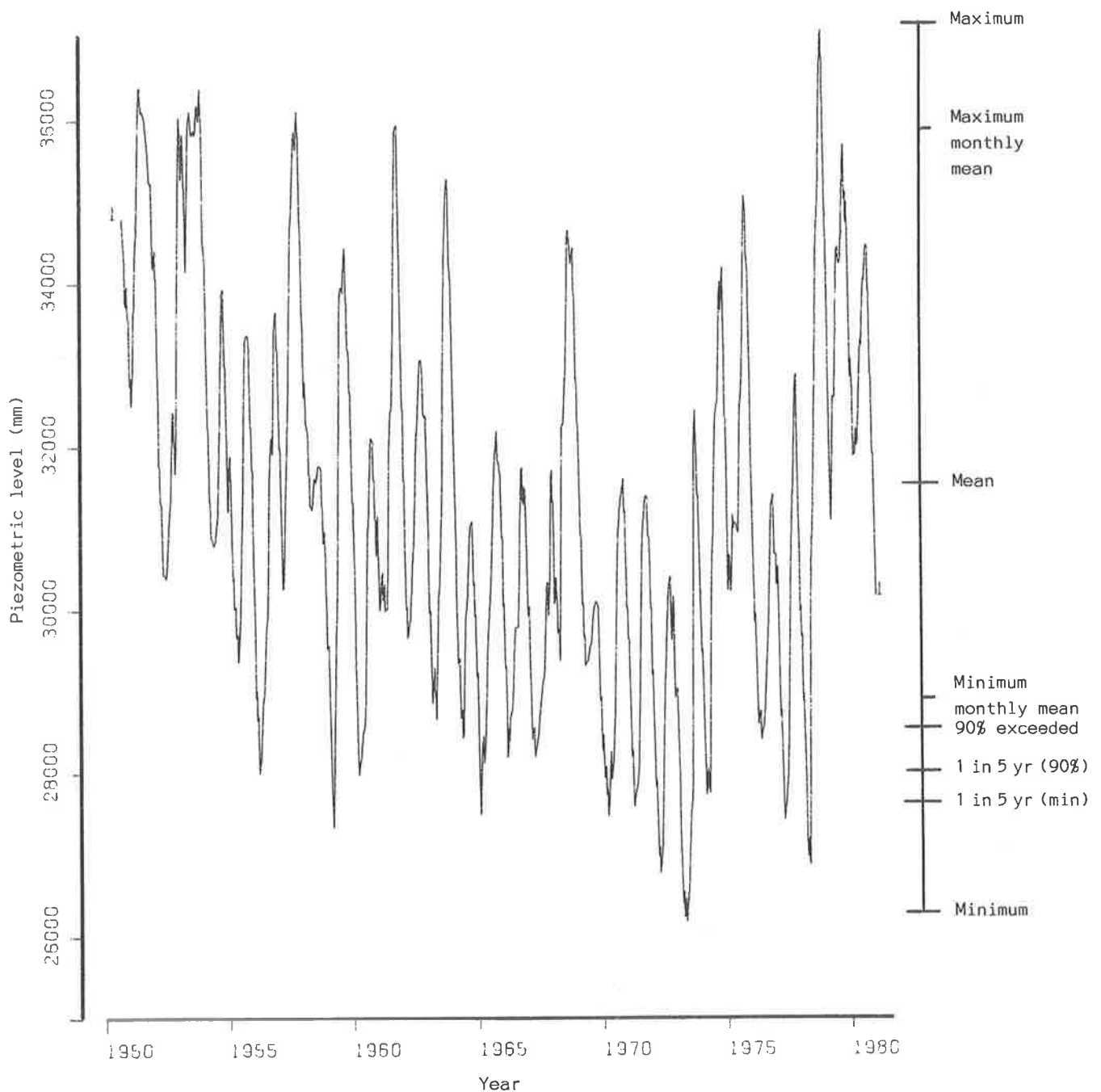


Figure 4.16 Simulated piezometric levels for node 122 showing a range of representative levels

is a constant for the particular simulation and n_t is the total number of model nodes. The h_{90} surface was adopted for presentation of the results of the eight simulations because it can be calculated quite simply for every node and each simulation, can be approximately related to the surface of absolute minima and conveys a useful indication of reliability of ground water levels.

4.4.3 Impact of Ground Water Development - Spatial Description

The results of the simulation of schemes 3, 4, 6 and 9 with the high water use strategy (simulations I, II, III and VII) are illustrated in figures 4.17, 4.18, 4.19 and 4.20, respectively. In the (a) section of each of these figures the size of the ground water development area is shown, together with contours of the corresponding depth to ground water exceeded for only 10% of the 30-year simulation period. The contours of depth to ground water have been drawn in the areas for which accurate topographic data are available.

For simulation I (figure 4.17 (a)) only a small section of the scheme 3 ground water development area experiences depths to ground water greater than 30 m, and nowhere within the area do depths exceed 35 m. Simulation II (figure 4.18 (a)) shows that within the scheme 4 ground water development area the maximum depth to ground water is less than 40 m. The corresponding maximum depths for simulations III and VII (figures 4.19 (a) and 4.20 (a)) are less than 52 m (scheme 6) and less than 70 m (scheme 9). The increasing maximum depths are largely the result of the natural difference between ground surface levels and ground water levels. Although there is a successive lowering of ground water levels for each larger ground water development area, the changes are smaller than the natural variation in ground water depth across the area.

The alternative ground water development options are shown shaded in the (a) section of figures 4.17 to 4.20. The corresponding changes in ground water levels are shown in the (b) section. The change is expressed in terms of the difference between the steady-state equilibrium ground water levels with no ground water development and the levels exceeded for 90% of the simulation period.

For simulation I (figure 4.17 (b)) the maximum reduction in ground water levels is 9 m, occurring in a very small region on the Ashburton River boundary of the model. The simulation indicates a reduction in ground water levels of more than 5 m over most of the scheme 3 ground water development area adjacent to the Ashburton River. There is less than 3 m reduction in ground water levels in the corresponding area adjacent to the Rakaia River. For simulation I, the minimum ground water levels are approximately 39% (i.e., $A = 1.39$ in eqn 4.29) further below the equilibrium levels than the levels exceeded 90% of the time.

Simulation II (figure 4.18 (b)) shows that the scheme 4 ground water development option repeats the scheme 3 maximum reduction adjacent to the Ashburton River.

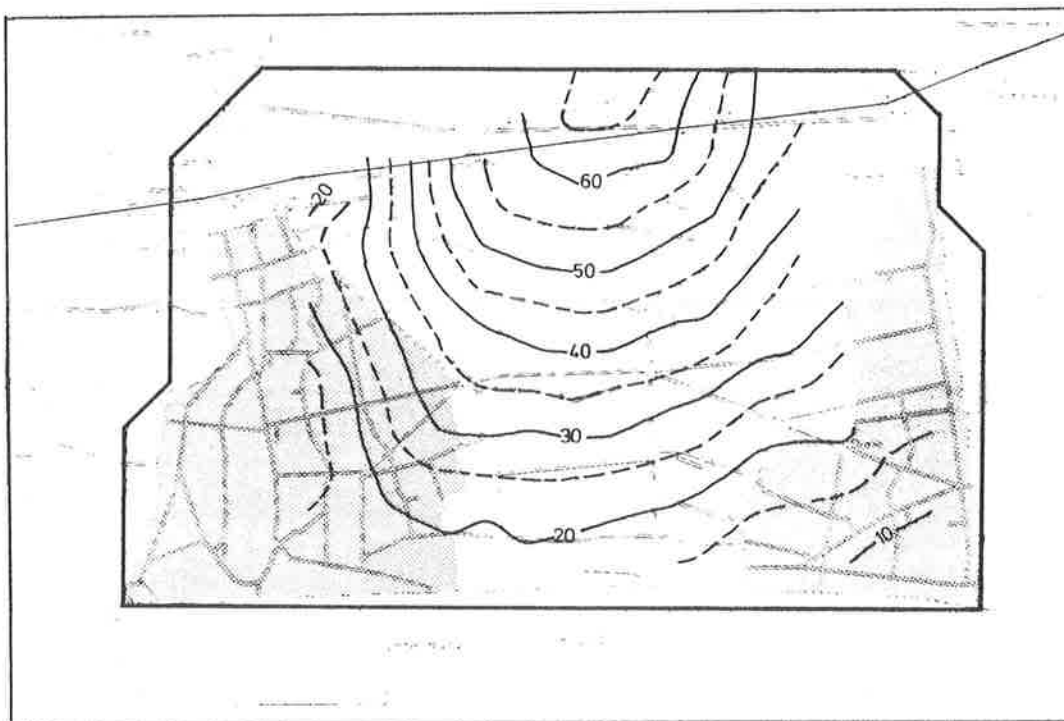


Figure 4.17(a) Simulation I (scheme 3/high water use). The shaded area is irrigated from ground water for scheme 3. Contours are depths to water exceeded less than 10% of the 30 year simulation period

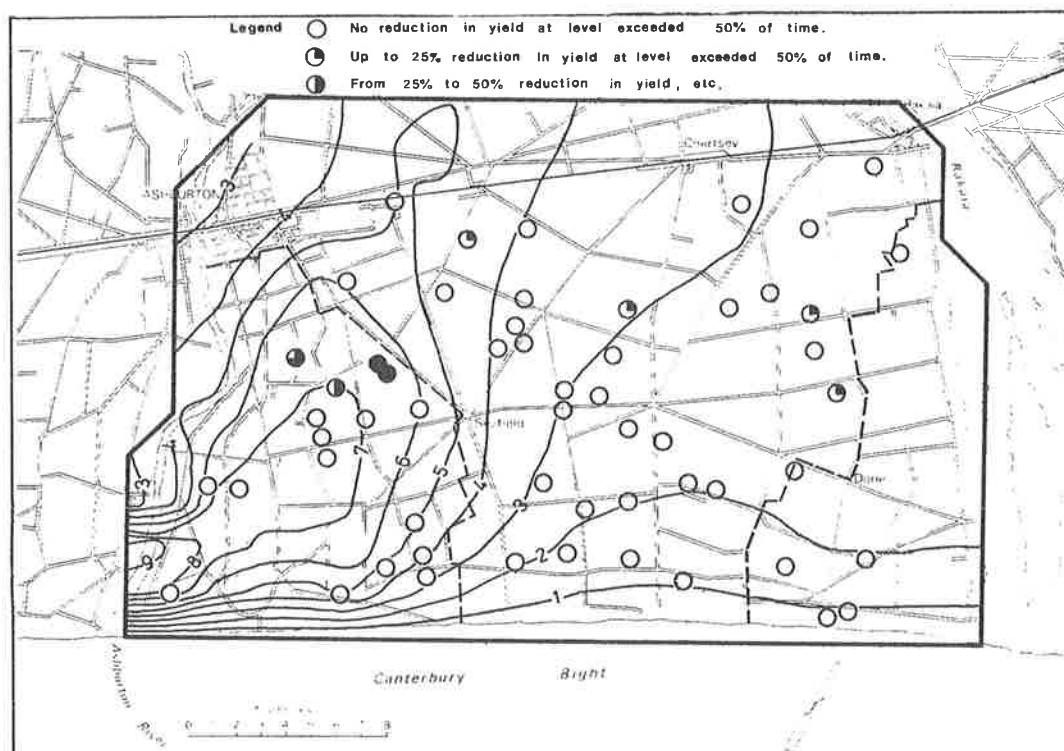


Figure 4.17(b) Simulation I - contours are the difference between initial equilibrium levels and the level exceeded more than 90% of the time (m). Circles show wells included in assessment of impact of ground water development

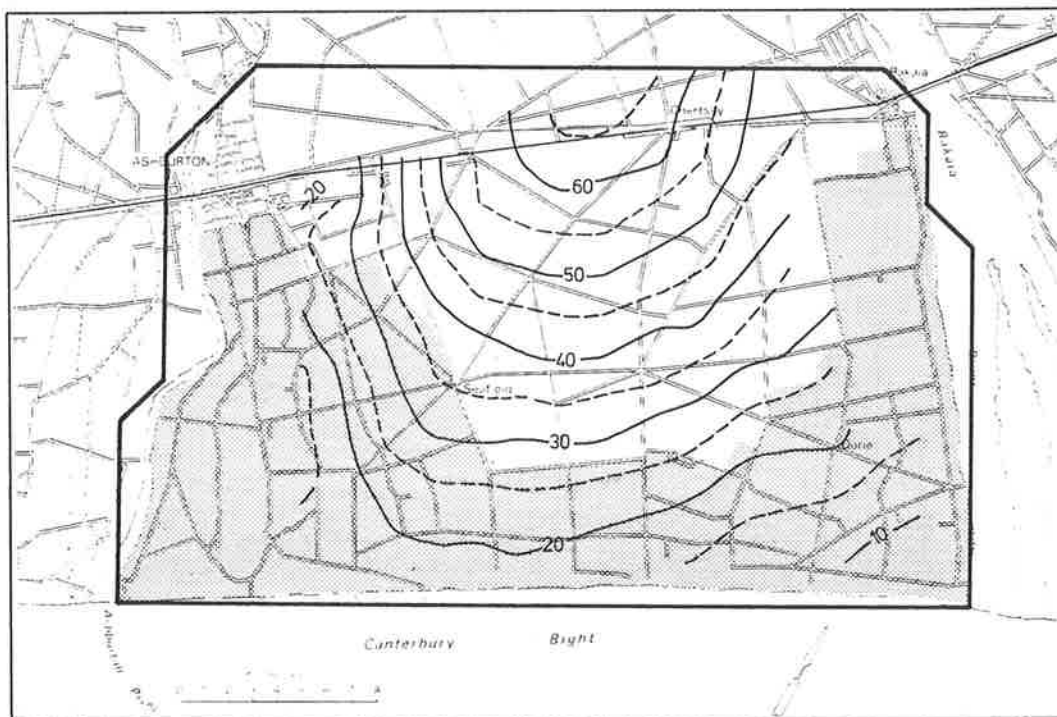


Figure 4.18(a) Simulation II (scheme 4/high water use). See figure 4.17(a) for legend

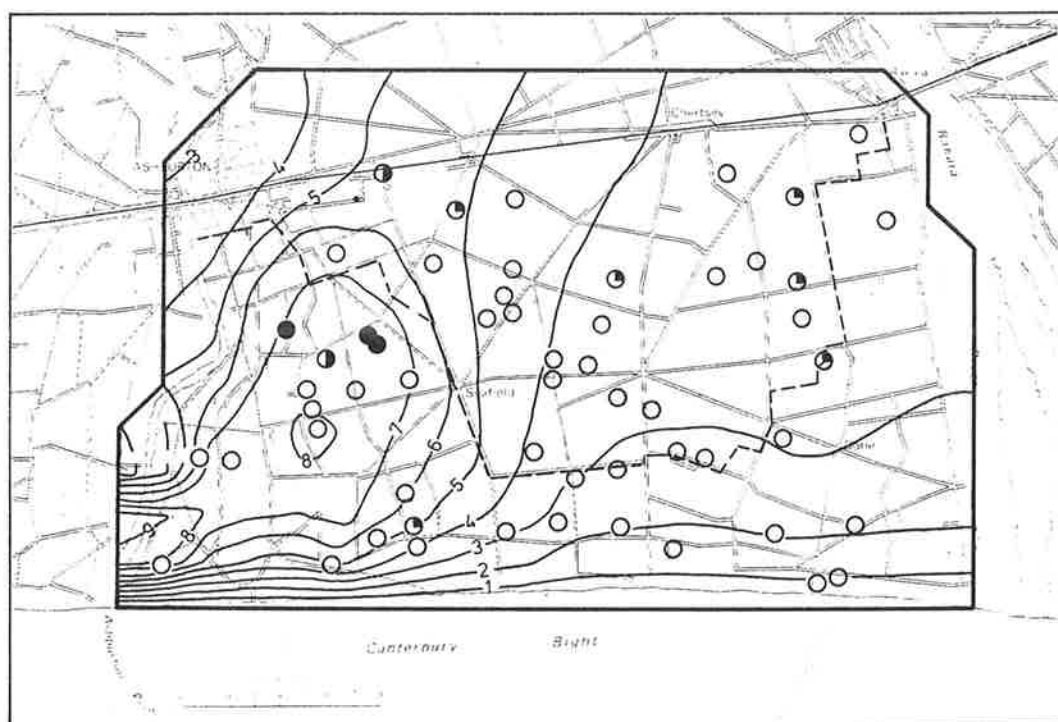


Figure 4.18(b) Simulation II. See figure 4.17(b) for legend

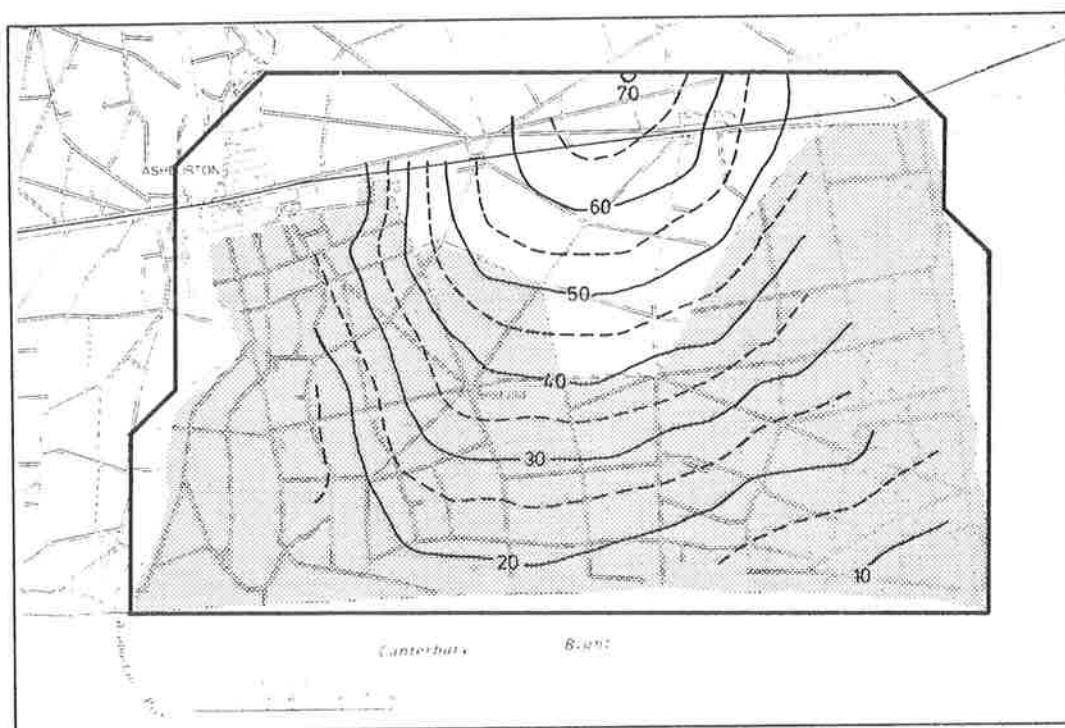


Figure 4.19(a) Simulation III (scheme 6/high water use). See figure 4.17(a) for legend

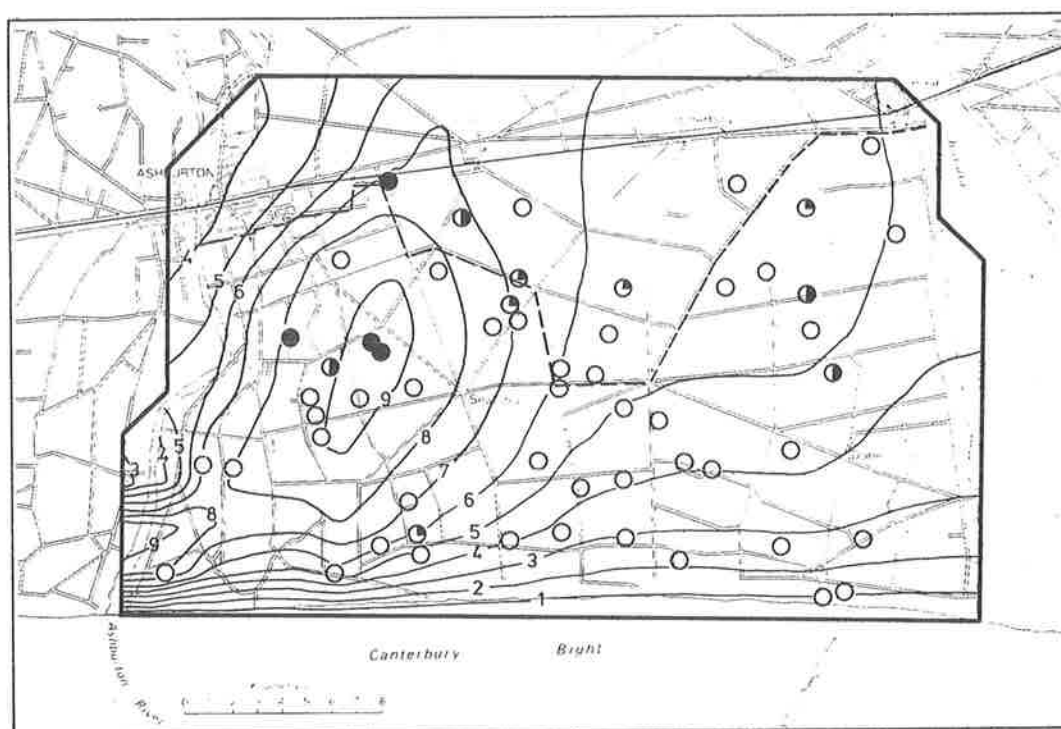


Figure 4.19(b) Simulation III. See figure 4.17(b) for legend

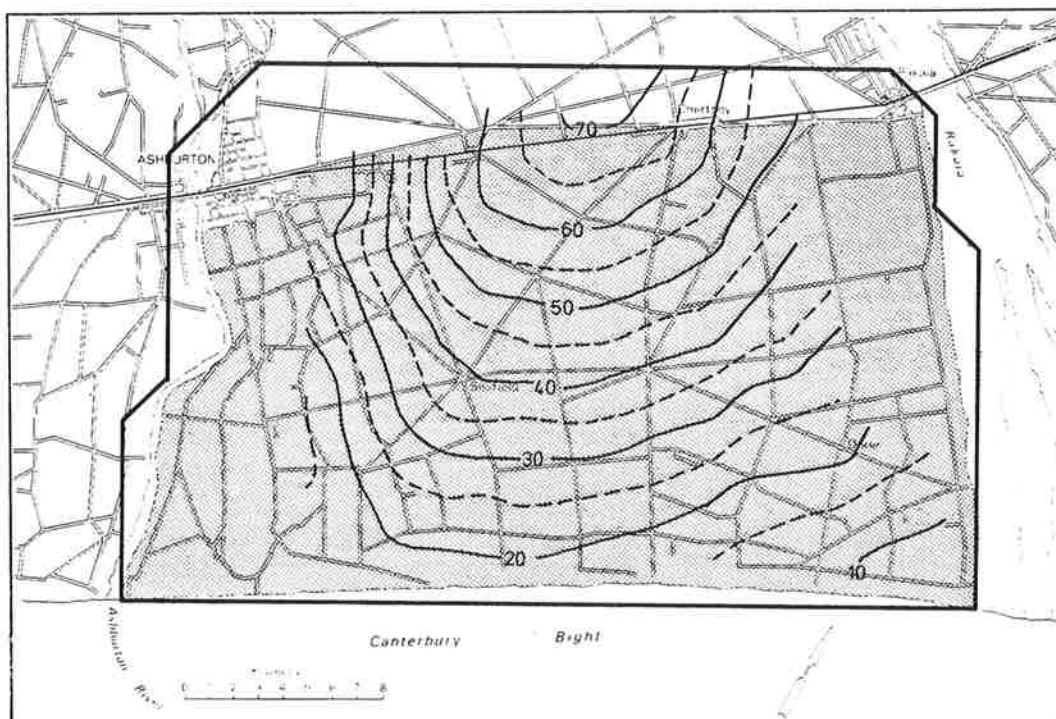


Figure 4.20(a) Simulation VII (scheme 9/high water use). See figure 4.17(a) for legend

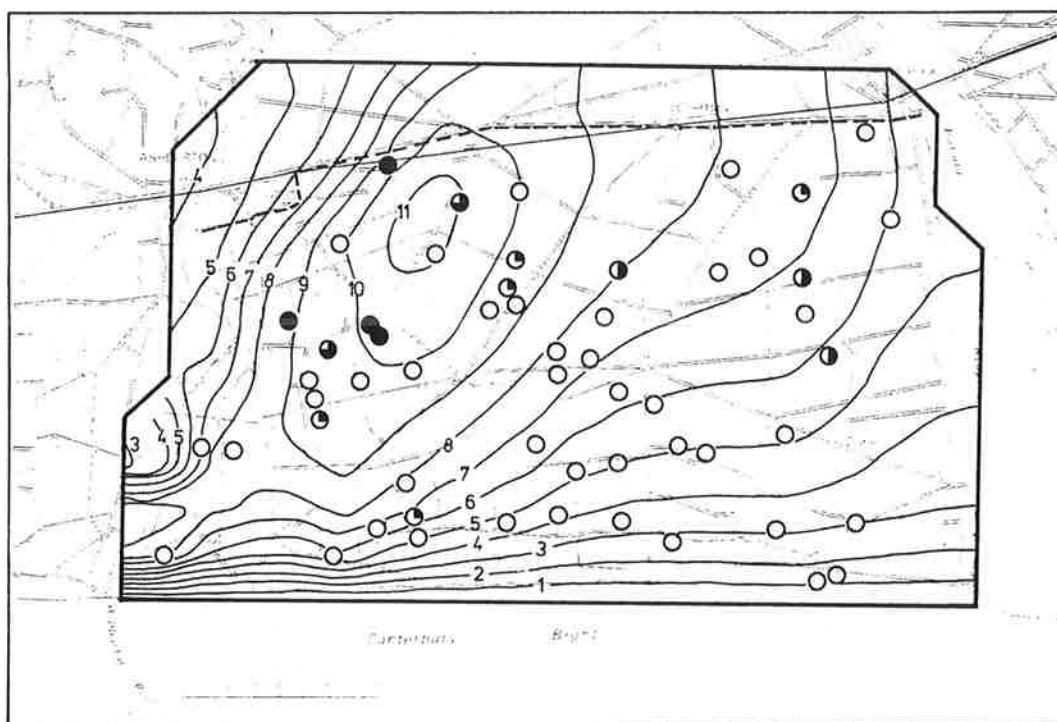


Figure 4.20(b) Simulation VII. See figure 4.17(b) for legend

In addition, ground water level reductions exceeding 8 m are indicated in the middle of the Ashburton River side of the scheme 4 area. The reduction in ground water levels is less than 4 m for the Rakaia River side of the scheme. Minimum ground water levels are approximately 36% (i.e., $A = 1.36$ in eqn 4.29) further below the equilibrium levels than the levels exceeded 90% of the time.

The scheme 6 ground water development option used in simulation III (figure 4.19 (b)) also produces the local 9 m ground water level reduction adjacent to the Ashburton River. Reductions exceed 9 m in part of the Ashburton River side of the scheme area, but are less than 4.5 m on the Rakaia River side. The minimum ground water levels for simulation III are approximately 32% further below the equilibrium levels than the levels exceeded 90% of the time.

Simulation VII (figure 4.20 (b)) indicates that the scheme 9 ground water development option produces ground water level reductions exceeding 11 m in part of the scheme area. As before, reductions on the Ashburton River side of the scheme area exceed those on the Rakaia River side. For this option the minimum ground water levels are approximately 29% further below the equilibrium levels than the levels exceeded 90% of the time.

Though all the ground water development options considered produce reductions in ground water levels adjacent to the coastal boundary, there is a significant positive gradient maintained at that boundary, even for the most extensive of the ground water development options. There is, therefore, little risk of saltwater intrusion on a regional scale. However, these results are based on the assumption that ground water withdrawals are uniformly distributed over each 334 ha model node area rather than being concentrated at a well. Hence the calculated levels and gradients are regional and do not indicate the local effect of pumping at a well. Some care should still be exercised when large wells are proposed, because they might cause major localised drawdown near the coast.

4.4.4 Effects on Existing Wells

The impact of ground water development on existing wells can be assessed by comparing the calculated regional ground water levels with the minimum piezometric level required to maintain a water supply at individual wells. The minimum piezometric level can be estimated for those wells with adequate data on well-head level, top of screen level and measured pumping drawdown, by

assuming that at least 3 m is required above the top of screen level to allow for the normal practice of installing submersible pumps above the screen (figure 4.21). The construction details and hydraulic data are only available for the 56 wells shown in figure 4.22, from an approximate total of 140. These details are tabulated in the Appendix.

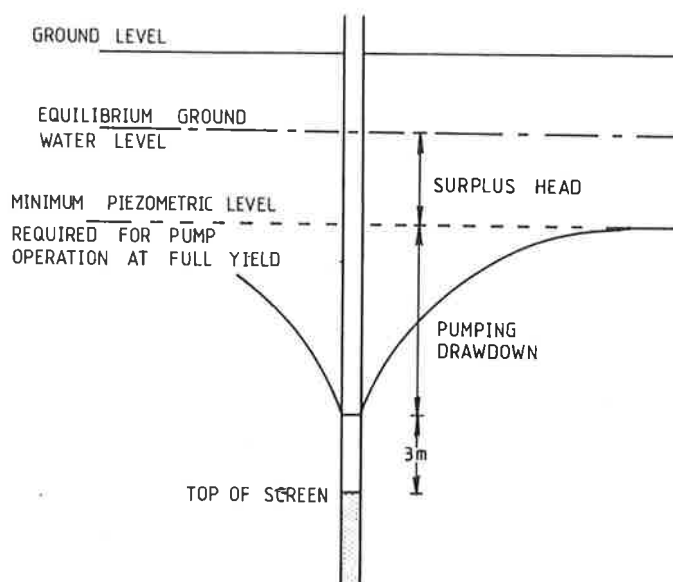


Figure 4.21 Schematic illustration of typical well showing local drawdown

The impact of the alternative ground water development options was assessed by calculating for each of the 56 wells, the percentage reduction in yield which is exceeded 50% of the time for simulation I, II, III and VII. The results of these comparisons are shown in figures 4.17(b), 4.18(b), 4.19(b) and 4.20(b), respectively, and are summarised in table 4.5.

Table 4.5 Impact of ground water development on existing wells (based on 56 wells with adequate data - figure 4.22).

| Simulation No. | | Up to 25% Reduction | 25% to 50% Reduction | 50% to 75% Reduction | Over 75% Reduction |
|----------------|------------|------------------------|-------------------------|-------------------------|-----------------------|
| I | (scheme 3) | 7% | 2% | 2% | 4% |
| II | (scheme 4) | 11% | 4% | - | 5% |
| III | (scheme 6) | 9% | 7% | - | 7% |
| VII | (scheme 9) | 9% | 5% | 4% | 7% |

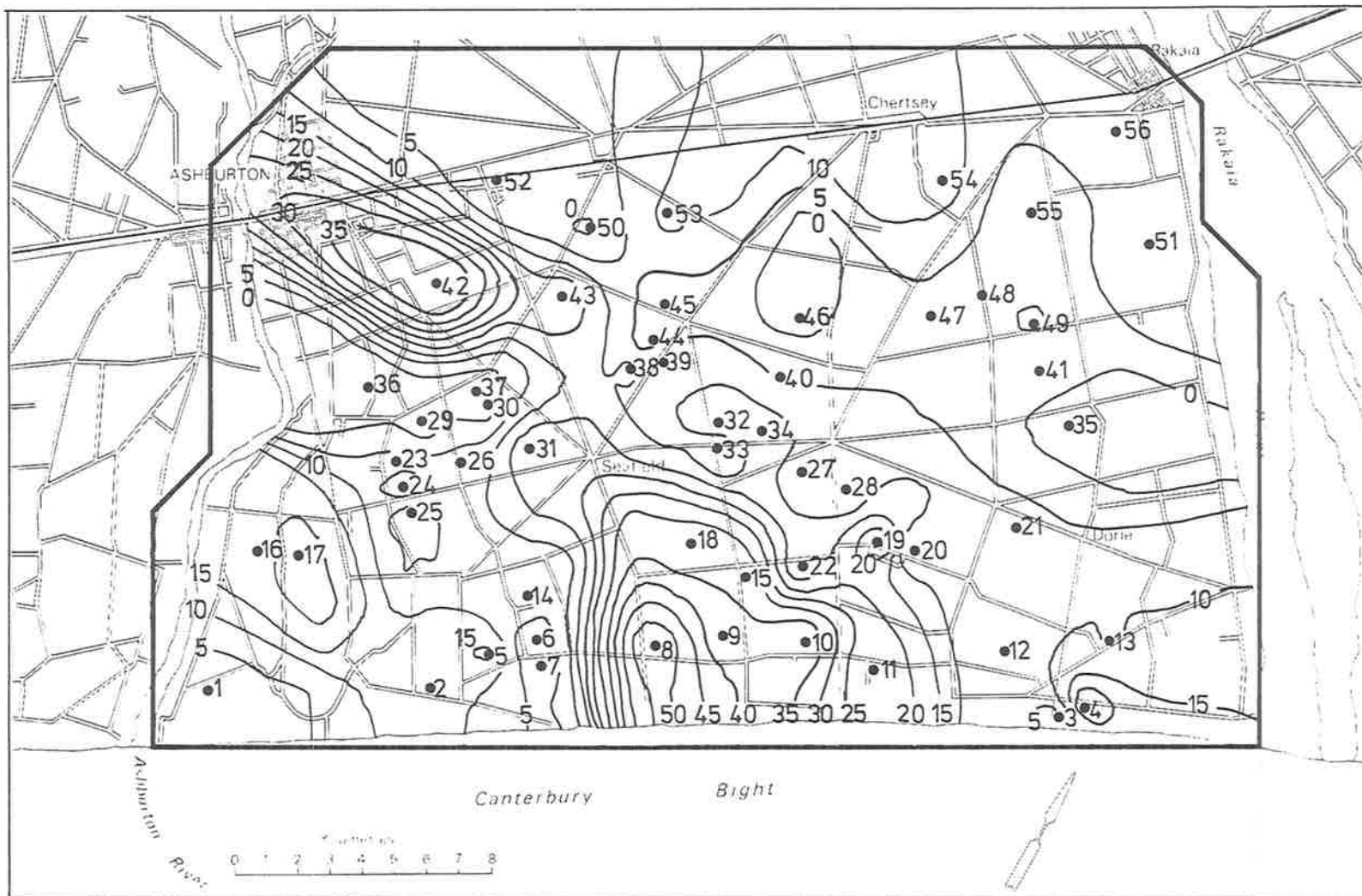


Figure 4.22 Location of the 56 existing wells used in assessment of impact of ground water development (see Appendix). Contours of the difference between the minimum allowable piezometric levels at each well and the "no development" equilibrium levels

The calculated minimum piezometric head was compared to the equilibrium ground water levels to produce the contours of surplus head in figure 4.22. They show that there are some areas with very little surplus head, even under equilibrium conditions. It is obvious that the minimum piezometric head varies considerably across the region modelled.

4.4.5 Alternative Irrigation Development Options

In addition to the four basic irrigation development simulations (Nos. I, II, III and VII), a further four simulations were completed to illustrate the effects of alternative scheme shape (simulation IV), alternative irrigation water use strategy (simulations V and VIII) and artificial recharge (simulation VI).

The scheme 7 area (figure 4.23) was chosen to equal that of scheme 4, and involved a change in shape intended to avoid ground water development in areas with little spare head above the minimum piezometric levels. The results of the change in the scheme area shape are illustrated by the contours in figure 4.23, which show the difference between the levels exceeded 90% of the time for simulations II and IV. The differences are relatively small with an increase in levels of about 1.5 m near Ashburton and a decrease of about 1 m around Seafield. These changes are small compared to the changes from equilibrium levels resulting from either scheme 4 or scheme 7.

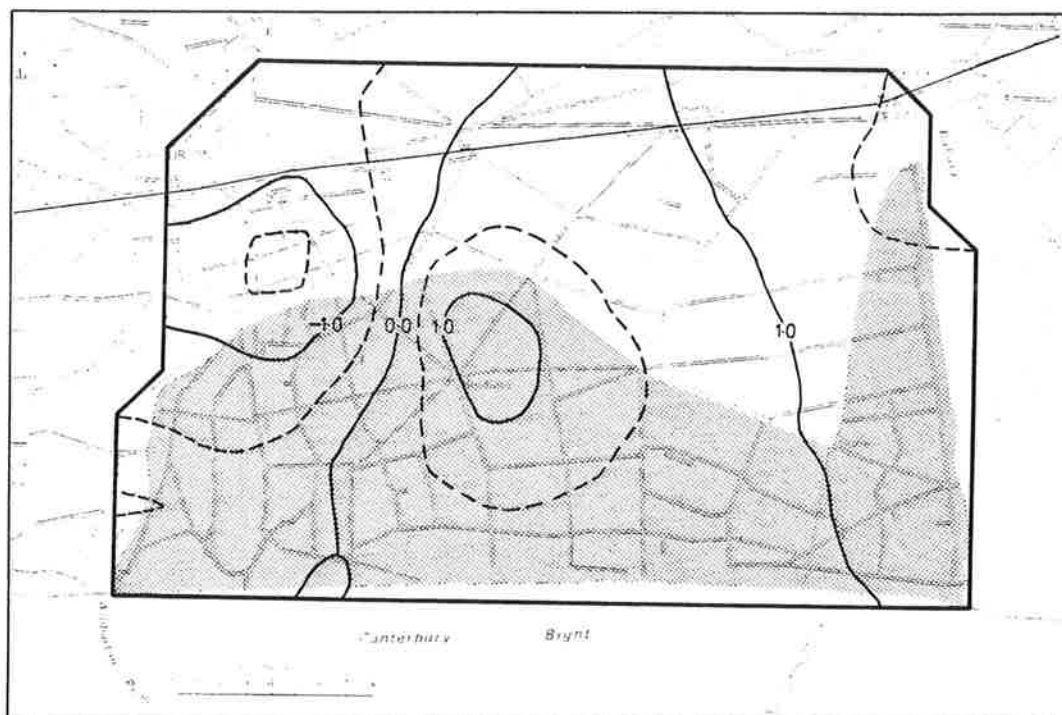


Figure 4.23 Comparison of simulations II and IV showing the effect of a change in scheme shape from scheme 4 (figure 4.18(a)) to scheme 7 (shaded here). Contours (m) are changes in the H90 surface. Negative values indicate simulation IV levels are higher than simulation II.

All the simulations described so far used the high water use strategy defined in section 4.3.1. The effects of the alternative low water strategy were illustrated by simulating ground water response to irrigation development with the lower water demands for scheme 6 (simulation V) and scheme 9 (simulation VIII). The result of the lower water use is illustrated by the change in the levels exceeded 90% of the time in figures 4.24 (scheme 6) and 4.25 (scheme 9). In both schemes there is, of course, a general increase in ground water levels. For scheme 6 there is a substantial area on the Ashburton River side of the region with an increase of more than 2.5 m, and for scheme 9 the increase exceeds 3.5 m in places. These changes reduce the impact on the ground water levels by approximately 30% in both schemes as a result of the 44% reduction in irrigation demand (section 4.3.1).

Simulation VI included artificial recharge in the area indicated in figure 4.26 and produces an increase in the ground water levels exceeded 90% of the time compared to simulation III. The increases exceed 6 m in a small area immediately adjacent to the artificial recharge strip. Increases of more than 2 m extend into the area where there is relatively little spare head above minimum piezometric levels. However, the changes have only a slight impact on the extent to which existing wells would be affected by ground water development.

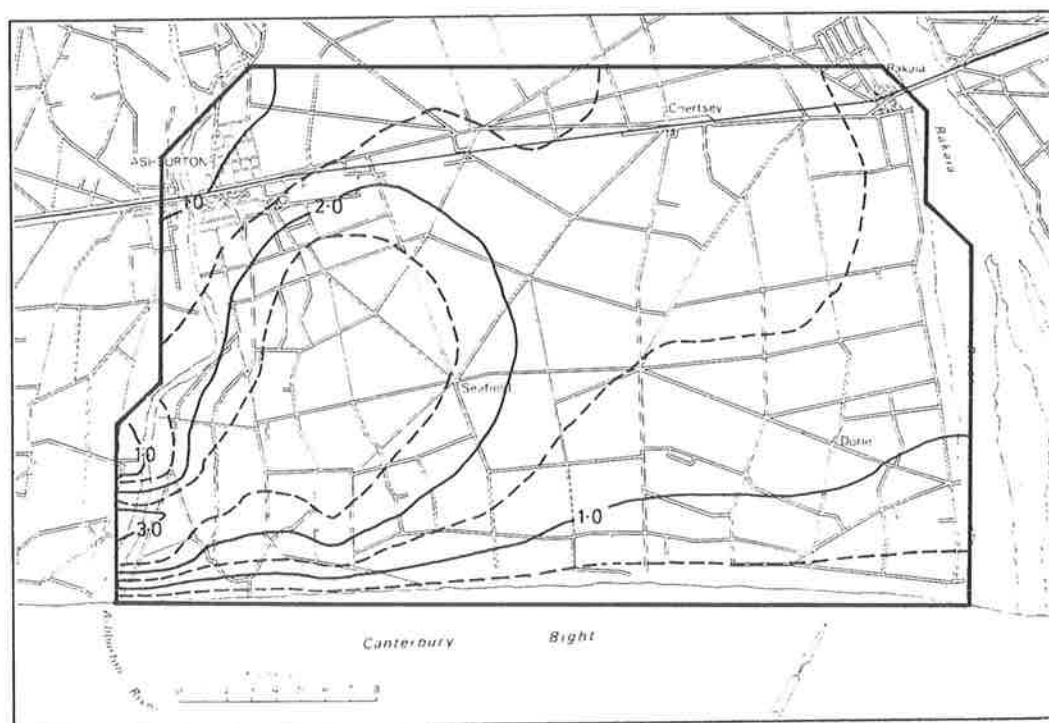


Figure 4.24 Comparison of simulations III and V (high/low water use strategies) on scheme 6. Contours show increase in level (m) resulting from lower irrigation demand

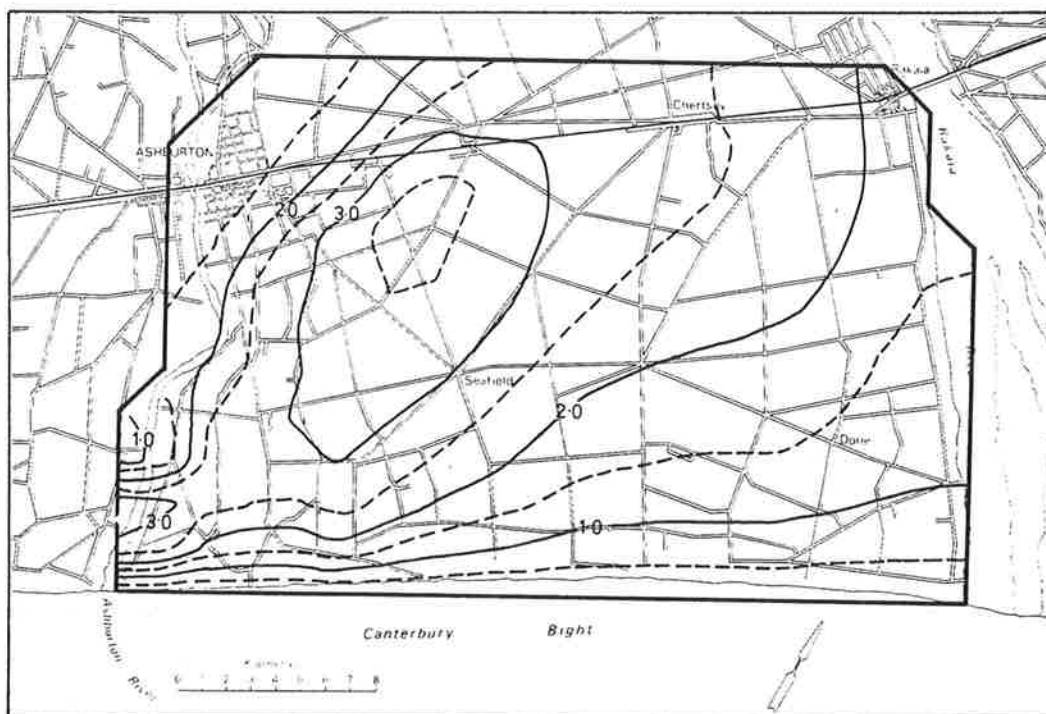


Figure 4.25 Comparison of simulations VII and VIII (low water use strategy) on scheme 9. Contours show increase in level (m) resulting from the lower irrigation demand

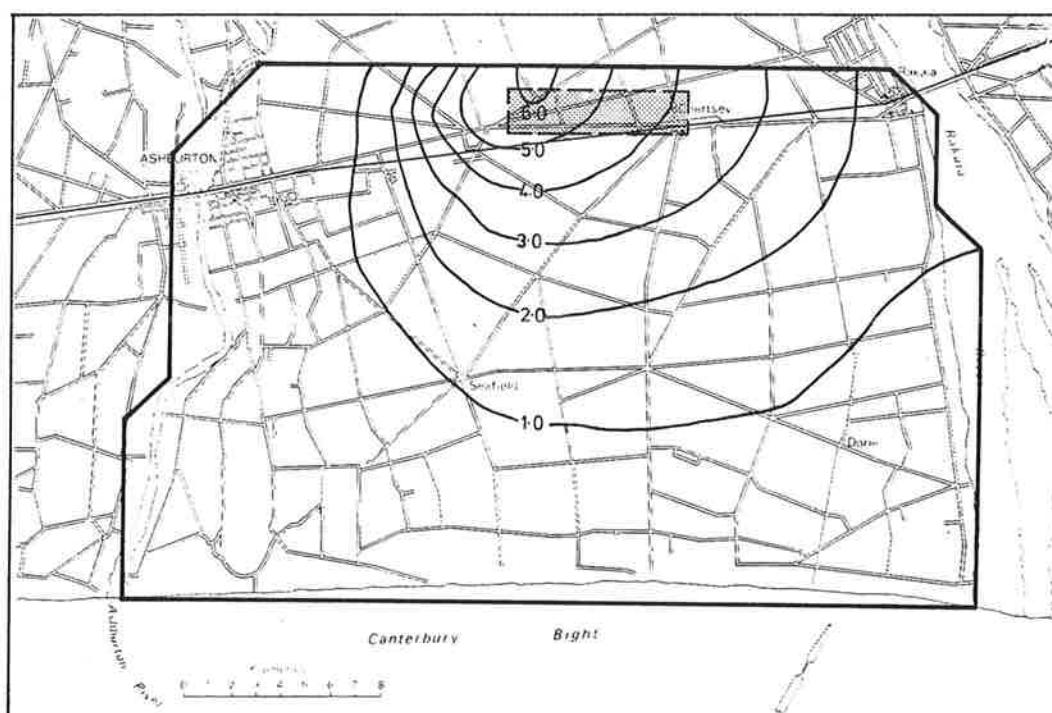


Figure 4.26 Comparison of simulations III and VI. Contours show increase in level (m) due to winter (6 months) artificial recharge at four nodes within the shaded area for scheme 6

4.4.6 Impact of Ground Water Development - Temporal Description

In the preceding sections the impact of ground water development has been described in terms of specific levels - the minimum levels and the levels exceeded 90% of the time. The finite difference model, however, calculated ground water levels for every node at 10-day time intervals for the 30 year simulation period. To provide a more complete description of the model results, the ground water level hydrographs for selected model nodes are plotted in figures 4.27 and 4.28. The location of the selected nodes (Nos. 122, 150 and 232) are shown in figure 4.8. Node 122 is adjacent to the Charing Cross observation well and was used in the unsteady model calibration. Node 150 is in the centre of the area with deepest ground water and node 232 is on the Rakaia River side of the model, adjacent to the Griggs Rd observation well.

The long-term responses of ground water levels at the three nodes for simulations 0, I, II, III and VII are shown in figure 4.27. Because the temporal pattern of ground water abstraction is the same for each of these development options, the ground water hydrographs predictably follow a similar pattern with the larger ground water development area producing lower levels and greater fluctuations. In every case there is an initial period of several years transient behaviour while the ground water system adjusts to the change in the water balance resulting from ground water abstraction. The plots show the effect on ground water levels of a winter period with little drainage, followed by a summer of high irrigation demand as, for example, in 1958-59 (cf. figure 4.5).

The effect of the alternative low water irrigation use strategy on long-term response of the ground water system is illustrated with the node 122 hydrographs for simulation 0, VII and VIII in figure 4.28 (a). The plots show the reduction in the impact of ground water development resulting from the lower water use.

The effect of artificial recharge on the long-term behaviour of the ground water system is shown in figure 4.28 (b) for node 150. The effect is too slight to be detected at nodes 122 and 232. The regular 6-monthly periods of artificial recharge cause ground water levels to continue rising after the end of the winter drainage period. Because artificial recharge was applied regardless of ground water conditions, the simulation resulted in greater ground water level fluctuations than for the no artificial recharge option.

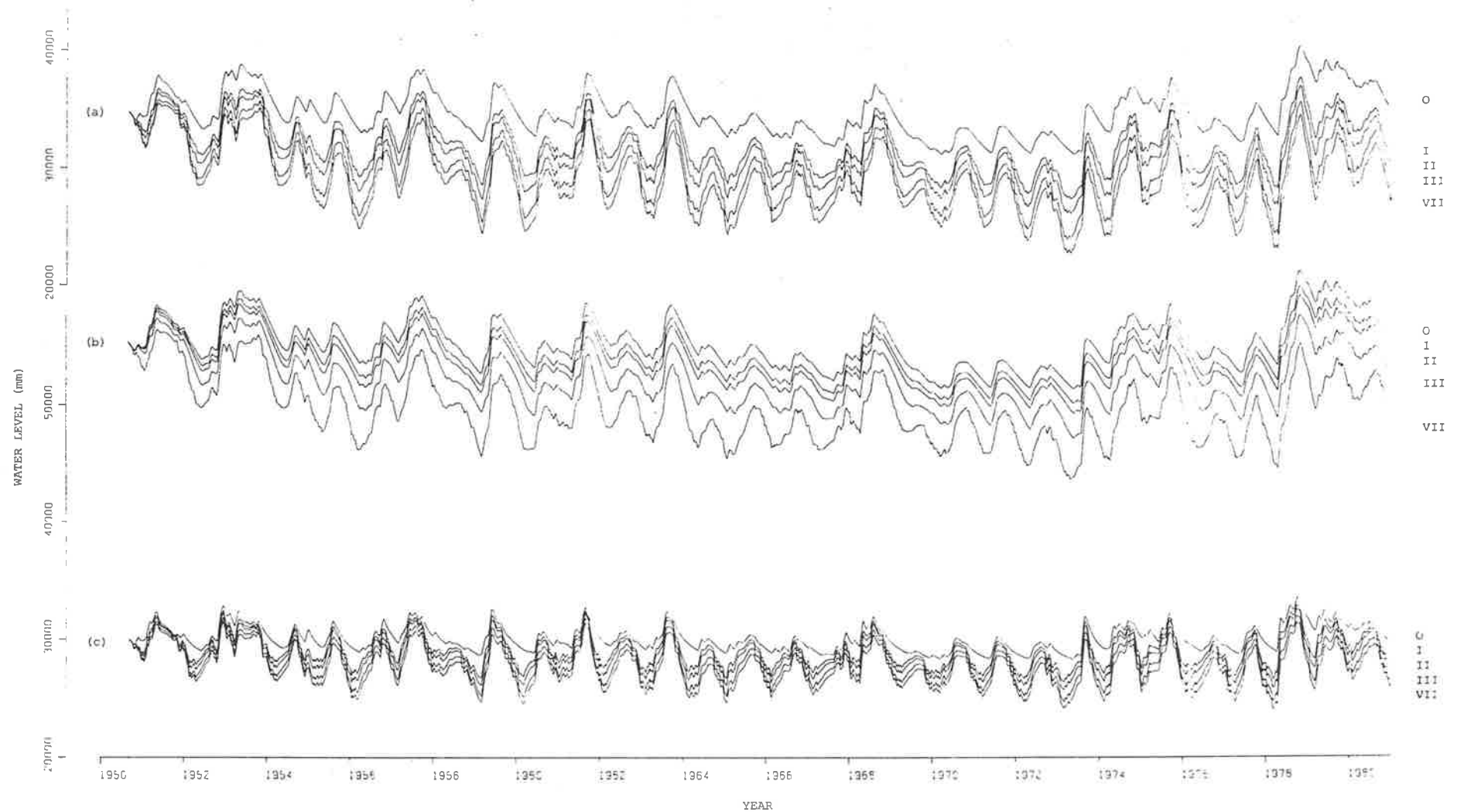


Figure 4.27 Long-term simulated piezometric levels at (a) node 122, (b) node 150 and (c) node 232 for simulations 0, I, II, III and VII

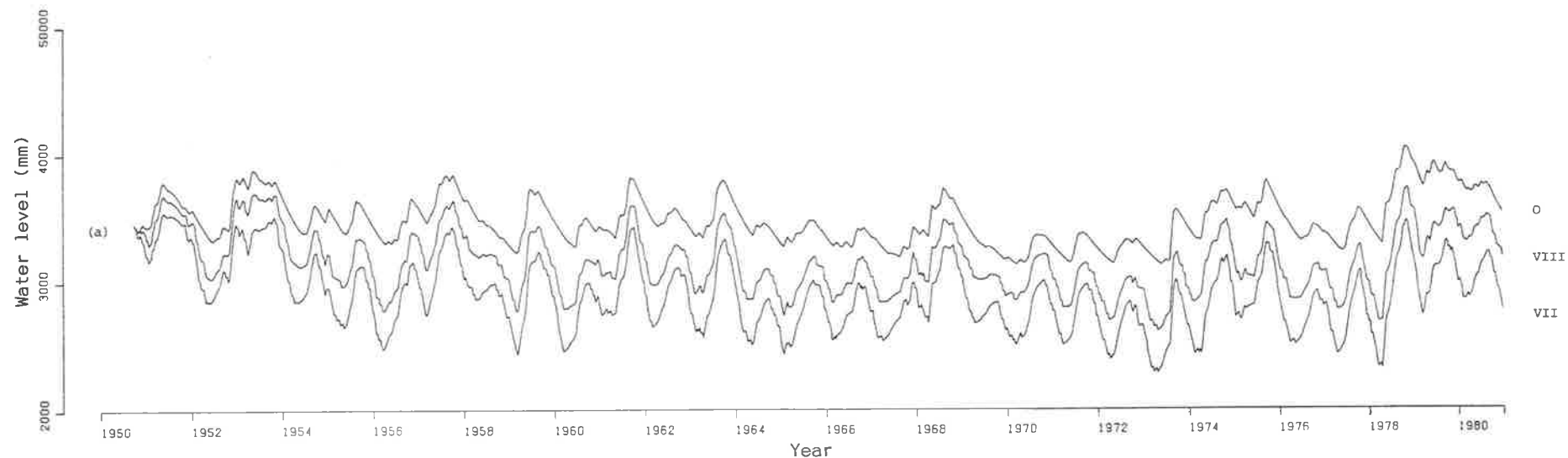


Figure 4.28(a) Long-term simulated piezometric levels at node 122 for simulations 0, VII and VIII (i.e., no development, scheme 9/high water use and scheme 9/low water use)

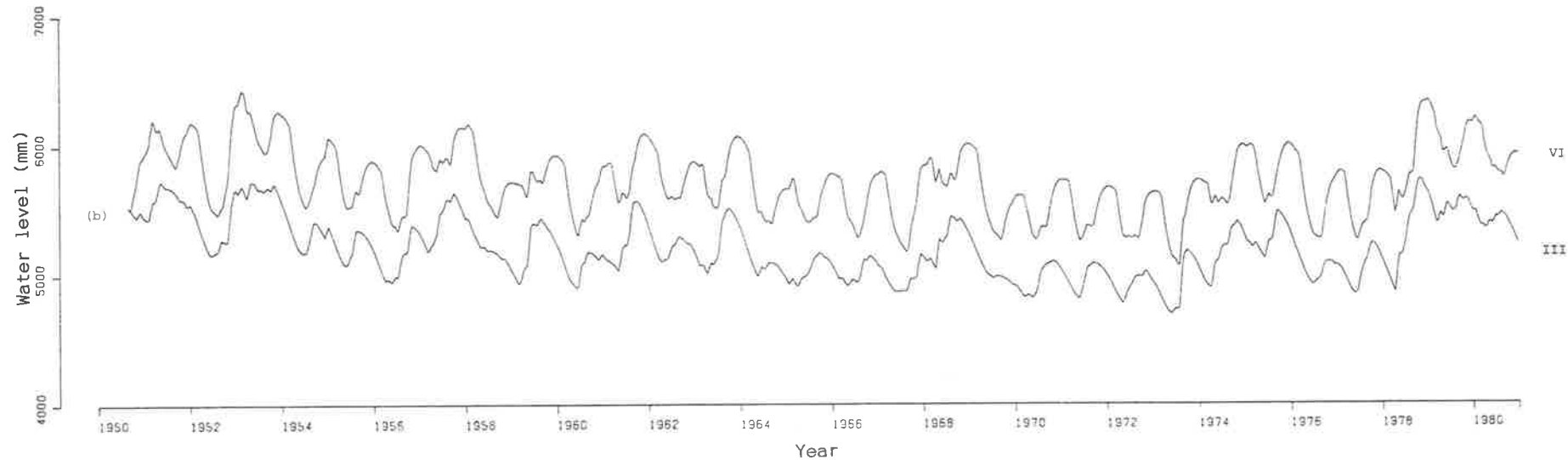


Figure 4.28(b) Long-term simulated piezometric levels at node 150 for simulations III and VI (i.e., scheme 6/high water use and the same scheme with artificial recharge)

The minimum, maximum and range of ground water levels for each of the three nodes and all simulations are given in table 4.6.

Table 4.6 Minimum, maximum and range of simulated levels (m) at selected nodes

| Simulation | Node 122 | | | Node 150 | | | Node 232 | | |
|------------|----------|-------|-------|----------|-------|-------|----------|-------|-------|
| | Min. | Max. | Range | Min. | Max. | Range | Min. | Max. | Range |
| O | 31.26 | 40.36 | 9.10 | 51.20 | 61.06 | 9.86 | 28.36 | 33.55 | 5.19 |
| I | 27.44 | 37.76 | 10.32 | 49.95 | 59.75 | 9.79 | 26.38 | 32.86 | 6.48 |
| II | 26.17 | 37.06 | 10.90 | 49.10 | 59.00 | 9.90 | 25.70 | 32.57 | 6.87 |
| III | 23.98 | 35.83 | 11.85 | 46.97 | 57.31 | 10.34 | 24.68 | 31.98 | 7.30 |
| IV | 25.26 | 36.95 | 11.70 | 48.85 | 58.88 | 10.04 | 25.98 | 32.54 | 6.56 |
| V | 26.78 | 37.79 | 11.00 | 48.67 | 58.80 | 10.13 | 26.12 | 32.78 | 6.66 |
| VI | 24.89 | 36.60 | 11.71 | 50.70 | 64.22 | 13.52 | 25.35 | 32.59 | 7.24 |
| VII | 22.80 | 35.50 | 12.69 | 43.51 | 56.32 | 12.81 | 24.00 | 31.55 | 7.55 |
| VIII | 26.08 | 37.15 | 11.08 | 46.59 | 57.83 | 11.24 | 25.73 | 32.44 | 6.71 |

4.4.7 Leakage Zone Effects

The unsteady behaviour of the ground water levels results in fluctuations in the leakage rates to the aquifer. As the extent of ground water development increases, so do the leakage flows. The leakage rates were calculated for every 10-day time-step for each 30-year simulation. The minimum, mean and maximum leakage flow rates for the Ashburton River leakage zone and the leakage zone adjacent to the Rakaia River are tabulated in table 4.7.

Table 4.7 Minimum, mean and maximum simulated leakage zone flows ($\text{m}^3 \text{s}^{-1}$) (positive flow indicates aquifer recharge)

| Simulation No. | Ashburton R. zone | | | Rakaia R. zone | | |
|----------------|-------------------|------|------|----------------|------|------|
| | Min. | Mean | Max. | Min. | Mean | Max. |
| O | -0.65 | 0.34 | 0.94 | 2.11 | 3.14 | 3.68 |
| I | -0.16 | 0.87 | 1.70 | 2.32 | 3.39 | 4.13 |
| II | -0.10 | 0.91 | 1.76 | 2.42 | 3.53 | 4.37 |
| III | -0.04 | 1.02 | 1.88 | 2.62 | 3.74 | 4.71 |
| IV | -0.21 | 0.75 | 1.49 | 2.41 | 3.47 | 4.21 |
| V | -0.27 | 0.72 | 1.52 | 2.37 | 3.47 | 4.28 |
| VI | -0.03 | 0.95 | 1.81 | 2.41 | 3.50 | 4.45 |
| VII | -0.01 | 1.10 | 1.97 | 2.79 | 3.91 | 4.92 |
| VIII | -0.20 | 0.76 | 1.57 | 2.48 | 3.57 | 4.43 |

The leakage response to changes in ground water levels is highly dependent on the assumptions incorporated in the finite difference model calibration. Since the river/aquifer interaction is probably the least well defined aspect of the ground water system, the model results have to be regarded as merely giving an indication of the potential impact on leakage flows.

Though the simulated magnitude of leakage from the Rakaia River always exceeds that of the Ashburton River, the increases in leakage induced by ground water development are proportionately higher on the Ashburton River side. This is principally because of the larger ground water fluctuations in this area, resulting from its relatively lower transmissivities, predicted by the steady-state calibration.

5 : SUMMARY AND CONCLUSIONS

5.1 INTRODUCTION

The study examined, measured, and made predictions about the ground water resource between the Rakaia and Ashburton Rivers. It did not consider the economic costs or consequences of ground water development.

The field information and soil moisture model are described in sections 2 and 3, respectively. These data enabled a water budget for the system to be prepared, and also provided the constraints for the calibration of the two-dimensional unsteady flow model described in section 4. This model covers only the area between SE 1 and the ocean, as this is the area where ground water use is concentrated at present and major future development is likely.

5.2 SUMMARY

5.2.1 Hydrogeology

The water yielding characteristics of the gravels of the study area are best near the rivers and the coast; interglacial, and especially post-glacial alluvium are better than glacial outwash material. There are no extensive, clearly defined aquifers, but three particular depths were identified at which transmissivities tend to be better. These are suggested to derive from deposits laid down during the last two interglacial and post-glacial periods. Hydraulic conductivity decreases with depth.

In some restricted areas aquifers are more clearly defined, but these appear to be interconnected at the larger scale, and overall the system behaves as semi-confined or unconfined, with substantial storativity. The heterogeneity of the material is very marked in all areas, but further inland the permeability decreases and the variability increases. Thus, there is greater risk of sinking a dry or unsatisfactory well. The inclusion of an area within the region to be spray irrigated from ground water does not indicate that a good well can be drilled at that particular site.

5.2.2 Piezometric Levels

Depth to standing water levels is generally less than 5 m in areas close to the rivers, about 10 m at the coast and 60 m at Chertsey. Further inland, near

Lauriston and Lyndhurst, depth to ground water exceeds 100 m. Natural seasonal variation close to the river is less than a metre, but in areas of deeper ground water, i.e., Seafield, Pendarves and Chertsey, it can be as much as 12 m. There is no evidence of long-term changes in ground water levels, either from irrigation return water or increased pumpage.

5.2.3 Hydrochemistry

Ground water quality is generally good, with the exception that nitrate-nitrogen levels approach or exceed the WHO recommended level of 10 g m^{-3} in some wells beneath, and downstream of areas where border-strip irrigation is practised. The source of this nitrate is urine from intensively grazed pasture.

Nitrate-nitrogen, together with other water quality determinands, have been used to delineate those areas which are recharged from rivers, and by runoff from the foothills, dryland farming areas and border-strip irrigated areas.

5.2.4 Aquifer Recharge

The major recharge for the ground water system is drainage from precipitation, although this varies markedly from winter to summer and from year to year. In a dry summer there is no recharge from precipitation. Precipitation contributes about 57% of the total recharge in an average year.

The rivers interact with the aquifer system. The Ashburton River, however, does not make a significant net contribution to the aquifers under present ground water conditions. The Rakaia River loses about 7 to 21% of the mean annual flow from the surface channels, but most of this becomes underflow. Nevertheless, about 18% of the recharge to the aquifer comes from the Rakaia River and this is a relatively constant value.

A network of stock races abstracts more than $4 \text{ m}^3 \text{ sec}^{-1}$ from both the Ashburton and Rakaia Rivers, nearly all of which leaks into the ground water system. Leakage from these races and the RDR amounts to a steady 16% of the overall recharge.

The remaining recharge derives from excess water applied seasonally to the ALIS, about 9% of the total. Should other border-strip irrigation schemes be constructed in the area, they would also contribute to the ground water recharge.

5.2.5 Aquifer Output

The major output from the aquifer is submarine leakage, which is unmeasured. Wakanui and Mount Harding Creeks are the only surface flows within the area and are only about 5% of the estimated average recharge. Present average seasonal irrigation use is probably no more than 5% of average annual recharge, but is increasing rapidly. Dry season irrigation may be twice the average figure, i.e., up to 220 mm.

Municipal and industrial use of ground water makes up less than 1% of the resource.

5.2.6 Model Summary

Three separate models were developed for this study, the first two primarily providing information for the third.

A simple soil moisture model was used to estimate recharge from both precipitation and excess irrigation water. For Winchmore, with an average annual rainfall of 760 mm, the corresponding recharge was 307 mm. Typically, border-strip irrigation produces a further 500 mm of drainage at Winchmore.

The soil moisture model was also used to estimate the potential irrigation demand (i.e., pumpage) over the period 1950-1980 for which suitable climatic data are available. Demand estimated for five water use strategies ranged from a mean annual figure of 167 up to 326 mm. The simulation demonstrated that soil moisture holding capacity had only a small effect on both drainage values and irrigation demand.

A lumped parameter ground water model was used to define a representative time lag between drainage leaving the soil profile and recharge arriving at the water table. This model also provided an estimate of the general aquifer storativity (0.044).

The major modelling effort was the two-dimensional finite difference flow model. In the steady-state version, it enabled solution of the inverse problem, i.e., determining the distribution of transmissivity from the piezometric contours. Finally, the unsteady version was used to simulate the aquifer response to different irrigation development options. A high water (326 mm) and a low (182 mm) water use strategy were variously applied to four suggested irrigation scheme areas and compared with the "no scheme" situation over the period 1950-1980.

5.3 CONCLUSIONS

5.3.1 Prospects for Expansion of Ground Water Use

At the present time there is a large surplus of input to the aquifer system compared to output. Therefore, scope exists for substantial expansion of irrigation using ground water (section 3.7).

5.3.2 Piezometric Level Controls

Drainage from present irrigation schemes may have some short-term effect on piezometric levels, but in areas away from the coast and rivers the dominant control is precipitation (section 2.6).

5.3.3 Ground Water Quality Changes

Irrigation has already caused detectable changes in ground water quality and further degradation will occur. Nitrate-nitrogen levels in the upper 30 m of ground water may rise to 15-20 g m⁻³ (section 2.7.5).

5.3.4 Potable Water Supplies

If a satisfactory potable water supply is to be maintained, existing domestic wells would need to be deepened or a rural water supply scheme constructed to replace the present stock race system, which is probably no more than 5% efficient. This would leave more water in the rivers (especially significant for the Ashburton River), but would reduce the recharge to ground water (sections 3.3 and 3.7).

5.3.5 Reduction of Ashburton River Flows

Substantial drawdown of the water table caused by pumping adjacent to the Ashburton River would induce recharge to the aquifers, and hence significantly reduce river flows from the river junction to the mouth (sections 2.4.2 and 4.4.7; and table 4.7). Flow in the Wakanui Creek would also be markedly reduced.

5.3.6 Reduction of Rakaia River Flows

Induced recharge would also occur from the Rakaia River, but because of the geological structure close to the river the response to drawdown would be much slower and the magnitude of this extra recharge would be insignificant in relation to the size and variability of Rakaia River flows (sections 2.4.1 and 4.4.7; and table 4.7).

5.3.7 Water Availability

In terms of a simple water budget all of the various spray irrigation options could be supplied from the ground water resource. In fact, the entire area between SH 1 and the coast could be accommodated (figures 4.17, 4.18, 4.19 and 4.20). However, in areas distant from the coast and rivers, water availability is restricted by low aquifer permeability, and ground water irrigation may not be possible (section 2.2).

5.3.8 Consequences of Development

The consequences of any of these irrigation developments would be increased regional drawdown, higher pumping costs and the reduction in output of a percentage of the existing wells. For example, irrigation of the entire area between SH 1 and the coast (55 443 ha) from ground water with an average annual application of 326 mm of water would give a maximum drawdown, exceeded less than 10% of the time, of 11 m (figure 4.20 (b)); 25% of the existing wells would be adversely affected to a significant extent (table 4.5).

5.3.9 Saltwater Intrusion

For all the options examined, the hydraulic gradient at the coast would remain positive and therefore intrusion of saltwater into the aquifers is unlikely to occur (section 4.4.3).

5.3.10 Artificial Recharge

Recharge of the aquifers with Rakaia River water is technically feasible. To have a significant effect on drawdowns, however, the recharge rate would have to be the same order of magnitude as the rate of abstraction for irrigation (section 4.4.5).

5.3.11 Accuracy of Prediction

The complexity of the aquifer system is such that the model is only an approximation to reality. The results, therefore, must not be interpreted precisely. In general, predicted drawdowns are considered to be accurate to within 20-25%. Accuracy is even less in the river recharge zones. This degree of accuracy is satisfactory for comparing different options and evaluating the opportunities for, and consequences of, large scale irrigation development in the area between the Ashburton and Rakaia Rivers.

6 : ACKNOWLEDGEMENTS

We gratefully acknowledge the assistance of staff of the South Canterbury Regional Water Board who collaborated in some of the project field work.

Our colleagues in the Hydrology Centre also assisted in field work and in reviewing draft manuscripts.

Particular thanks are due to Barbara Vaile for her contribution to the preparation of the material for publication.

7 : REFERENCES

- Bear, J. 1972 : *Dynamics of fluids in porous media*. American Elsevier, New York, 764 p.
- Bradley, W.C.; Fahnestock, R.K.; Rowekamp, E.P. 1972: Coarse sediment transport by flood flows on Knik River, Alaska. *Geological Society of America Bulletin* 83:1261-84.
- Broadbent, M. 1978: Seismic refraction surveys for Canterbury groundwater research. *Geophysics Division Report No. 131*. Department of Scientific and Industrial Research, 91 p.
- Burden, R.J. 1982: Hydrochemical variation in a water-table aquifer beneath grazed pastureland. *Journal of Hydrology (NZ)* 21(1):61-75.
- Cedergren, H.R. 1977: (2nd Edn.). *Seepage, drainage and flow nets*. Wiley-Interscience, New York, 534 p.
- Clark, L. 1977: The analysis and planning of step drawdown tests. *Quarterly Journal of Engineering Geology (UK)* 10:125-43.
- Collins, B.W. 1950: Ground water in North Canterbury, between the Waimakariri and Ashley Rivers. *New Zealand Journal of Science and Technology* 30B(5): 249-68.
- Day, M.C. 1976: A model for steady groundwater flow in North Canterbury. *Civil Engineering Research Report 76-5*. University of Canterbury, 33 p.
- Drost, W.; Klotz, D.; Koch, A.; Moser, H.; Neumaier, F.; Rauert, W. 1968: Point dilution methods of investigating ground water flow by means of radioisotopes. *Water Resources Research* 4(1):125-46.
- Eden, R.N.; Hazel, C.P. 1973: Computer and graphical analysis of variable discharge pumping tests of wells. *Civil Engineering Transactions, Institution of Engineers, Australia, Paper 3194*:5-10.
- Halevy, E.; Moser, H.; Zellhofer, O.; Zuber, A. 1967: Borehole dilution techniques : a critical review. In Proceedings of a symposium on isotopes in hydrology. International Atomic Energy Agency, Vienna, 1966, pp. 531-64.
- Heine, R.W. 1976: Comparison of methods of estimating potential evapotranspiration in Canterbury. *New Zealand Journal of Science* 19:255-64.
- Hopper, M.J. 1973: Harwell subroutine library: a catalogue of subroutines. *United Kingdom Atomic Energy Authority, Report 7477*. Harwell, 118 p.
- Hunt, B.W. 1976: Some computer models for ground water flow. *Civil Engineering Research Report 76-11*. University of Canterbury, 24 p.

- Hunt, B.W.; Wilson, D.D. 1974: Graphical calculation of aquifer transmissivities in Northern Canterbury, New Zealand. *Journal of Hydrology (NZ)* 13(2):66-80.
- Klotz, D.; Moser, P.; Trimborn, P. 1979: Single borehole techniques. Present status and examples of recent applications. In Proceedings of a symposium on isotopes in hydrology. International Atomic Energy Authority, Vienna, 1978, pp. 159-79.
- Maidment, D.R.; Lewthwaite, W.J.; Hamblett, S.G. 1980: Rakaia water use and irrigation development. *Water and Soil Miscellaneous Publication No. 19*. Ministry of Works and Development, Wellington, 47 p.
- Mandell, S. 1974: The ground water resources of the Canterbury Plains. *Lincoln Papers in Water Resources No. 12*. New Zealand Agricultural Engineering Institute, 59 p.
- Nash, J.E.; Sutcliffe, J.V. 1970: River flow forecasting through conceptual models, part 1 - a discussion of principles. *Journal of Hydrology (NZ)* 10:282-90.
- Oborn, L.E. 1955: The hydro-geology of the Canterbury Plains between the Rakaia and Ashley Rivers. Unpublished M.Sc. thesis, University of Otago, Dunedin.
- Oborn, L.E. 1960: The incompetent and elastic nature of the Christchurch artesian system. *New Zealand Journal of Geology and Geophysics* 3(1):81-97.
- Oborn, L.E.; Suggate, R.P. 1959: Sheet 21 - Christchurch (1st Edn), Geological Map of New Zealand, 1:250,000. Department of Scientific and Industrial Research, Wellington.
- Quin, B.F. 1979: The effects of surface irrigation on drainage and ground water quality. In The quality and movement of ground water in alluvial aquifers of New Zealand. Proceedings of a symposium, Lincoln College, November 1978. pp. 139-45.
- Quin, B.F.; Burden, R.J. 1979: The effects of land use and hydrology on ground water quality in mid-Canterbury, New Zealand. *Progress in Water Technology* 11(6):433-48.
- Rushton, K.R.; Redshaw, S.C. 1979: *Seepage and ground water flow*. Wiley Interscience, Chichester, 339 p.
- Ruston, K.R.; Ward, C. 1979: The estimation of ground water recharge. *Journal of Hydrology* 41:345-61.
- Scott, G.L. 1980: Near surface hydraulic stratigraphy of the Canterbury Plains between the Ashburton and Rakaia Rivers, New Zealand. *Journal of Hydrology (NZ)* 19(1):68-74.

- Smart, G.M. 1978: The development and application of analytical techniques for planning of irrigation systems. Unpublished Ph.D. thesis, Lincoln College, 151 p.
- Smith, G.D. 1965: *Numerical solution of partial differential equations*. Oxford University Press. pp. 149-51.
- Soons, J.M.; Gullentops, F.W. 1973: Glacial advances in Rakaia Valley. *New Zealand Journal of Geology and Geophysics* 16(3):425-38.
- Stephen, G.D. 1972: The water resources of the Rakaia catchment. Unpublished report, North Canterbury Catchment Board, Christchurch, 41 p.
- Suggate, R.P. 1958: Late quaternary deposits of the Christchurch metropolitan area. *New Zealand Journal of Geology and Geophysics* 1(1):103-22.
- Suggate, R.P. 1963: The fan surfaces of the Central Canterbury Plain. *New Zealand Journal of Geology and Geophysics* 6(2):281-87.
- Suggate, R.P. 1973: Sheet 21 - Christchurch (2nd Edn). Geological Map of New Zealand, 1:250 000. Department of Scientific and Industrial Research, Wellington.
- Walsh, R.P.; Scarf, F. 1980: The water resources of the Ashburton and Hinds Rivers. *Publication No. 31*. South Canterbury Catchment Board and Regional Water Board, Timaru, 40 p.
- Wilson, D.D. 1973: The significance of geology in some current water resource problems, Canterbury Plains, New Zealand. *Journal of Hydrology (NZ)* 12(2):103-18.
- Wilson, D.D. 1976: Hydrogeology of metropolitan Christchurch. *Journal of Hydrology (NZ)* 15(2):101-20.
- Wilson, D.D. 1979: Geology of aquifers. In *Proceedings of Technical Groups* 5(3), New Zealand Institution of Engineers, pp. 395-416.

APPENDIX

DETAILS OF SELECTED EXISTING WELLS

| Well | Well Head R.L. | Depth to Top of Screen | Normal Pumping Drawdown | Min. Piezo. Level | S.W.L. 4/82 | Well | Well Head R.L. | Depth to Top of Screen | Normal Pumping Drawdown | Min. Piezo Level | S.W.L. 4/82 |
|------|----------------|------------------------|-------------------------|-------------------|-------------|------|----------------|------------------------|-------------------------|------------------|-------------|
| 1 | 27.4 | 26.0 | 4.3 | 8.7 | 20.0 | 29 | 67.5 | 30.0 | 12.2 | 52.7 | 55.0 |
| 2 | 26.7 | 29.8 | 0.6 | 0.5 | 10.0 | 30 | 71.0 | 30.0 | 1.9 | 45.9 | 48.0 |
| 3 | 14.9 | 46.6 | 30.5 | 1.8 | 5.0 | 31 | 64.1 | 56.4 | 4.6 | 15.3 | 39.1 |
| 4 | 14.1 | 64.6 | 27.4 | -20.1 | 3.7 | 32 | 69.2 | 69.8 | 13.4 | 15.8 | 22.9 |
| 5 | 23.2 | 31.7 | 4.6 | -0.9 | 16.0 | 33 | 62.4 | 67.0 | 9.8 | 22.9 | 8.2 |
| 6 | 33.5 | 30.5 | 9.1 | 15.1 | 15.5 | 34 | 66.4 | 61.0 | 5.4 | 13.8 | 25.0 |
| 7 | 29.4 | 30.0 | 5.5 | 7.9 | 13.3 | 35 | 57.1 | 38.7 | 11.25 | 32.7 | 33.5 |
| 8 | 29.1 | 77.3 | 3.73 | -41.5 | 7.8 | 36 | 71.0 | 20.0 | 6.4 | 60.4 | 68.7 |
| 9 | 31.3 | 60.0 | 1.5 | -24.2 | 9.1 | 37 | 75.0 | 30.0 | 1.8 | 49.8 | 53.0 |
| 10 | 27.7 | 59.7 | 0.3 | -28.7 | 7.0 | 38 | 75.1 | 60.1 | 9.1 | 27.1 | 38.0 |
| 11 | 25.0 | 69.5 | 30.0 | -11.5 | 5.0 | 39 | 78.3 | 61.0 | 7.62 | 27.9 | 32.5 |
| 12 | 22.7 | 22.6 | 2.4 | 5.5 | 7.7 | 40 | 76.9 | 75.6 | 23.2 | 27.5 | 29.0 |
| 13 | 20.3 | 26.0 | 5.0 | 2.8 | 9.2 | 41 | 63.4 | 51.8 | 18.3 | 32.9 | 35.1 |
| 14 | 37.1 | 30.1 | 3.0 | 13.0 | 24.0 | 42 | 91.5 | 82.6 | 11.7 | 23.6 | 82.0 |
| 15 | 38.5 | 61.0 | 2.0 | -17.5 | 13.0 | 43 | 91.8 | 68.7 | 4.8 | 30.9 | 50.0 |
| 16 | 45.7 | 30.0 | 3.16 | 21.9 | 40.0 | 44 | 86.8 | 64.9 | 12.2 | 37.1 | 39.1 |
| 17 | 42.7 | 32.4 | 1.6 | 14.9 | 38.0 | 45 | 89.4 | 65.2 | 12.2 | 39.4 | 43.0 |
| 18 | 48.3 | 64.6 | 2.0 | -11.3 | 17.8 | 46 | 87.0 | 70.4 | 19.2 | 38.8 | 34.0 |
| 19 | 41.9 | 61.5 | 11.6 | -5.0 | 15.0 | 47 | 82.3 | 58.6 | 6.7 | 33.4 | 40.0 |
| 20 | 42.1 | 43.9 | 12.5 | 13.7 | 15.0 | 48 | 78.6 | 51.0 | 7.3 | 37.9 | ? |
| 21 | 41.8 | 33.0 | 4.7 | 16.5 | 21.0 | 49 | 58.6 | 28.7 | 7.9 | 40.8 | 51.0 |
| 22 | 43.1 | 77.3 | 37.8 | 6.6 | 13.0 | 50 | 110.0 | 67.2 | 9.1 | 54.9 | 60.0 |
| 23 | 71.3 | 48.5 | 15.0 | 40.8 | 45.0 | 51 | 81.4 | 41.0 | 1.2 | 44.6 | 58.0 |
| 24 | 51.6 | 29.1 | 3.7 | 26.5 | 45.0 | 52 | 112.7 | 40.8 | 0.4 | 75.3 | 83.3 |
| 25 | 49.6 | 25.0 | 9.0 | 36.6 | 42.0 | 53 | 105.5 | 71.7 | 2.9 | 39.7 | 45.5 |
| 26 | 58.2 | 30.0 | 0.97 | 32.2 | 44.0 | 54 | 95.8 | 67.0 | 8.4 | 40.2 | 49.0 |
| 27 | 57.4 | 60.1 | 15.2 | 15.5 | 21.2 | 55 | 92.5 | 64.3 | 20.1 | 51.3 | 50.0 |
| 28 | 54.0 | 59.7 | 21.3 | 18.6 | 21.0 | 56 | 103.3 | 54.1 | 2.7 | 54.9 | 68.0 |

S.W.L. 4/82 is the static water-level measured or estimated from the April 1982 piezometric survey.

Min. Piezo. Level is the minimum piezometric level estimated from normal pumping drawdown as described in section 4.4.4.

PUBLICATIONS OF THE HYDROLOGY CENTRE, CHRISTCHURCH

EDITED BY B.H. VAILE

Copies of publications in this series are available from:

Technical Information Officer
Hydrology Centre
Ministry of Works and Development
P.O. Box 1479
CHRISTCHURCH

- No. 1 LADEDA Plotting Handbook. R.D. Williams. May 1982.
- No. 2 Groundwater Tracing Experiments. L.W. Sinton and M.E. Close. December 1983.
- No. 3 Local Scour Around a Cylindrical Bridge Pier. A Davoren. June 1985.
- No. 4 micro-TIDEDA User's Manual. S.M. Thompson and M.W. Rodgers. June 1985.
- No. 5 Hydrology Field Office Practice. D.A. McMillan. June 1985.
- No. 6 Ground Water Resources Between the Rakaia and Ashburton Rivers. D.M. Scott and H.R. Thorpe. March 1986.
- No. 7 Hydrological Data Standards, Procedures and Quality Assurance. A.I. McKerchar. In Press.
- No. 8 TRACE/POLAR Users Manual. P.R. Van Berkel and R.D. Williams. April 1986.

PUBLICATIONS OF THE HYDROLOGY CENTRE, CHRISTCHURCH

EDITED BY B.H. VAILE

Copies of publications in this series are available from:

Technical Information Officer
Hydrology Centre
Ministry of Works and Development
P.O. Box 1479
CHRISTCHURCH

- No. 1 LADEDA Plotting Handbook. R.D. Williams. May 1982.
- No. 2 Groundwater Tracing Experiments. L.W. Sinton and M.E. Close.
December 1983.
- No. 3 Local Scour Around a Cylindrical Bridge Pier. A Davoren.
June 1985.
- No. 4 micro-TIDEDA User's Manual. S.M. Thompson and M.W. Rodgers.
June 1985.
- No. 5 Hydrology Field Office Practice. D.A. McMillan. June 1985.
- No. 6 Ground Water Resources Between the Rakaia and Ashburton
Rivers. D.M. Scott and H.R. Thorpe. March 1986.
- No. 7 Hydrological Data Standards, Procedures and Quality
Assurance. A.I. McKerchar. In Press.
- No. 8 TRACE/POLAR Users Manual. P.R. Van Berkel and
R.D. Williams. April 1986.